Univerzita Tomáše Bati ve Zlíně
Fakulta technologická

Doctoral Thesis

Polymerní nanočástice pro enkapsulaci a kontrolované uvolňování bioaktivních látek

Polymeric nanoparticles for encapsulation and controlled release of bioactive compounds

Author: Antonio Di Martino, M.Sc.

Study programme: P2808/Chemistry and material technology

Study course: 2808V009/ Chemistry and material technology

Supervisor: doc. Ing. Vladimír Sedlařík, Ph.D.

Zlin, 2016

Klíčová slova: *enkapsulace, chitosan, polylaktid, nanočástice, cytostatika*

Key words: *encapsulation, chitosan, polylactide, nanoparticles, cytostatic*

ACKNOWLEDGEMENTS

ABSTRAKT

ABSTRACT

INTRODUCTION

1. THEORETICAL PART

1.1 Nanoparticles for drug delivery applications

1.2 Polymeric Nanoparticles

1.3 Release kinetic models

1.4 Considerations on nanoparticles cytotoxicity

1.5 Pharmacokinetic and pharmacodynamics

1.6 *In-vitro-In-vivo* correlation (IVIVC) model

1.7 Chitosan and chitosan grafted-PLA as carrier and coating agent

1.8 Chitosan derivatives

AIMS OF THE WORK

2. EXPERIMENTAL PART

2.1 Materials, sample preparation and characterization methods

3. RESULTS AND DISCUSSION

3.1 Polysaccharides based nanocomplexes for encapsulation and controlled release of anticancer drugs

3.2 Chitosan grafted PLA and carboxy functionalized PLA for doxorubicin and temozolomide co-therapy

3.3 Chitosan grafted low molecular weight PLA for protein encapsulation and burst reduction

SUMMARY REMARKS

CONTRIBUTIONS TO SCIENCE AND PRACTICE

REFERENCES

LIST OF TABLES

LIST OF FIGURES

LIST OF ABBREVIATIONS

CURRICULUM VITAE

LIST OF PUBLICATIONS

ACKNOWLEDGEMENTS

I would like to express my deeply gratitude to my scientific supervisor doc. Ing. Vladimir Sedlarik, Ph. D for his support and for creating the best conditions to carry out my research.

Special thanks also to my research group and the staff of Polymer Centre for their availability and kindness.

Apart from my colleagues and friends, I would like to thanks my relatives for always being by my side.

ABSTRAKT

Tato práce se zabývá vývojem a charakterizací nových materiálů pro enkapsulaci a následné kontrolované uvolňování bioaktivních látek, cytostatik, se zaměřením na částicové amfifilní systémy na bázi chitosanu. Tento polysacharid byl modifikován polymerem kyseliny mléčné, polylaktidu. Významná část práce je věnována popisu vlivu strukturních parametrů polylaktidu na výsledné chování připravených nanočástic a kinetiku uvolňování modelové bioaktivní látky do prostředí o různých vlastnostech. Dále byl popsán průběh simultánní enkapsulace a následné uvolňování modelových látek pro systémy obsahující dva druhy cytostatik.

Klíčová slova: enkapsulace, chitosan, polylaktid, nanočástice, cytostatika

ABSTRACT

This doctoral thesis is aimed at development and characterization of novel materials for encapsulation and subsequent controlled release kinetics of the model compounds and cytostatic, with focus on nanoparticle amphiphilic systems based on chitosan. This polysaccharide was modified with polylactide. Description of the effect of polylactide structural characteristics on resultant behaviour of the prepared nanoparticle systems represents an important part of the thesis. Moreover, simultaneous encapsulation and release trend of two individual cytostatic were described.

Key words: encapsulation, chitosan, polylactide, nanoparticles, cytostatic

INTRODUCTION

In the last decades, new approaches and strategies have been developed in drug delivery area to control the rate, time and targeting of bioactive compounds in order to enhance therapeutic performances. This was the beginning of the so-called drug delivery systems (DDS). The main purpose of using a DDS is not only to deliver a biologically active compound in a controlled time and release rate but also to maintain drug level in the body within therapeutic window. The delivery of the drug in a specific area of the body is extremely important, in terms of lowering possible side effects, decreasing the concentration and the administration frequency and improving patient compliance (Koo et al., 2005, p.193-212).

Recently, a great support for preparation of more efficient and selective DDS comes from nanotechnology. Among the various type of DDS, nanoparticles (NPs) are the most promising due to the several advantages of nanoscale materials compared to bulk. DDS based on nanoparticles can be classified according to their size, surface properties, shape and material. Regarding the material, polymers represent an optimal platform due to the benefits connected with their structure such as wide range of molecular weight and polydispersity, architecture and presence of various functional groups which allow chemical modification (Liu et al., 2008, p. 1650-1662).

Polymeric materials used for preparation of NPs for drug delivery need to be biocompatible, biodegradable, non-immunogenic and non-toxic. Many polymers have been used as PLA, PGA, PCL, PA family but also natural such as proteins or peptides and polysaccharides (Liu et al., 2008, 1650-1662).

Among all mentioned the use of polysaccharides and their derivatives represent the main trend due to the favourable properties in particular in solution where are considered as polyelectrolytes as they can be positively or negatively charged according with their composition.

Polyelectrolytes (PE) are macromolecules carrying a number of functional groups which are charged or can become charged under suitable conditions. PE can be classified according to the nature (natural, synthetic or chemically modified), composition (homopolymer, copolymer) and molecular structure (linear, branched, cross-linked) (Luo and Wang, 2014, p. 353-367). By mixing oppositely charged polyelectrolyte solutions, polyelectrolyte complexes (PECs) are formed. Structurally, PECs are polymer-polymer complexes bound together by electrostatic interactions, hydrogen bonds, ion dipole and hydrophobic interactions (Llina & Varlamov, 2005). Formation and complex stability depend on several factors, i.e. the degree of ionization,

charge density, position of ionic groups, charge distribution, ionic strength, molecular weight, chain flexibility, contact time, ratio and order of mixing (Berger et al., 2004,p. 35-52.).

PECs based on polysaccharide and derivatives has been extensively investigated for biomedical application, especially in drug delivery (Cooper et al., 2005, p. 52-78. and Jayakumar et al., 2010,p. 142-150) Several bioactive compounds have been entrapped, adsorbed or chemically linked to PECs spacing from anticancer drugs like doxorubicin (Chen et al., 2011, p. 2586-2592 ; Di Martino and Sedlarik, 2014, p. 134-145), paclitaxel (Lee et al., 2008, p. 6442-6449), 5-Fluorouracile (Nagarwal et al., 2011,p. 272-278.) to antibiotics and antimicrobic (De Campos et al., 2001.p. 159-168 ; Katiyar et al., 2014,p. 117-124.); psycho active drugs (Varshosaz et al., 2015,p. 65-73); peptides and proteins; (Di Martino et al., 2015,p. 912-921 ; Dionisio et al., 2013, p. 102-113) nucleic acids (Bordi et al., 2013p. 184-190, Laroui et al., 2014, p. 41-53 and Li et al., 2014, p. 160) and the behaviour of the systems have been deeply investigated, as reported in literature (Wang et al., 2007, p. 336-343; Hu et al., 2011,   p. 1128-1133; Hu et al.2010, p. 323-334) indicating the advantages of these systems compared to other drug delivery systems.

Encapsulation of bioactive compounds into polysaccharides based NPs or complexes presents several advantages compared to the free drug (Danhier et al., 2012, p. 505-522). The carrier work as an envelope to protect the drug from the external environment, improve solubility and the duration of action in particular in case of hydrophobic drug in biological environment (Fernandez et al., 2011, p. 1628-1651). Moreover, using specific carriers increases the selectivity, decreases the dose and administration frequency and subsequently the related side effects of the considered drug.

The presented thesis is devoted to the preparation of nanoparticles based on chitosan and chitosan modified with various formulations of low molecular weight polylactic acid for encapsulation and controlled release of different bioactive molecules, in particular three anticancer drugs and a model protein.

In the first section a general overview of nanoparticles preparation methods, characterization, encapsulation and evaluation of the release kinetics by mathematical models are reported. At the end a general introduction to chitosan and its derivatives as carrier and coating agent for drug delivery application is given.

In the second section, the experimental part, the method used for nanoparticles preparation and characterization, encapsulation and release studies of different drugs and the most significate results are illustrated.

Table 1 Advantages and disadvantages related to DDS (Coelho et al., 2010, p. 164-209)

Advantages	Disadvantages
Extension of duration of action and bioavailability of the drug	Possibility of toxicity of the materials
Minimization of drug degradation and loss	Harmful degradation products
Prevention and reduction of side effects	Necessity of surgical intervention either on systems application or removal
Reduction of dosing frequency	Patients' discomfort with DDS device usage
Minimization of drug concentration fluctuations in plasma level	High cost of final product
Improvement of drug utilization	
Improvement of patient compliance	

1. THEORETICAL PART

1.1 Nanoparticles for drug delivery applications

Nanoparticle research is currently an area of intense scientific research, due to a wide variety of potential applications in biomedical, optical, and electronic fields.

Nanoparticles (NPs) are microscopic particles with at least one dimension less than 100 nm and are considered as a bridge between bulk materials and atomic or molecular structures. In a bulk material, mechanical, electronic, optical, chemical and biological properties should be independent from the size while at the nanoscale size-dependence is observed. The properties of materials change as their size shifts from macro to nanoscale. The reason is related to the high surface area in the nanoparticles (Hewakuruppu et al. 2014, p. 6041-6050), for example considering that the surface area of a cubic centimetre of a solid material is 6 m^2 while in 1 nm particle it is 1000 times higher.

Considering that most of the chemical reactions involving solids occur at the surface, where chemical bonds are incomplete, the example above indicates the high reactivity of nanoparticles.

NPs are classified in terms of chemical composition, surface properties, preparation methods and shape. Various engineered nanomaterials with the same chemical composition can have various shapes like spheres, tubes, fibres, ring and planes. According to the shape, the physical properties change even if the chemical composition is the same, because the pattern of molecular bonds differs.

Nanoparticles find application in various fields as e.g. agriculture, electronics, optics, cosmetics, pharmaceutical and biomedical industry. A great interest is focused on biomedical applications in particular for drug delivery.

Nanoparticles used in drug delivery are divided in two main platforms: i) organic (liposomes, polymeric NPs, dendrimers) and ii) inorganic platform (Au NPs, silica materials, magnetic and carbon-based materials).

Organic platform

Liposomes

Liposomes are self-assembled vesicles developed from amphiphilic phospholipids consisting in a spherical bilayer structure surrounding aqueous domain. The size can range from 50 nm to several micrometres (Sunderland et al., 2006, p. 70-93). Biological properties, including biocompatibility and biodegradability, isolation of drugs from the surrounding environment, the ability to entrap rather hydrophilic than hydrophobic drugs and the opportunity to tune size and surface properties make liposomes highly interesting for drug delivery applications.

Nowadays, liposomes are the most clinically established nanosystems for drug delivery showing high efficacy in reducing systemic effects and toxicity and improving drug circulation time (Zhao et al., 2009, p. 68-78). Examples of marketed liposomes are: i) Doxil® and ii) Caelyx® where the active molecule is doxorubicin for treatment of Kaposi's sarcoma, breast and ovarian cancer; iii) Depocyt©, containing cytarabine for lymphomatous meningitis treatment; iv) Daunoxome, containing daunorubicin for Kaposi's sarcoma and v) AmBisome®, containing Amphotericin B for treatment of fungal infections.

Besides all the peculiarities, liposomes are subjected to some limitations related to the low encapsulation efficiency, fast burst release, poor storage stability and lack of tuneable

drug release (Mao et al., 2001, p. 399-421). Surface modification represents one strategy to improve stability and structural integrity of liposomes after administration. One of the common ways to modify the surface is by attaching PEG units, poly (methacrylic acid-co-cholesteryl methacrylate), and PAA to improve the circulation time in blood (Bilensoy et al., 2009, p. 170-176).
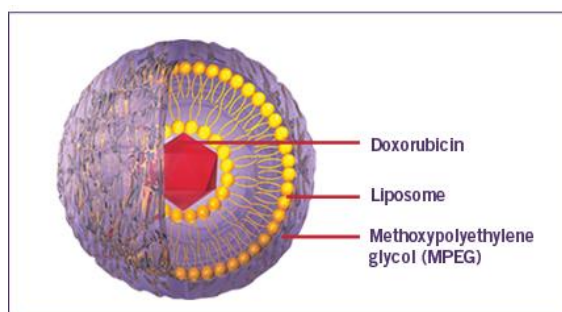

Fig. 1 Representation of marked liposome based formulation Doxil®

Polymeric nanoparticles (NPs)

Polymeric *NPs* present size in the range 10 to 1000 nm and various shapes from spherical to branched or core-shell. They have been made from synthetic (polylactide, polylactide-polyglycolide copolymers, polyacrylates (Schmaljohann, 2005, p. 1655-1670) and polycaprolactones (Bilensoy et al., 2009, p. 170-176) or natural polymers like albumin, gelatine (Saraog et al., 2010, p. 143-149) alginate, collagen and chitosan (Mao et al., 2001, p. 399-421). According to the starting material, various methods have been used to prepare polymeric based nanoparticles (see section 3.3). In the last decades, advances in polymer science and engineering have resulted in the development of stimuli-sensitive polymers. Their physicochemical properties can be changed by application of physical (temperature, ultrasound, light, electricity and mechanical stress), chemical (pH and ionic strength), and biological (enzymes) stimuli. Examples of polymeric nanoparticles available in the market are: I) Adagen ®, containing adenosine deaminase for treatment of adenosine deaminase deficiency; II) Onscaspar®, L-asparaginase for acute lymphoblastic leukemia; III) Pegasys ®, Pegylated IFN-a-2a, for hepatitis C and Genexol ®-PM, containing Paclitaxel used in cancer therapy.

Dendrimers

Dendrimers are synthetic, branched macromolecules that form a tree-like structure with low polydispersivity (Singh et al., 2008, p. 2239-2252). The opportunity to control the chemical composition and molecular weight of these structures allows predicting biocompatibility, biodegradability and toxicity of the final product. Two main approaches are used to synthesize dendrimers: i) divergent, which goes from the core and the reactions are carried on the single molecule; and ii) convergent, the synthesis begins at the periphery and stops at the core (Singh et al., 2008, p. 2239-2252). An example of dendrimer widely used in drug delivery research is polyamidoamine that has been conjugated with different target molecules like folic acid and antigen antibody. Since the clinical experience with dendrimers has been limited so far, it is hard to tell whether the dendrimers are intrinsically safe or not.
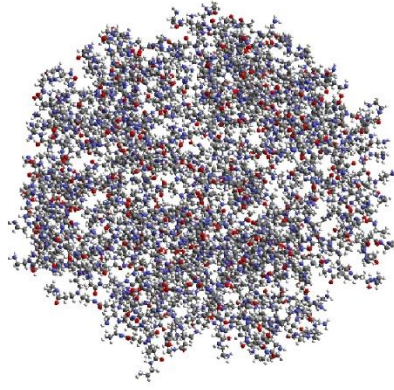
Fig. 2 Representation of molecular modelling of dendrimer

Inorganic Platform

Inorganic nanoparticles can be defined as particles of metal oxide or metallic composition possessing at least one length scale in the nanometre range. These nanostructures exhibit distinct chemical, physical and biological properties, and functionality compared to macro-scale structures. The preparation of inorganic nanoparticles offers several challenges. There is not a one-fits-all type of production process for nanoparticles but (Lee et al., 2006, p. 229-235) the traditional preparation method is by sol–gel route where the control of its particle growth occurs by changing thermal or pH conditions of the solution. Other methods widely used are spry-drying that is more suitable for scale up process and micro-emulsion (Trommelen and Crosby, 2004, p. 857-867). Inorganic nanoparticles are attracting great interest in the field of nanomedicine even if associated with long-term tissue damage, toxicity, immunogenicity, carcinogenesis, and inflammation (Huang et al., 2011, p. 344-357).

Gold nanoparticles

The interest in biomedical use of AuNPs has peaked over the past decade due to its intrinsic optical properties that can be used directly or indirectly for the treatment and diagnosis of diseases (Kumar et al., 2011, p.22). Potential applications of AuNPs have been studied recently and administered in phase I & II of clinical trials for cancer treatment.
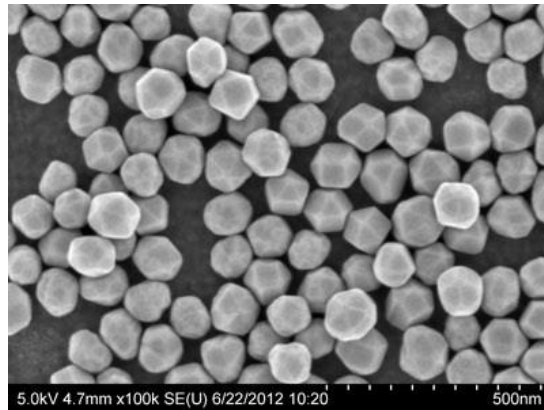
Fig. 3 SEM micrograph of standard gold nanoparticles. Source Cytodiagnostic.
www.cytodiagnostic.com

Magnetic nanoparticles

Magnetic nanoparticles present various attributes such as easy handling, possibility of passive and active targeting, simply detection and enhanced uptake by target tissue, which makes them suitable for drug delivery application. The main drawback of magnetic nanoparticles is the tendency to aggregate in large clusters with subsequent losing of the advantages related to the nano-size. Magnetic nanoparticles can be divided into i) pure metals like cobalt (Meng et al., 2011, p. 977-984), nickel (Kale et al., 2012, p. 452-459), manganese (Sayed et al., 2011, p. 3363-3369), iron (Smolensky et al. 2011, p. 189-199) and ii) alloys and oxides.

Iron oxide nanoparticles are the only type approved for clinical use. Such restriction is due to the lack of knowledge about side effects which the mentioned metals have on the human body. Various drugs and their therapeutic activity after incorporation into iron oxide nanocarriers have been tested. Some examples are i) antineoplastic and chemotherapeutic agents (like cisplatin (Yang et al., 2006, p. 185-190) and doxorubicin (Gaihre et al., 2009, 180-189)); ii) antibiotics (ciprofloxacine (Bajpai et al., 2011, p. 357-369)) and iii) neurotransmitters (Dopamine (Losic et al., 2010, p. 6323-6325)). Toxicity and influence of iron oxide nanoparticles on cellular function have been investigated and reported (Wilczewska et al., 2012, p. 1020-1037) as well. Depending on the administration route they may interact with extracellular components, cell membrane of macrophages, endothelial cells, skin epithelium, respiratory and gastrointestinal tracts (Mahmoudi et al., 2010, p. 300-309). Furthermore, after inhalation they are able to cross the blood-brain barrier and easily reach the brain. Surface chemistry and hydrodynamic size play an important role in the biodistribution,

internalization and circulation time of magnetic nanoparticles (Yoo et al., 2010, p. 2298-2307; Wang et al., 2010, p.861)
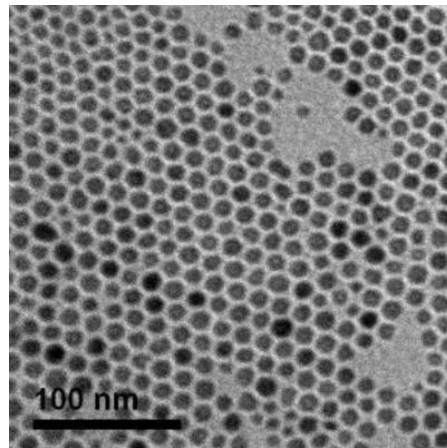
Fig. 4 TEM micrograph of Iron oxides nanoparticles. Source cytodiagnostic.
www.cytodiagnostic.com

Carbon-based nanocarriers

Carbon-based drug delivery systems are classified in i) nanotubes (CNTs) and ii) nanohorns (CNH) (Wilczewska et al., 2012, p. 1020-1037).

CNTs are formed by rolling single (SWCNTs-single walled carbon nanotubes) or multi (MWCNTs-multi walled carbon nanotubes) layers of graphite. These structures are characterized by huge surface area and excellent electronic and thermal conductivity properties (Beg et al., 2011, p. 141-163). CNTs present low biocompatibility, but it can be enhanced by anchoring PAMAM dendrimers (Zhang et al., 2010, p. 18-25), amphiphilic copolymers (Di Crescenzo et al., 2011, p. 925-928) or PEG (Bhirde et al., 2010, p. 1535-1546) on the surface or by dispersion in hyaluronic acid matrix (Shin et al., 2011). Furthermore, due to the mechanical strength, CNTs have been used as support material to improve properties of other carriers, either polymeric or non-polymeric based (Shin et al., 2011). Bioactive molecules can be immobilized in CNTs in three main ways: i) encapsulation (Arsawang et al., 2011, p. 591-596); ii) chemical adsorption on the surface by electrostatic, hydrophobic, $\pi-\pi\Box$ interactions and H-bonds (Chen et al., 2011) and iii) by attachment after functionalization. Examples of drug immobilized in CNTs are Cisplatin (Tripisciano et al., 2010, p. 141-146), Gemcitabine (Arsawang et al., 2011, p. 591-596), Doxorubicin, Amphotericin B (Prajapati et al., 2011) and Dexamethasone (Luo et al., 2011, p. 6316-6323). An

advantage of using CNTs for controlled release application is the possibility opportunity to control the release by electrical or chemical stimuli.

CNHs, are a type of SWCNTs, which possesses similar properties to nanotubes. They can be easily prepared at low cost and high purity as no metal catalysts are required. Drugs can be immobilized by adsorption on walls or by nanoprecipitation (Ajima et al., 2008, p. 2057-2064).

The potential toxicity of carbon-based nanomaterial is mainly linked with the geometrical structure (Jia et al., 2005, p. 1378-1383) in fact in case of nanotubes, the toxicity is connected to results with the high length to diameter ratio. However, the presence of impurities like residual metals or amorphous carbon that induces oxidative stress cannot be omitted (Dobrovolskaia and McNeil, 2007, p. 469-478). Some studies reported the similarity in carcinogenic potential between CNTs and silicate minerals (Poland et al., 2008, p. 423-428).
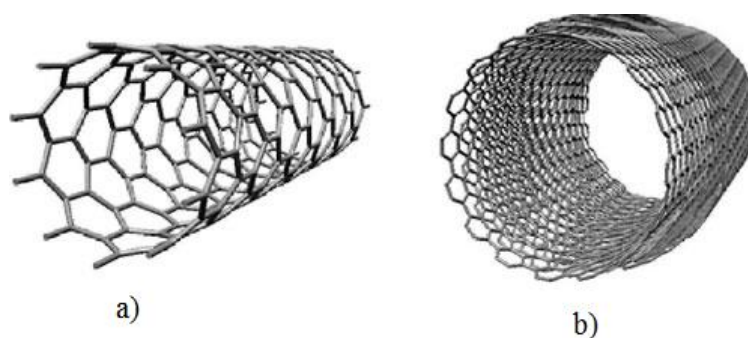

Fig. 5 Schematic representation of a) SWCNT and b) MWCNT

Silica-based nanocarriers

Drug delivery systems based on silica are divided in xerogels and mesoporous silica nanoparticles (MSNs) (Wei et al., 2010, p. 4066-4079).

MCM-41 (Mobil composition of matter), SBA-15 (Santa Barbara University mesoporous silica material) and HMS (Hollow mesoporous spheres) are the most used and characterized among MSNs (Amato, 2010). MCM-41 represents hexagonal

arrangement of the mesoporous while SBA-15 a well-ordered hexagonal connected system of pores (Wei et al., 2010, p. 4066-4079).

The MSNs properties make them an excellent material for various pharmaceutical and biomedical applications. The structure enables the incorporation of both small (Di Pasqua et al., 2009, p. 1343-1349) and large molecules (Kim et al., 2012, p. 435-442.), adsorption of DNA, and gene transfer (Slowing et al., 2008, p. 1278-1288). This gives a possibility of using these nanomaterials in a combined therapy. Bioactive compounds are loaded into mesoporous silica mainly by chemical and physical adsorption (Di Pasqua et al., 2009, p. 1343-1349). Examples of drugs loaded in MSNs are antineoplastic antibiotics and cardiac medications (Popovici et al., 2010, p. 704-714). Usually the drug release is driven by diffusion through the porous structure. Regarding the toxicity, nanoparticle size plays an important role affecting pharmacokinetic parameters, such as tissue distribution as reported in various studies (Cho et al., 2009, p. 177-183). However, toxicological data are still controversial as in some cases high toxicity is reported, especially hepatotoxicity, while in other no organ toxicity is presented (Kumar et al., 2010, p. 699-708).
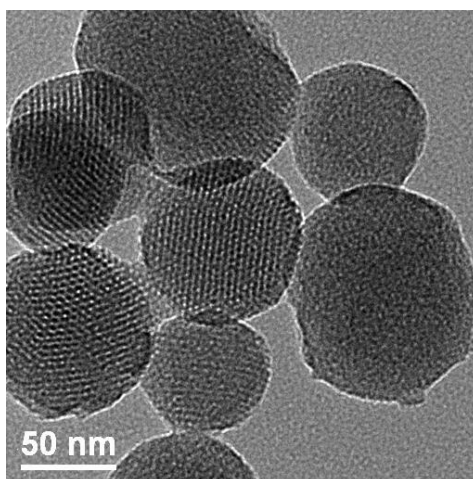

Fig.6 TEM micrograph of mesoporous silica nanoparticles

1.2 Polymeric Nanoparticles

Polymeric nanostructures represent due to their unique properties and large potential in biomedical applications a growing area in the biomaterials science (Bielawski et al., 2011, p. 364-372). Polymers, either natural or synthetic, used for preparation of drug delivery systems have to possess definite requirements as i) biocompatible backbone and degradation products; ii) mechanical properties which meet application needs; iii) degradation kinetics matching a biological process; iv) processability; v) chemical, structural and application versatility and vi) economically acceptable shelf life (Safari and Zarnega, 2014, p. 85-99). Nowadays, besides the use of natural and synthetic polymer, design DDS comprising natural and synthetic block represents a promising strategy, because an advantage from both polymeric classes can be obtained; biodegradability and biocompatibility from the natural and good mechanical properties from the synthetic (Sahoo et al., 2010, p. 106-113).

Currently available polymer-based DDS can be classified into four different categories: i) *diffusion-controlled;* ii) *chemically controlled;* iii) *solvent-activated;* and iv) *magnetically controlled* (Koo et al., 2005, p. 193-212).

Diffusion-controlled systems enclose both reservoir and matrix systems. The first are based on a polymeric membrane that surrounds a core containing the drug, while the second on a polymeric matrix in which the drug is distributed homogeneously;

Chemically controlled systems include polymer-drug conjugates in which drug molecules are linked to a polymeric backbone by a spacer. Once inside the body the linkage is cleaved by hydrolysis or enzymatically.

Magnetically controlled systems. Compared to the previous systems, magnetically responsive carrier presents two major advantages; i) high efficiency in vivo targeting and ii) controllable release of the loaded molecules at the microvascular level. Magnetically responsive systems are particularly interesting for cancer therapy.

Examples of polymeric based nanoparticles available in the market are: i) Adagen ®, containing adenosine deaminase for treatment of adenosine deaminase deficiency; ii) Onscaspan ®, L-asparaginase for acute lymphoblastic leukemia; iii) Pegasys ®, Pegylated IFN-a-2a, for hepatitis C and Genexol ®-PM, containing paclitaxel used in cancer therapy.

Natural polymers

Natural polymers, due to their biodegradability and biocompatibility are very attractive materials. However, limitations related to antigenicity, risk of viral infection and non-uniformity in the properties from batch-to-batch occur (Nair and Laurencin, 2006, p. 762-798). The main groups of natural polymers for nanoparticles preparation are protein and polysaccharides. From natural polysaccharides a wide range of derivatives has been obtained by chemical modification, showing improved properties compared to the native one.

Proteins

Proteins are macromolecules composed by amino acid residues, linked together by peptide bonds. They are the main structural components in animal and plant tissues. Collagen, gelatin and albumin represent the most used proteins for DDS preparation.

Collagen is the most abundant protein in the human body and the major component of skin, cartilage and bone. It is non-toxic, biodegradable and low-immunogenic. Collagen has been used as DDS, in a variety of shapes such as microspheres, mini-rods and sponges (MaHam et al.2009, p. 1706-1721). Collagen micro-particles have been tested as a carrier system for various bioactive compounds such as steroids and cytotoxic drugs.

Gelatin is a mixture of peptides and proteins produced by partial hydrolysis of collagen extracted from the skin, bones, and connective tissues of animals. Due to its high solubility in water and poor mechanical properties, crosslinking with other materials may be necessary (Lin et al., 2009, p. 939-944). Micro and nano-spheres of gelatine have been used for the entrapment of some anti-cancer drugs such as doxorubicin, 5-fluoruoracil, bleomycin and mitomycin C.

Albumin is the most abundant protein in the human blood plasma. It is hydrosoluble and presents a molecular weight of about 66 kDa. Characteristics like biodegradability, non-toxicity and non-immunogenicity make albumin a very promising material for biomedical/ pharmaceutical applications. Albumin microspheres have proved to be a suitable carrier for drugs used in cancer treatment due to the use of albumin by cancer cells as a source of nitrogen and energy (Wunder et al., 2003, p. 4793-4801)

Polysaccharides

Polysaccharides are high molecular weight compounds made of repeating monosaccharide units linked by glycoside linkages. According to the source, they present a wide range of properties and structures. The presence of reactive groups (-NH$_2$, COOH, SO$_4^{-2}$ and –OH) allow chemical modification improving the properties. Chitosan, alginate, dextran and polygalacturonic acid are frequently used for DDS preparation (Bigucci et al., 2008, p. 435-441).

Chitosan is a cationic polysaccharide obtained by alkaline deacetylation of chitin. It is insoluble in water and in organic solvents, but it can be dissolved in mildly acidic water solutions. The wide use of chitosan in biomedical and pharmaceutical applications is possible due to the high biodegradability, low toxicity, good biocompatibility, mucoadhesivity and antibacterial properties. A few examples of drugs entrapped in chitosan nanoparticles are paclitaxel, doxorubicin, daunomycin, 5-fluorouracil and camptothecin (Ta et al., 2008, p. 205-216). According to the structural characteristics, chitosan nanoparticles are mainly prepared by four mechanisms: i) covalent crosslinking; ii) ionic crosslinking, iii) polyelectrolyte complexation, and iv) self-assembly of hydrophobically modified polysaccharides (Il'ina, and Varlamov, 2005, p.5-11)

Alginic acid is a polysaccharide extracted from brown algae composed of β-D-mannuronic acid and α-L-glucoronic acid units. Beside the biocompatibility and non-immunogenicity, it presents the disadvantage of not being enzymatically degraded by mammals (Nair & Laurencin, 2007, p. 762-798). Angiogenic growth factors, like VEGF and bFGF and heparin have been entrapped in alginic acid based nanoparticles systems with high encapsulation rate.

Dextran is a polysaccharide of bacterial origin with backbone made of D-glucopyranose units α-1,6-linked and branches of D-glucopyranose units in the positions α-1,2-, α-1,3- or α-1,4-. Biodegradability, biocompatibility, non-immunogenicity and non-antigenicity make it a suitable material for biomedical application. Microspheres based on dextran and derivatives have been used for the controlled release of proteins, anti-inflammatory and cytotoxic drugs (Hornig et al., 2009, p. 56-62).

Polygalacturonic acid or pectic acid is a water soluble product of pectin degradation in plants. Although it has a long history of use in food industry the application in biomedical field and in particular in controlled release is still at the beginning. Various drugs have been incorporated, using simple procedures, with high loading efficiency.

Furthermore, chemical modifications have improved the polysaccharide properties. Comparative studies of other biopolymers like chitosan and alginic acid are underway in order to establish the advantages of pectic acid compared to others.

Cellulose and derivatives

Cellulose is the most abundant biopolymer in nature. Its composed of D-glucose units linked by β (1→4) glycoside bond. The presence of hydroxyl causes strong intermolecular and intramolecular H-bonds among the chains, making cellulose insoluble in water and organic solvents. The difficulty to dissolve cellulose makes further chemical modification necessary. Hydroxypropyl methylcellulose and ethyl cellulose represent the most used cellulose derivatives for biomedical application.

Hydroxypropyl methylcellulose (HPMC) is widely used for drug delivery system preparation due to the swelling properties. HPMC has been used as a carrier for several drugs and factors influencing the release behaviour have been analysed.

Ethyl cellulose (EC) is a non-ionic cellulose ether, insoluble in water, but soluble in some polar organic solvents. EC has been used for the controlled release of diclofenac sodium (Murthy and Chowdary, 2005, p. 216-219), ketoprofen (Yamada et al., 2001, p. 271-282), betamethazone and nimesulide (Madhusudhan et al., 2009).

Synthetic Polymers

Synthetic polymers offer a wide variety of compositions with tuneable properties. These materials open the possibility of developing new DDS with selected properties by changing the building blocks or the preparation technique. Synthetic polymers can also be either biodegradable or non-biodegradable. Biodegradable are those containing in their backbone linkages such as ester, orthoester, amide, urea or urethane which are easily cleaved. However, introduction of these linkages in non-biodegradable polymers make them biodegradable.

Biodegradable synthetic polymers

Polyesters: Poly (lactic acid) (PLA), and poly (lactic co-glycolic acid) (PLGA) are largely used for preparation of drug delivery devices due to their biodegradability, biocompatibility, low immunogenicity and low toxicity. A tailored degradation rate of these copolymers can be achieved by varying the stereochemistry (D or L-lactic acid monomer) and the PLA/PGA (poly (glycolic acid)) ratios. Compared to PLA, PLGA is preferred due to its higher degradation rate. Micro and nanoparticles of PLGA have been used in the controlled delivery of proteins, vaccines, genes, antigens, grow factors and anti-cancer drugs. Moreover, their potential application in gene delivery has been demonstrated (Csaba et al., 2005, p. 271-278) and also they have proved to be efficient in protecting the genetic material from the nuclease attack and high transfection efficiencies were obtained (He et al., 2004, p. 660-663).

Poly(ortho esters): The development of poly(orthoesters) (POE) is related to the necessity of having more hydrophobic polymers, containing hydrolytically labile chemical bonds, with a surface erosion degradation instead of a bulk degradation mechanism (Nair and Laurecin, 2007, p. 762-798). Currently, four families of POE are known: *POE I, POE II, POE III* and *POE IV.*

POE I is obtained by transesterification reaction between a diol and a dimethoxytetrahydrofuran; *POE II* is synthesized from diols and diketene acetal 3,9-bis (ethylidene 2,4,8,10-tetraoxaspiro[5,5] undecane) presenting high hydrophobicity; *POE III* is obtained by a reaction between a triol and an ortho ester, and *POE IV*, a modification of *POE II* , is made of units of lactic acid or glycolic acid incorporated in the polymer backbone. *POE IV* presents a number of advantages over the other *POEs*, as the possibility of controlling the polymer properties and erosion rate, high stability at room temperature and drug release dependent on erosion mechanism (Nair and Laurecin, 2007, 762-798).

Poly(alkyl cyanoacrylates) (PACA) are biodegradable acrylate polymers, with a wide range of applications in biomedical/ pharmaceutical field. PACA exhibits high rates of degradation ranging from hours to days, according to the length of the alkyl (R) chain. The development of PACA particles for drug delivery purposes has started two decades ago (Vauthier et al., 2007, p. 641-663) and a wide range of drugs has been successfully encapsulated including peptides, proteins, oligonucleotides, anti-cancer, anti-infectious and anti-inflammatory compounds. A comprehensive review on the methods of preparation, potential applications, and drugs commonly incorporated was done by Vauthier and co-authors (Vauthier et al., 2007, p. 641-663).

Non-biodegradable synthetic polymers (*Acrylic Polymers*)

Poly(methyl methacrylate) (PMMA) was the first acrylic polymer used in a biomedical application, as intraocular lenses, due to the high biocompatibility and stability. Besides the use of PMMA based materials in ophthalmology, it has been used in orthopaedics for managing open fractures, total joint arthroplasty and chronic osteomyelitis. Example of PMMA application in drug delivery comes from a microdevice coated with lectins, which was successfully used in delivering to the gastrointestinal tract (Tao et al., 2003, p. 215-228).

Poly(2-hydroxyethyl methacrylate) (PHEMA) possesses a similar structure to PMMA where the pendant methylester group in PMMA is substituted by a pendant hydroxyethyl ester group. PHEMA is a biostable polymer, with the ability of forming hydrogels and easy to manipulate, offers the possibility of having tailor-made materials for specific applications. The use of PHEMA based materials in controlled release applications is well-known in particular for cancer (Chouhan and Bajpai, 2009, p. 1103-1114) and neurological diseases treatment (Jhaveri et al., 2009, p. 174-183).

Preparation methods

Numerous techniques are available for preparation of polymeric nanoparticles belonging either to *top-down* or *bottom-up* processes.

Top-down: start from a bulk material and break it in smaller components mechanically, chemically or by other form of energy;

Bottom-up: synthesize the material from atomic or molecular precursor by chemical reaction.

The choice of the preparation method is driven by the required properties of the final product and the possibility to control size, shape, distribution, composition and agglomeration during the preparation. In case of biomedical application, surfactants, reactants and organic solvents must be completely removed.

Solvent evaporation

Solvent evaporation is one of the oldest and largely employed techniques to prepare polymeric nanoparticles using a dispersion of preformed polymers. Two main strategies are used: i) single-emulsions, e.g. oil-in-water (o/w) and ii) double-emulsions, e.g. (water-in-oil)-in-water, (w/o)/w (Rao and Geckeler, 2011, p. 887-913). These methods utilize high-speed homogenization or ultrasonication, followed by evaporation of the solvent by magnetic stirring or under reduced pressure. Solidified nanoparticles can be collected by ultracentrifugation and washed in order to remove additives such as surfactants. Examples of nanoparticles prepared by solvent evaporation are reported.

Table 2 Examples of polymeric nanoparticles prepared by solvent evaporation Adapted from Rao and Geckeler, 2011, p. 887-91

Polymer	Organic solvent	Stabilizer	Emulsion	Particle size (nm)
POP	CH_3COCH_3	Poloxamine 908	o/w	200
PLGA	CH_2Cl_2/CH_3COCH_3	PVA	o/w	60–200
PLGA	CH_2Cl_2	Span 40	(w/o)/w	200
PLGA	$CHCl_3$	Sucrose	(w/o)/w	268 ± 4
PEO-mPAE	CH_3CH_2OH	SDS	(w/o)/w	76
PS copolymer	THF	Pluronic F-108	o/w	100–150

Salting-out

Salting-out is a modified version of solvent evaporation where the use of surfactants and chlorinated solvents is not required. The emulsion is formulated with a solvent which is normally totally miscible with water, i.e., acetone, and emulsification in the aqueous phase is achieved without employing any high-shear forces (Ganachaud and Katz, 2005, p. 209-216). For salting-out effect high concentration of salts like magnesium chloride, calcium chloride and magnesium acetate or sucrose are dissolved in the aqueous phase (Galindo-Rodriguez, 2004, p. 1428-1439). The miscibility properties of water with other solvents are modified as these components dissolve in water. A reverse salting-out effect, obtained by dilution of the emulsion with a large excess of water, leads to the precipitation of the polymer dissolved in the droplets of the emulsion. The migration of the solvent from the emulsion droplets is induced due to the reduction of the salt or sucrose concentration in the continuous phase of the emulsion. A compilation of the polymer nanoparticles prepared by employing the salting-out method is given in Table 3

Nanoprecipitation

Nanoprecipitation is a simple, fast and reproducible method for nanospheres and nanocapsules preparation. Nanoprecipitation consists of three basic components: i) polymer; ii) solvent and; iii) non-solvent of the polymer. The polymer solvent has to be miscible with water and easy to remove by evaporation (i.e. ethanol, acetone, hexane, methylene chloride or dioxane). Acetone is the most employed in this technique alone (Mishra et al., 2010, p. 9-24) or in binary blends such as acetone-water or acetone-ethanol (Rao and Geckeler, 2011, p. 887-913). The non-solvent phase consists of one or a mixture of non-solvents with synthetic surfactants. In table 4 examples of polymers, solvents, non-solvents and stabilizing agents used in the nanoprecipitation formulations and particle size are reported. As can be seen most of them are synthetic but natural polymers like allylic starch (Tan et al., 2009, p. 855-859) and dextran (Hornig et al., 2009, p. 56-62) are also employed. Surfactants are not required for nanoparticles formation but the presence avoids the agglomeration phenomena, which take place in case of long storage periods.

Table 3 Examples of polymer nanoparticles prepared by the salting-out method. Adapted from Rao and Geckeler, 2011, p. 887-913

Polymer	Salting-out agent	Organic solvent	Particle size (nm)
PDLLA	$Mg(CH_3COO)_2 \cdot 4 H_2O$	CH_3COCH_3	295
PEO	$MgCl_2 \cdot 6H_2O$	CH_3COCH_3	280 ± 03
PLGA	$MgCl_2 \cdot 6H_2O$	THF	>200
PLGA	$CaCl_2$	CH_3CN	480
PDLLA	$MgCl_2 \cdot 6H_2O$	CH_3COCH_3	279 ± 10
PDLLA	$MgCl_2 \cdot 6H_2O$	CH_3COCH_3	248
PTMC	$MgCl_2 \cdot 6H_2O$	THF	183–251

Table 4 Examples of polymer nanoparticles prepared by nanoprecipitation.
Adapted from Rao and Geckeler, 2011, p. 887-913

Polymer	Solvent	Non-solvent	Stabilizing agent	Particle size (nm)
PLGA	CH_3COCH_3	H_2O	PVA	95–560
PBCA	CH_3COCH_3	H_2O	Pluronic F68	269 ± 4
Allylic starch	CH_3COCH_3	H_2O	Dextran	270
PHB	CH_3COCH_3	H_2O	Tween 80	100–125
Dextran ester	CH_3COCH_3	H_2O	–	77
PLGA	CH_3COCH_3/ CH3CH2OH	H_2O	Tween 20	63–90

Dialysis

It represents a simple method to obtain small nanoparticles with low polydispersive index (PDI). Polymer is dissolved in an organic solvent and placed inside a dialysis tube with proper molecular weight cut-off (MWCO). The dialysis is performed against a non-solvent miscible with the former one. The displacement of the solvent inside the membrane is followed by the progressive aggregation of polymer due to a loss of solubility and the formation of homogeneous suspensions of nanoparticles (Errico et al., 2009). Table 5 reports examples of polymers and other parameters used in this technique.

Supercritical fluid technology

In contrast to the previous methods where organic solvents are involved, production of polymeric nanoparticles by supercritical fluid technology represents a more environmentally friendly technique. The opportunity to obtain highly pure nanoparticles without any traces of solvent or reactants makes this technology remarkably interesting for biomedical application (Cocero et al., 2009, p. 546-555). Two principal processes have been developed for the production of nanoparticles by this technology: i) RESS and ii) RESOLV.

In RESS (Rapid Expansion of Supercritical Solution) the supercritical fluid is used to dissolve the solid material under high pressure and temperature forming a homogeneous supercritical phase. Afterwards, the solution is expanded through a nozzle forming small particles. At the expansion point a drop in pressure forces the dissolved material to precipitate. The crystals that are instantly formed enclose a small amount of the solvent that, due to the expansion, changes from supercritical fluid to its normal state, thus breaking the crystal from inside-out. The particles that are formed this way have a diameter of a few hundred nanometers. RESOLV (Rapid Expansion of Supercritical sOlution into Liquid solVent) is a modification of RESS where the supercritical solution is rapidly expanded into a liquid solvent. Compared to RESS, this technique allows the formation of polymeric nanoparticles with diameter less than 100 nm and a subsequent protection from agglomeration (Vemavarapu et al., 2005, p. 1-16).

Table 5 Summary of the experimental conditions for the preparation of polymer nanoparticles using the dialysis method. Adapted from Rao and Geckeler, 2011, p. 887-913.

Polymer	Solvent	MWCO (kg/mol)	Dialysis time (h)	Particle size (nm)
PBG-PEO	DMF	–	24	250–362
PDLLA-P(NIPAM-MAA)	DMSO	12–14	48	84–338
PDLLA	DMF	0.8–15	12	321
TosDex	DMAc	0.3-5	96	345–500
PA	DMSO	0.2	72	50–130

Ionotropic gelation

The method is based on the ability of polyelectrolytes to crosslink in presence of counter ions to form nanoparticles also called "gelispheres" which are capable of extensive gelation and swelling in biological fluids (Patil et al., 2012, p. 27-32). Examples of natural and synthetic polymers used in Ionotropic gelation are reported in table 6.

Table 6 Example of natural and synthetic polymers used in IG technique for nanoparticles preparation

Natural polymers	Synthetic polymers
Alginate	Poly lactic acid (PLA)
Dextran	Poly methacrylate (PMA)
Pectic acid	Poly ethylene glycol (PEG)
Chitosan	Poly-N-Isopropylacrylamide (PNIPAM)
Hyaluronic acid	Polyethylenimina (PEI)
Fibrin	Polyethylen glycole diacrylate (PEGDA)
Collagen	

Factors, which greatly influence the particles properties obtained by ionotropic gelation, are: i) polymer and crosslinking electrolyte concentration; ii) charge ratio; iii) temperature; iv) pH; v) ionic strength and vi) stirring.

Several drugs belonging to different therapeutic classes have been encapsulated, mostly in natural polymer matrix by ionotropic gelation method; such as prednisolone; ibuprofen (Win et al., 2003, p. 305-310); simvastatin (Boppana et al., 2010, p. 137-143); captopril and a long list of anticancer drugs.

Polyelectrolytes complexation method

Polyelectrolyte complexes (PECs) are formed by association of two oppositely charged polyions (e.g. polymer-polymer, polymer-drug and polymer-drug-polymer). The complexes are formed by electrostatic interaction avoiding the use of chemical crosslinking agents making the products more suitable for biomedical application. pH, ionic strength of the dissolution media, temperature, charges ratio and stirring represent important variables that directly affect dimension, surface charge and stability of the PEC.

As reported in Figure 2 three main steps are presented: i) formation of primary complex by Coulomb forces; ii) development of new bonds and/or corrections of the polymer chains distortions which leads to the formation of intracomplexes; iii) intercomplex aggregation driven by hydrophobic interactions (Lankalapalli and Kolapalli, 2009, p. 481). Generally, PECs are characterized by measurements of turbidity, pH and ionic strength, weight ratio of polymer in the media, viscosity, light scattering, IR and NMR, thermal analysis and X-ray diffraction.

Various parameters influence the formation of PECs such as ion site, charge density, polyelectrolyte concentration, ionic strength and temperature (Schonhoff,2003). For example, by changing the ionic strength of the media by addition of salts the ionic strength of the solution increases causing a screening effect, which weakens the complexation between polyions, and, consequently, changing in the density, size and shape of the PEC in solution occurs (Weinbreck et al. 2003, p. 293-303).
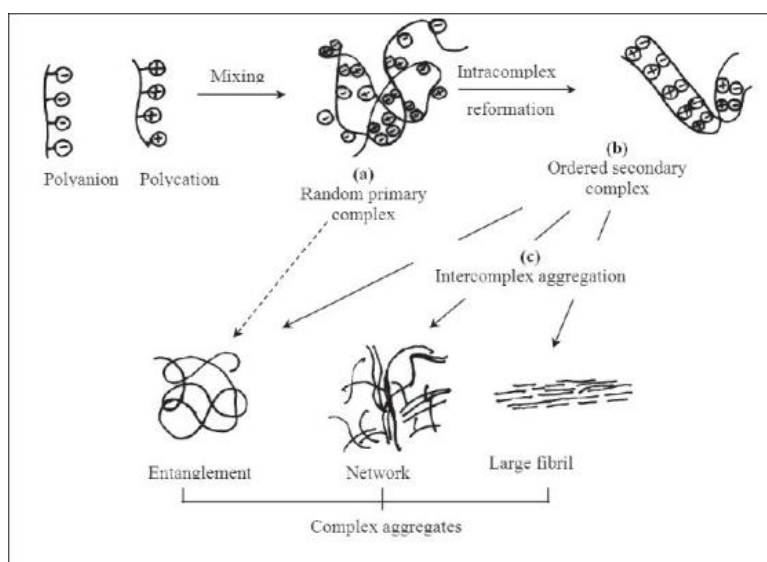

Fig.7 Schematic representation of polyelectrolytes complexes formation (Lankalapalli and Kolapalli, 2009, p. 481).

Characterization methods

Generally, nanoparticles for DDS application are initially characterized in terms of size, morphology and surface charge as they directly influence the physical stability and in-vivo distribution.

Particle size

The most popular method to evaluate nanoparticles dimension is by photo-correlation spectroscopy (PCS) or dynamic light scattering (DLS). DLS determines the dimension of nanoparticles in colloidal suspension in nano and submicron ranges. The Brownian motion of the nanoparticles in solution causes a Doppler shift of the monochromatic light which hits the particles causing a change in the wavelength of the incoming light. These variations are directly connected with the size of the particles. By measuring the diffusion coefficient (D_f) and using the auto correlation function information regarding the size distribution particles motion in the media are obtained.

Morphology

Besides the size and size distribution, morphology is another important parameter to evaluate. Scanning and transmission electron microscopy are the two main methods used to evaluate the nanoparticles morphology in solid phase and in suspension.

Scanning electron microscopy (SEM) gives a direct visualization of the nanoparticles morphology and size. Limited information regarding size distribution and the true particle population average represent the main drawback. Analysis can be conducted only on dry powder coated with a conductive metal (gold) and surface characteristics are obtained by the secondary electrons emitted after hitting by a focused beam of electrons. Generally, the nanoparticles dimension is comparable with the average values obtained by DLS.

Transmission electron microscopy (TEM): Contrary to SEM, TEM allows to investigate morphology and nanoparticles dimension in dry form and in solution. It represents an advantage in case of polymeric nanoparticles which are sensible to freeze-drying treatment (e.g. chitosan). Surface characteristics are given by an electron beam that passes through the sample. Like for SEM, the dimension values are generally comparable with that obtained by DLS (Molpeceres et al., 2000, p. 599-614).

Atomic force microscopy (AFM) provides a topographical map of the sample based on the interactions between the sample surface and a probe tip. The advantage of AFM is the ability to investigate non-conductive samples without any pre-treatment. It is

highly important in case of highly sensitive sample (biological sample) (Shi et al., 2003, p. 479-484). Compared with the previous techniques AFM provides a real image, which helps to understand the effect of the external environment on the sample. Moreover, a more accurate description of size and size distribution is obtained without any mathematical elaboration.

Surface charge

The nanoparticles stability in solution and the interaction with the external environment is evaluated by ζ-potential measurements, which is an indirect measure of the surface charge. Precisely, it represents the potential difference between the outer Helmoltz plane and the surface of shear. It represents a useful way to predict the stability and the effect of the media on the stability.

Surface hydrophobicity

It can be evaluated through different techniques: i) hydrophobic interactions chromatography, ii) biphasic partitioning, iii) adsorption of probes, iv) contact angle measurements etc. The presence of specific chemical groups on the surface can be proved by X-ray photon correlation spectroscopy.

Microencapsulation

Microencapsulation is defined as a technology to entrap a material (solid, liquid or gas) inside a micro or nano scale system in order to immobilize, protect, release or structure it (DeVos et al., 2010, p. 292-302).

The host system is classified according to the dimension and preparation methods into:

- Micro: capsules, spheres, particles or emulsions
- Nano: capsules, spheres, particles or emulsions
- Micelles
- Liposomes
- Molecular inclusion

It has been useful in the immobilization of drugs, cells and other biopharmaceutical molecules providing protection from the surrounding environment and controlled release. The characteristics of the capsules are strictly connected to the final biopharmaceutical goals of the encapsulated product (Duchesneau al., 2012, p.2013).

Various techniques are available for microencapsulation of bioactive compound for biomedical applications. These are based on chemical, physical or psychochemical approaches. Chemical methods include: i) solvent evaporation; ii) interfacial crosslinking; iii) interfacial polycondensation; iv) in situ and v) matrix polymerization. Regarding physical methods, the most common are: i) spray drying; ii) fluid-bed/pan coating; iii) centrifugal extrusion; iv) vibrating nozzle and v) spinning disk. Physicochemical methods include: i) ionotropic gelation; ii) polyelectrolyte complexation; iii) coacervation and iv) supercritical fluid technology (Duchesneau et al., 2012, p.2013).
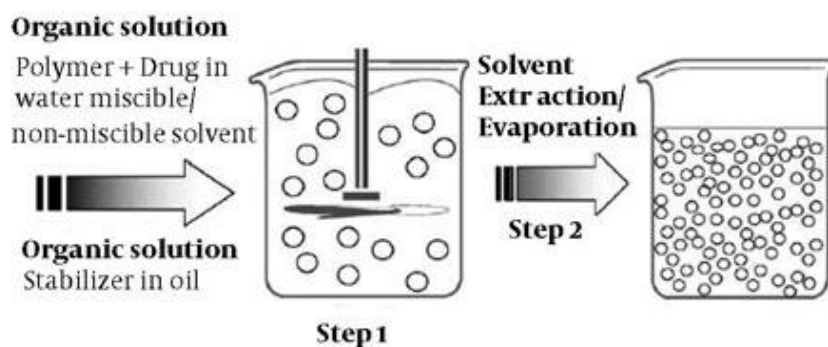

Organic solution
Polymer + Drug in water miscible/ non-miscible solvent

Organic solution
Stabilizer in oil

Solvent Extraction/ Evaporation

Step 1

Step 2

Fig. 8 Schematic representation of the single emulsification-extraction/ evaporation technique (Jelvehgari and Montazam, 2012, p.144)
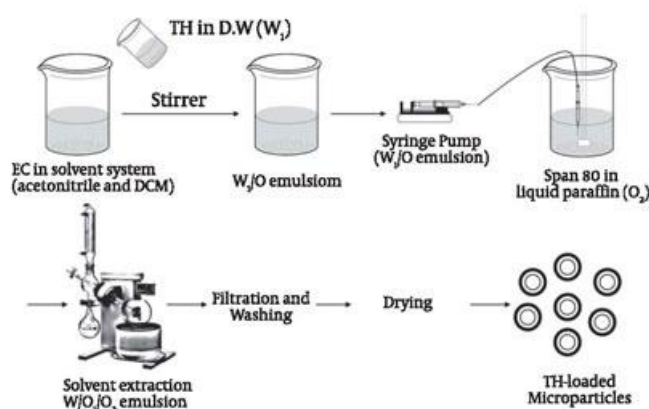
Fig. 9 Schematic representation of EC microparticles preparation using double-emulsification called the W/O1/O2 method. (Jelvehgari and Montazam, 2012, p.144)

According to the method, the bioactive compound and carrier, the compound can be homogeneously or heterogeneously located in the core, on the surface or in both area of the carrier at different percentage. The location of the drug in the system directly influences the release rate.

To evaluate the efficiency of the process and the amount of bioactive compounds loaded into the system two main parameters are generally considered; the encapsulation efficiency *(EE)* and the drug loading *(DL)*, both expressed in percentage. *EE* and *DL* are obtained by the following Equations 1 and 2, respectively.

$$\% \, EE = \left(\frac{weight \; of \; entrapped \; drug}{Total \; amount \; of \; drug} \right) x \; 100 \qquad [1]$$

$$\% \, DL = \left(\frac{Weight \; of \; entrapped \; drug}{Total \; weight \; of \; nanoparticles} \right) x \; 100 \qquad [2]$$

Another parameter which is used in case of nanoparticles systems is the particles yield (Y_P) obtained by Equation 3

$$\% \ Y_P = \left(\frac{Total \ weight \ of \ particles}{Weight \ of \ polymer + Total \ weight \ of \ drug} \right) x \ 100 \qquad [3]$$

In the last years' different approaches to deliver multiple compounds using a single carrier have been explored (Parhi et al., 2012, p. 1044-1052). A multi-drug treatment is particularly promising in cancer therapy as it can overcome the development of chemo-resistance, which is the main cause of therapeutic failure (Kunjachan et al., 2013, p. 1852-1865). It has been widely demonstrated that during chemo-treatment cancer cells acquire defence mechanisms such as overexpression of drug efflux pumps, increasing drug metabolism or express altered drug target which diminishes the therapeutic efficacy of the drug (Kievit et al., 2011, p. 76-83). In clinic, it is well-known that combination of chemotherapy drugs reduces the drug resistance (Zhu et al., 2010, p. 2408-2416). However, due to the variety of pharmacokinetics, biodistribution and membrane transport properties it is difficult to make a combination therapy schedule, in particular in terms of dosage.

The challenge in drug delivery is to combine nanotechnology with chemotherapy to obtain carrier able to transport and deliver more than one substance to the target, in the right order and at the right time.

Many approaches have been reported for multi-drug encapsulation into polymeric nanoparticles. They can be divided into three categories:

i) direct encapsulation of the drugs into the polymeric core;

ii) create a separate compartment in the nanoparticles for drug loading;

iii) conjugation of the drugs directly to the polymer backbone.

In the first case the drugs are mixed with the polymeric solution during the preparation process. This process is easy to develop but limitations connected to the chemical properties of the compound are presented (e.g. difficulty to obtain *EE* for hydrophilic compound) (Hu et al., 2010, p. 323-334).

The second approach consists in the development of a multi-compartment system to increase the loading capacity of hydrophilic drugs. It can be obtained by taking advantage of surface properties of polymeric nanoparticles (Zhang et al. 2007, p. 1268-1271).

In the last approach multiple types of drugs can be attached to a single polymer chain before nanoparticles preparation. What differentiates this approach from the previous is the ability to control the molar ratios of different drugs as it bypasses the complex nature of drug-drug and drug-polymer interactions involved in the physical drug encapsulation techniques.

Examples of nanoparticles loaded with multi-drug are reported in Table 7

Table 7 Examples of multi-drug formulations and their status (Adapted from Hu et al., 2010, p. 323-334)

Drugs	Indication	Status
GCB and DOX	Prostate cancer and various cancer types	In vivo
DOX-WOR	Breast cancer and various cancer types	In vitro
CA4 and DOX	Lung carcinoma, melanoma and various cancer types	In vivo
PTX and Bcl-2-targeted siRNA	Breast cancer	In vitro
PTX and VEGF-siRNA	Prostate cancer and various cancer types	In vitro
DOX and DTX	Prostate cancer and various cancer types	In vitro
VCR and VER	Breast cancer	In vitro
DOX and CSA	Various cancer types	In vitro

1.2 Release kinetic models

According to the chemical and physical characteristics of the polymer and the loaded molecule, the release mechanism can be controlled by three main processes:

1)   Diffusion
2)   Swelling
3)   Erosion

In biodegradable polymers, such release is primarily driven by hydrolytic cleavage of polymer chains, even though diffusion may be still dominant when erosion is slow. Conversely, in non-biodegradable polymers, drug release is controlled by the concentration gradient via diffusion or matrix swelling *(Arifin et al., 2006, pp. 1274-1325; Vergnaud, 1993).*

Diffusion controlled systems

The release profile of diffusion controlled systems is obtained by Fick's second law that considers ideal boundary conditions, as follows:

$$\frac{\partial C}{\partial t} = \frac{1}{r^2} \times \frac{\partial}{\partial r} \times \frac{Dr^2}{\frac{\partial C}{\partial r}} \qquad [4]$$

where D is the diffusion coefficient and C the concentration of the loaded compound in the carrier. Depending on the area where drug diffusion occurs, a diffusion-controlled system can be classified as either a reservoir or matrix system. The former consists of a drug reservoir surrounded by the polymer matrix shell, while the latter involves the drug being dissolved or dispersed inside the polymer matrix.

A schematic illustration of said systems is given below; a reservoir system (Fig. 10a), and a matrix system - where the drug is dissolved (Fig. 10b) or dispersed (Fig. 10c).
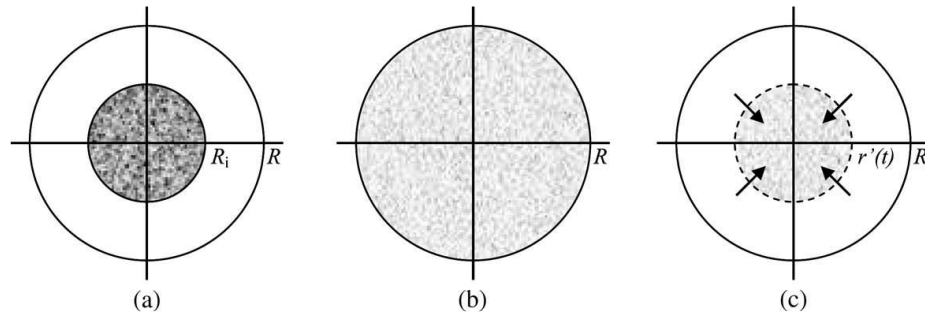
Fig. 10 Schematic representation of a) a reservoir system; b) a dissolved drug system and c) a dispersed drug system (Arifin et al., 2006, pp. 1274-1325)

The assumption for the reservoir model is that the drug is confined by a spherical shell of outer radius R and inner radius R_i. Thus, the drug must diffuse through a layer of thickness $(R-R_i)$ (Fig. 10a) (Arifin et al., 2006, pp. 1274-1325).

In the matrix system pertaining to dissolution of the drug, concentration of the drug as loaded (C_0) is lower than the saturation concentration (C_s), meaning that the drug is uniformly dissolved in the matrix.

In the case where the drug is dispersed, two compartments are present: (i) the "core", where undissolved solute exists at concentration C_0; and (ii) the dissolved or diffusion area, where all solute is dissolved.

Distinct separation for these two areas is valid when $C_0 > C_s$.

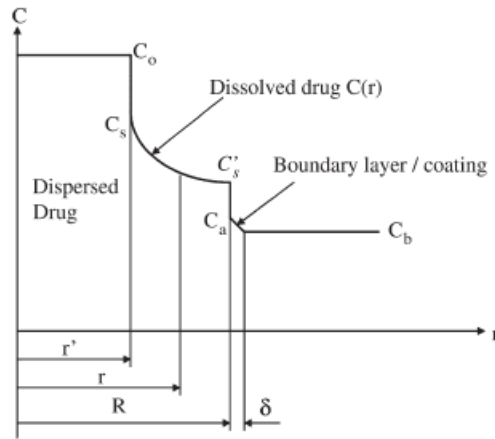Figure 11 depicts a schematic illustration of concentration profiles for the dispersed drug system.

Fig. 11: Schematic representation of concentration profiles pertaining to the dispersed drug system under ideal sink conditions (Arifin et al., 2006, pp. 1274-1325)

Swelling-controlled systems

These demonstrate a superior level of control over the drug release process, particularly when the diffusivity of the drug in the polymer is low. These systems are usually based on hydrophilic polymers, which tend to swell as water penetration occurs, thereby causing relaxation of the polymer chains. The percentage of swelling and degree of disentanglement are directly linked to the concentration of the polymer (Fig. 12) (Ju et al., 1995, pp. 1455-1463).
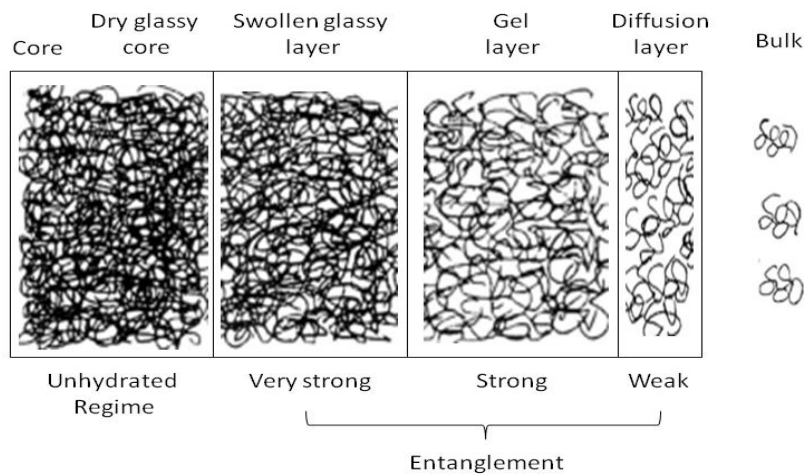

Fig. 12: Schematic illustration of polymer matrix disentanglement as a function of polymer concentration in a swelling-controlled drug system (Ju et al., 1995, pp. 1455-1463)

As illustrated in Fig. 12, the amount of media in the polymer matrix influences the level of disentanglement. In an instance of of strong entanglement, the swelled matrix forms a rubbery region where diffusion and drug mobility takes place. Conversely, in an area characterized by weak entanglement, the given polymer actually dissolves at the interface. In such a case, deviation from Fick's second law is observed, and the release process is controlled by diffusion of the drug inside the matrix, polymer matrix disentanglement and the dissolution process.

Examples of hydrophilic polymers used in drug delivery that exhibit swelling behaviour include cellulose derivatives such as hydroxypropyl cellulose, polyvinyl alcohol (PVA) and poly(hydroxyethyl methacrylate). Usually swelling-controlled delivery systems are prepared as tablets, with the overall release process being strictly connected with the geometry of the given device. Various mathematical models have been developed in accordance with such geometry, (Arifin et al., 2006, pp. 1274-1325).

Erosion-controlled systems

Due to their chemistry and surface properties, bioerodible polymers represent an important class of materials in biomedical applications. Erosion kinetics can be tuned by modifying the composition of the polymer.

It is important to distinguish degradation from erosion. Degradation is a chemical process that refers to cleavage of the polymer chain/bond, whereas erosion indicates loss of polymer material under a chemical or physical process (Costa and Lobo, 2001, pp. 123-133).

Considering that erosion is a complex mechanism involving aspects such as drug dissolution, polymer degradation, porosity creation, change in microenvironment and pH, diffusion of the drug and autocatalytic effect, description tends to focus on two ideal scenarios - surface and bulk erosion. In the latter, external fluid penetrates the system, with said system maintaining its dimensional constant. However, in surface erosion, the size of the system decreases alongside occurrence of phenomena taking place at its external matrix boundary (Kumar et al., 2002, pp. 889-910).

Presently, several mathematical models are available that describe drug release from erosion-controlled systems. These models are divided in two main groups: empirical and mechanistic. The former does not take into account complex physicochemical phenomena, and is developed for surface-eroding systems that exhibit zero order release kinetics. As for the latter of the two groups, consideration is given to physicochemical

phenomena, which essentially comprise diffusional mass transfer and chemical reaction processes (Arifin et al., 2006, pp. 1274-1325).

Drug release mechanism in nanoscale

Over the past few decades, there has been a rise in interest in developing nanoparticles for drug delivery applications, particularly for cancer treatment.

One of the major challenges to drug delivery is the release of hydrophobic agents, which exhibit limited diffusivity through the polymer matrix, resulting in a slow release profile. A prime example is paclitaxel, used widely used for treating ovarian and breast cancer, and numerous studies have focused on improving its solubility.

The release profile of a highly hydrophobic drug from polymeric systems is principally influenced by the drug diffusion mechanism. Indeed, the drug dissolution mechanism has little effect on drug release, as solubility is low and the dissolution rate constant (k) small compared to the diffusion rate. In such a situation, the timescale for diffusion due to the relatively little size of nanoparticles is still less than that for dissolution. Therefore, the tendency is that the encapsulated drug is released through diffusion in the polymer matrix. In a crystalline polymer matrix, such as PLA, drug release is often very slow due to a correspondingly low diffusion coefficient.

Taking into consideration the Fickian diffusion model, it would be expected that the release profile could significantly alter by changing the particle dimension. However, this is not reflected in some experimentally determined release profiles that have been reported, especially for a hydrophobic drug (Liggins and Burt, 2001, pp. 19-33; Siepmann et al., 2005, pp. 2312-2319). Another important characteristic to highlight is the effect of drug loading on the release profile. In general, the diffusion model predicts a release profile on the basis of the fraction of initial loaded drug that is released over time. Many studies have observed that the release profile is dependent on drug loading in the polymer matrix. When designing controlled release devices for hydrophobic drugs, an important role is played by both factors pertaining to the dependence of drug diffusion coefficient, these constituting particle size and the effect of drug loading.

In addition to the difficulties encountered in hydrophobic drug delivery relating to slow release, discharging hydrophilic drugs such as proteins also represents a challenge. An intensive initial burst is often associated with hydrophilic molecules, followed by a phase of very slow drug release (Arifin et al., 2006, pp. 1274-1325; Wong and Wang, 2001, pp. 933-948).

One way to overcome it is by encapsulating the drug in double-walled composite particles; this dampens the initial burst effects and allows for sustained release over a longer period of time. An example of this in practice comprises double-walled microspheres for sustained delivery of a water-soluble radio sensitizer drug, etanidazole (Lee et al., 2002, pp. 437-452).

The main goals for delivery of hydrophilic drug molecules constitute development of nanoscale particles capable of site-specific targeting with sustained release over a longer period of time. This might be achieved by creating double-walled nanoparticles with a less permeable outer shell made of a hydrophobic matrix, with the aim of controlling the initial burst effect.

In vitro release models

In vitro release studies are key to evaluating and optimizing such a formulation. However, a lack of correlation between *in vitro* and *in vivo* release profiles exists. Physiological conditions are more complex than the buffer solutions, and the presence of various components such as proteins, cells and enzymes directly affects the release pattern. Utilizing a simulated medium for physiological release, e.g. intestinal, gastric and lachrymal fluids, saliva and blood serum, enhances accuracy of evaluation (Costa and Lobo, 2001, pp. 123-133).

The complex composition of biological fluids also presents a challenge to conventional analytical methods. The tools for overcoming such issues came about through rapid development of advanced analytical techniques, such as liquid chromatography coupled with mass spectroscopy, and the use of fluorescent probe and imaging techniques (Rothstein et al., 2009, pp. 1657-1664).

Various methods are available that enable evaluation of drug release from nanoparticle carriers, as follows: i) side-by-side diffusion using artificial or biological membranes; ii) dialysis bag diffusion; iii) reverse dialysis bag diffusion; iv) agitation followed by ultracentrifugation/centrifugation; and v) ultrafiltration. Usually a release study involves controlled agitation followed by centrifugation. As separating nanoparticles from the release media is both time-consuming and technically complex, the dialysis technique is generally preferred. However, these methods prove difficult to replicate and scale-up for industrial use.

In order to evaluate and predict release kinetics, different mathematical models have been established. Even though models representing real physiological conditions have yet to be developed, the aim is to evaluate the transport mechanism and structure-function relationships. Mathematical approaches to investigating release kinetics can be split into three main categories:

a) Statistical methods (MANOVA: multivariate analysis of variance)

b) Model-dependent methods (zero-order, first-order, Higuchi, Korsmeyer-Peppas, Hixson-Crowell, Baker-Lonsdale, Weibull, Hopfenberg and others) (Costa and Lobo, 2001, pp. 123-133)

c) Model-independent methods

Statistical methods

Multivariate analysis of variance (MANOVA)

MANOVA is a General Linear Model used to quantify strength between variables (Zientek and Thompson, 2009, pp. 343-352).

MANOVA is a mathematically extended version of ANOVA more suitable in situations involving two or more dependent variables.

Model dependent methods

Model dependent methods are based on mathematical function to describe dissolution profiles. The most frequently applied models are detailed below.

Zero-order model:

This describes drug dissolution from systems lacking disaggregation followed by slow release. The representative equation is:

$$Q_t = Q_0 + K_0 t \qquad\qquad [5]$$

where Q_t represents the amount of drug dissolved at time t, Q_0 the initial amount of drug in the media ($Q_0 = 0$ generally) and K_0 represents the zero-order release constant expressed in concentration/time.

The *in vitro* data obtained are reported as the cumulative amount of drug release contrasted with time.

This model can be applied to describe release from transdermal systems, as well as matrix tablets with low-soluble drugs and osmotic systems (Freitas and Marchetti, 2005, p. 201-211)

First-order model

First-order release can be expressed by the equation:

$$\frac{dC}{dt} = -K_1 c \qquad\qquad [6]$$

where K_1 represents the first-order constant expressed in time^{-1}. Another way to express the equation is in logarithmic form:

$$log\ C = logC_0 - \frac{K_1 t}{2.303} \qquad\qquad [7]$$

where C_0 is concentration of the drug and *t* is time. The resultant data are plotted as the log cumulative percentage of drug remaining contrasted with time.

This model can be used to describe the release of water-soluble drugs from porous matrices.

Higuchi model

This was originally conceived for planar systems but was extended to encompass other geometries and porous systems. It is based on 6 hypotheses, as follows: i) initial drug concentration in the matrix actually exceeds drug solubility; ii) drug diffusion occurs only in one dimension; iii) drug particles are smaller than system thickness; iv) swelling and dissolution of the matrix are negligible; v) drug diffusivity is constant; and vi) perfect sink conditions. Expression of the model is given by the equation:

$$Q = A\ (D(\ 2C - C_S)C_S t)^{1/2} \qquad\qquad [8]$$

where *Q* is the amount of drug released at time *t* per unit area *A*, *C* is the initial drug concentration, C_s is the solubility of the drug in the matrix, and *D* drug diffusivity into the matrix.

This relation can be considered valid all the time except when total depletion of the drug in the system is achieved. Equation 7 can be expressed in a simpler manner, known as the simplified Higuchi model:

$$Q = K_H t^{1/2} \tag{9}$$

where K_H is the Higuchi constant (Arhewoh et al., 2004). The values obtained are plotted as cumulative percentage release contrasted with the square root of time. This equation is used to describe water-soluble drug dissolution from several pharmaceutical formulations, such as transdermal systems and matrix tablets.

Hixson-Crowell model

The equation derived where the regular area of particles is recognized as proportional to the cube roots of its volume is:

$$W_0^{1/3} = W_t^{1/3} + K_{HC} t \tag{10}$$

where W_0 is the initial amount of the drug in the system, W_t is the remaining amount at time t and KHC is a constant that incorporates the surface-volume ratio.

The equation describes the release rate of systems that exhibit change in surface area and diameter (Shoaib et al., 2006, pp. 119-124).

The data are plotted as the cube root of the percentage of drug remaining in the matrix contrasted with time. This equation is applied to the pharmaceutical form of tablets, where dissolution occurs in planes parallel to the surface of the drug (Chen and Cheng, 2007, pp. 907-913)

Korsmeyer-Peppas model

This model describes drug release by the following equation (Siepmann and Peppas, 2001, pp. 163-174):

$$\frac{Mt}{M\infty} = K t^n \tag{11}$$

where $\frac{Mt}{M\infty}$ is the fraction released at time t, K represents the release rate and n the release exponent.

Table 8 shows *n* values corresponding with release mechanisms from polymeric films.

Table 8 Interpretation of diffusional release mechanisms from polymeric films (Siepmann and Peppas, 2001, p. 163-174)

Release exponent (n)	Drug transport mechanism	Rate as function of time
0.5	Fickian diffusion	$t^{-0.5}$
0.45 < n = 0.89	Non-Fickian transport	t^{n-1}
0.89	Case II transport	Zero-order release
n> 0.89	Super case II transport	t^{n-1}

In order to obtain the correct *n* value, only the portion of release curve $Mt/M\infty$ < 0.6 should be utilized. Evaluating release kinetics involves plotting the resultant data as log cumulative drug release in per cent contrasted with logarithms of time.

Baker-Lonsdale model

This model was devised from the Higuchi model, and describes drug release from spherical matrices using the following equation:

$$f = \frac{Mt}{M\infty}\left[1 - (1 - \frac{Mt}{M\infty})^{3/2} = K_t \right. \tag{12}$$

where the release rate constant *K* corresponds to the slope (Polletto et al., 2007, pp. 70-80). The resultant data are plotted as [d $(Mt/M\infty)$]/ dt contrasted with the inverse of the root of time.

This model has been used to linearize release data obtained from microcapsule or microsphere formulations (Polletto et al., 2007, pp. 70-80).

Weibull model

An alternate dissolution process is described by the following equation:

$$M = M_0[1 - e^{-(t-T)^{\frac{b}{a}}}]$$ [13]

where M is the amount of drug dissolved as the function of time t, M_0 represents the total amount of drug released and T is the lag time. Parameter a, is a scale parameter that describes the dependence of time, while b represents the shape of the dissolution curve. In the case of b=1, such curvature corresponds to an exponential profile with K = 1/a, while for b >1 the curve appears sigmoidal (Dash et al., 2010, pp. 217-223). This model is useful for comparing the release profile of a drug from matrix-type systems (Kachrimanis and Malamataris, 2000, pp. 387-393).

Hopfenberg model

This model correlates with drug release from surface-eroding polymers as long as the surface area remains constant during the degradation process. The cumulative fraction of drug released at time t is given by:

$$\frac{Mt}{M\infty} = 1 - \left[\frac{1-K_0t}{C_L a}\right]^n$$ [14]

where K_0 (zero-order rate constant) describes the surface erosion process of the polymer, C_L is the initial drug loading, a is the half thickness of the system (radius in the case of sphere), and n is the exponent according to the geometry (n= 1 flat, n= 2 cylindrical, n= 3 spherical).

This model is used to identify the mechanism of release from the optimized oil spheres using data derived from a composite profile, the latter displaying site-specific biphasic release kinetics.

Table 9   Review of release kinetics models and their application

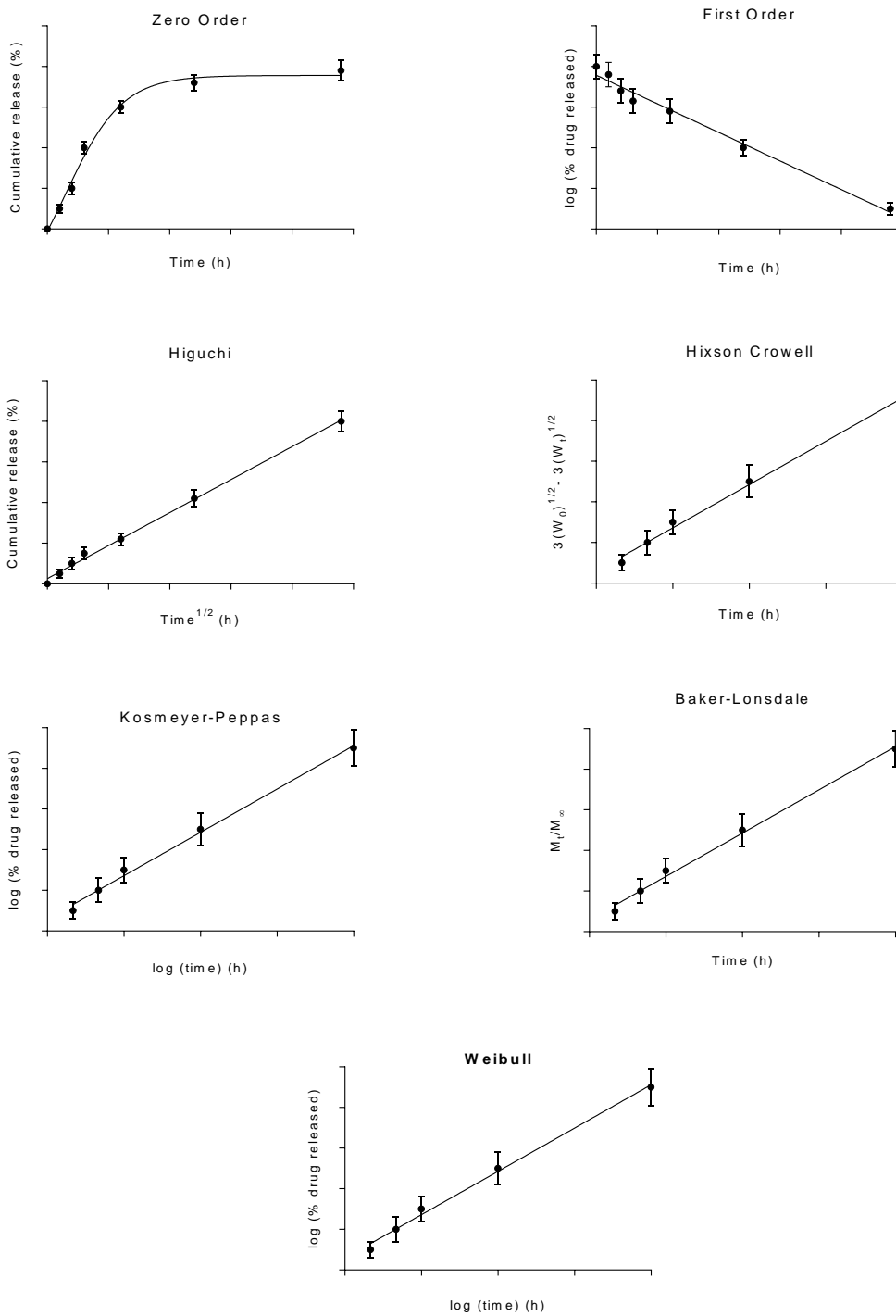| Model	Application
Zero-order	Osmotic and transdermal systems
First-order	Water-soluble drugs in porous matrix
Higuchi	Diffusion matrix formulations
Hixson-Crowell	Erodible matrix formulations
Weibull	Various systems
Korsmeyer-Peppas	Swellable systems
Baker-Lonsdale	Microcapsules or microspheres

Fig. 13 Graphical representation of the most frequently utilized mathematical models for release kinetics

1.3 Consideration of nanoparticle cytotoxicity

Engineered nanoparticles constitute one of the leading nanomaterials currently under investigation due to their applicability in various biomedical fields (Kong et al., 2011, pp. 929-941).

Therefore, the unintentional adverse effect of exposure to nanoparticles is of growing concern both academically and socially. Standardized procedures have yet to be outlined for evaluating nanoparticle toxicity (Stone et al., 2009, pp. 613-626; Dhawan and Sharma, 2010, pp. 589-605; Teeguarden et al., 2007, pp. 300-312). *In-vivo* studies are desirable when evaluating the effect of nanoparticles on the human body. However, most toxicity studies focus on *in-vitro* examinations due to the comparative simplicity of executing, controlling and interpreting such experiments compared with *in-vivo* tests. Taking the experimental conditions into consideration, well-defined *in-vitro* studies can mimic the *in-vivo* system, and function as a simple method for investigating the toxic effect of such materials. Therefore, more consideration must be placed on improving experimental procedures for toxicity assays so as to gain reliable data (Wörle-Knirsch et al., 2006, pp. 1261-1268; Casey et al., 2007, pp. 1425-1432; Ciofani et al., 2010, pp. 405-411; Park et al., 2009, pp. 108-116; Tolnai et al., 2001, pp. 2683-2687).

It is important to evaluate the most significant factors that affect cytotoxicity assays and the methods used to address them, especially regarding nanoparticles which people are extensively exposed to through various routes, such as intravenous administration, the respiratory tract, dermal exposure and ingestion. Choosing an appropriate cytotoxicity assay method is also an important consideration, since some may interfere with the toxic effect produced by the nanoparticle (Huang et al., 2000, pp. 3530-3531; Brown et al., 2007, pp. 69-79; Fortner et al., 2005, pp. 4307-4316).

Modifying the properties of the nanoparticle, following contact with biological media, poses an issue, as protein adsorption and aggregation can change the surface charge, composition and dimension of the nanoparticle (Gulson et al., 2006, pp. 1486-1488; Limbach et al., 2005, pp. 9370-9376; Lisunova et al., 2006, pp. 740-746; Kong et al., 2011, pp. 929-941).

Choice of cell types

The toxic effect of nanoparticles is highly dependent on the organs and type of cell encountered. For example, cancer cells are more resilient to nanoparticle toxicity than normal cells due to an increased rate of proliferation and metabolic activity (Nan et al., 2008, pp. 2150-2154; Chang et al., 2007, pp. 2064-2068). Obtaining complete evaluation of the effect of nanoparticles on the human body requires that cytotoxicity assays actually consider all the cells the nanoparticles encounter from administration until reaching the target site.

In biomedical applications, nanoparticles are often administrated by intravenous, subcutaneous, intramuscular or intraocular pathways, meaning that numerous cell types ranging from endothelium, blood, the spleen, liver, nervous system, heart and kidney are involved and have to be considered (Nemmar, 2002, pp. 998-1004; Oberdörster et al., 2002, pp. 1531-1543; Vickers et al., 2004, pp. 577-590).

In addition to understanding the effect of nanoparticles on specific cell types it is important to identify the systemic response. Nanoparticles can accumulate in certain areas of the body, depending on their composition and exposure route, or may be distributed throughout the body.

Due to the wide variety of affected cells and elicited responses by nanoparticle exposure, cytotoxicity assays should extend beyond a single cell study to the co-culture of multiple cell types. Combining various cells, such as macrophages, epithelial and endothelial cells, in a single assay would more closely mimic circumstances *in-vivo*, since numerous types of cells of *in-vivo* systems react systematically and simultaneously to the nanoparticle (Rothen-Rutishauser et al., 2005, pp. 281-289; Chithrani and Chan, 2007, pp. 1542-1550).

Nanoparticle characterization

The properties of the nanoparticle, such as size and shape, also play a major role in evaluating cytotoxicity, as demonstrated in various studies (Chithrani and Chan, 2007, pp. 1542-1550). It has been shown that cellular uptake, protein adsorption, accumulation in cell organelles and distribution throughout the body is directly connected to the size and shape of the nanoparticle. One reason for these effects is the correlation between particle size and surface area.

The surface area of the nanoparticle increases as size decreases, and the ratio of size of surface to total number of atoms or molecules increases exponentially as particle size diminishes.

It has been demonstrated that in various nanosystems, from quantum dots to silica nanotubes, there is a direct correlation between rise in toxicity and reduction in dimension (Pan et al., 2007, pp. 1941-1949).

It is also important to consider agglomeration phenomena, which can randomly and dramatically change the initial size and shape of the particles. Nanoparticles tend to easily agglomerate, but it is a simple matter to re-disperse them by ultrasound or vortex treatments. However, strongly bound particle agglomerates prove difficult to restore to their original, well-separated forms.

Maintaining the original size, shape and surface composition of the particle in a well-suspended state is crucial for obtaining reliable data on toxicity dependent on the size and shape of the nanoparticles. Recently, surface modification of nanoparticles, in particular through the use of PEG, has been applied to limit agglomeration of nanoparticles and non-specific adsorption of proteins (Oberdörster et al., 2007, pp. 1531-1543).

Nanoparticle concentration

Nanoparticle toxicity has been shown to be dependent on concentration. Determining an appropriate dose to utilize in a cytotoxicity assay is fundamental to understanding subsequent toxic effects under real conditions.

The concentration of particles introduced into cell cultures during cytotoxicity assays varies according to the parameter used to determine dosage of the nanoparticles. Usually the dose is expressed as mass per unit volume (e.g. µg/ml). In contrast to soluble chemicals, nanoparticles have a tendency to diffuse, settle and agglomerate in dispersion media, thereby influencing the transportation rate towards the adherent cells on the culture plate and affecting the effective dose within said cells (Teeguarden et al., 2007, pp. 300-312). Generally, concentration ranges at 5 - 500 ☐g/ml according to the parameters discussed above. Defining the dose for *in-vitro* studies is rather complicated and requires careful evaluation.

Cytotoxicity assays

Various assays are used to determine the toxic effects of nanoparticles on cell cultures, including lactate dehydrogenase (LDH) leakage, the 3-(4,5-dimethylthiazol-2- yl)-2,5-diphenyltetrazolium bromide (MTT) assay and identifying cytokine/chemokine production.

In order to discern which would be the most preferable assays, all potential interferences have to be considered to avoid false positives and false negatives. For example, interactions between the nanoparticles and dye have been cited as a potential major interference, leading to inaccurate results being recorded. As reported by Wörle-Knirsch (Wörle-Knirsch et al., 2006, pp. 1261-1268), single-walled carbon nanotubes attached to MTT-formazan crystals - formed after the reduction of MTT - proved not to be soluble in the solvents used to dissolve the MTT-formazan; consequently, reduction in cell viability was observed in the MTT test.

Disturbance of toxicity assays through the presence of metallic nanoparticles has also been reported (Kong et al., 2011, pp. 929-941; Kong et al., 2011, pp. 929-941). In the case of a gold nanoparticle, dead cells were imaged with commonly used fluorescent propidium iodide (PI). Normally, the fluorescent PI molecules cannot penetrate the cell membrane. However, in the experiment, the PI entered the cell during endocytosis of the nanospheres and resulted in a false-positive toxicity result.

In addition to the potential interferences highlighted above, light absorption and scattering by the nanoparticles can create inaccuracies in the data, since many nanoparticles absorb in the UV-Vis range (Kong et al., 2011, pp. 929-941).

The types of toxic effects that are actually analysed also represent an important factor for consideration when selecting an appropriate cytotoxicity assay. *In-vitro* toxicity assays often measure the extent of cell death caused by nanoparticles. However, in some cases, sub-lethal cellular changes may occur, which alter certain functions of the cell but do not result in cell death. These 'secondary' effects must be carefully characterized by genomic and proteomic array tests. Other forms of cellular damage, such as membrane damage, metabolic abnormality and inflammatory responses, can be characterized via LDH leakage, MTT assay and cytokine/chemokine measurements. Selecting cytotoxicity assays that are deemed capable of identifying the diverse range of potential induced responses is critical to fully understanding the toxic effects of nanoparticles.

1.4 Pharmacokinetics and pharmacodynamics

The human body is a complex organism, in which biological, physiological and biochemical processes directly influence the course of the administered drugs (Laub and Gallo, 2006, pp. 393-395).

The specifics of these processes are grouped and commonly referred to as:

Absorption: the process of getting the drug into the body

Distribution: the process of distributing the drug in tissues

Metabolism: the process of changing the drug into metabolites

Excretion: the process of removing the drug and associated metabolites from the body

Together these are referred as "ADME" and are influenced by the genetic make-up, age and gender of the subject, and the state of their disease.

The action of a drug is related to the concentration of active product heading towards receptor sites with the intention of influencing the biochemical functions. (Peters, 2008, pp. 261-275).

Pharmacokinetics (PK) is the application of mathematical models to absorption, distribution, metabolism, and excretion of drugs in the body. PK is primarily concerned with evaluating the concentration and rate of drug availability to the target site; it is not limited to the parent drug molecule, but is also applicable to active or inactive metabolites.

PK parameters can be descriptive or conceptual. Descriptive results are simple in nature and applied in a concentration-time profile where knowledge of body-drug interaction is not required. Analysis evaluates the concentration of drug as time progresses, resulting in the production of a 'plasma concentration-time curve'. Various indices like maximum plasma concentration (C_{max}), time to maximum plasma concentration (T_{max}) and area under the plasma concentration curve (AUC) can be calculated (Bois, 2009, pp. 154-161). Conversely, from a conceptual perspective, an understanding of drug-body interactions needs to be considered.

The pharmacodynamics (PD) process describes all issues concerned with the pharmacological actions of a drug. (Csajka and Verotta, 2006, pp. 227-279). Just like PK, PD is not limited to the parent drug molecule itself, but will also assess identified metabolites (Danhof et al., 2008, pp. 186-191).

In PD, the "dose-response curve" is used to describe the relationship between the concentration of drug at the site of action and the intensity of the pharmacological effect caused. Graphs can then be used to analyse individual drug activity, or permit comparison so as to assess potency, the amount of drug needed to produce similar effects or the drug concentration required to produce the maximum effect (Meibohm and Derendorf, 1997).
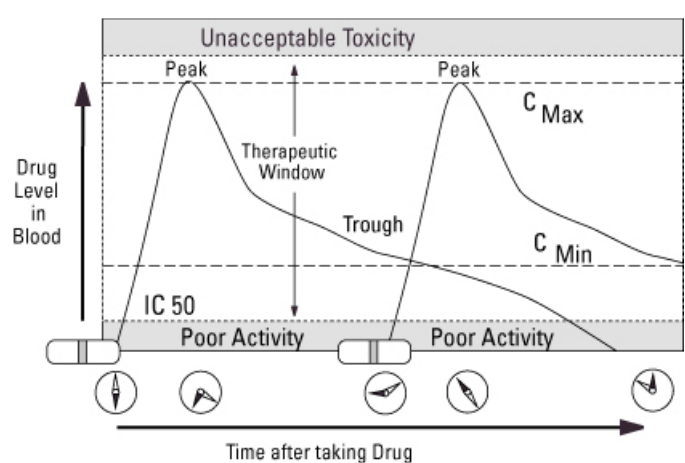

Fig. 14 Dose responsive curve; "The Ups and Downs of Drug Levels: A Pharmacokinetics Primer" by Bob Munk, The Body, July/August 2

1.5 *In-vitro-in-vivo* correlation (IVIVC) model

In-vitro–in-vivo correlation (IVIVC) models allow for prediction of *In-vivo* performances of a drug based on i*n-vitro* release profiles.

Generally, *in-vitro* properties are related to drug dissolution or release, while the *in-vivo* response pertains to plasma concentration and the amount absorbed.

The establishment of an IVIVC model can provide a surrogate for bioequivalence studies, improve product quality, and reduce regulatory charge (Lu et al., 2011, pp. 142-148).

It is recognized that correlations exist between *in-vitro* drug dissolution and *in-vivo* drug absorption. However, limited progress has been made towards developing a comprehensive model capable of predicting *in-vivo* drug absorption based on dissolution. This is due to the existence of several complex factors that contribute to the process of drug dissolution and absorption. These factors can be classified into three groups: physicochemical, biopharmaceutical and physiological. In order to develop a model that can demonstrate good correlation between *in-vitro* drug dissolution and *in-vivo* absorption, these factors have to be properly considered. (Lu et al., 2011, pp. 142-148)

Physicochemical factors

These play an important role in predicting drug absorption *in-vivo*. For orally administered drugs, dissolution is a prerequisite to absorption and clinical efficacy. Several physicochemical properties like solubility, pH, salt forms and particle size influence dissolution. The Noyes-Whitney equation, which describes rate of dissolution as a function of change in drug concentration over time, represents a simple means to describing model dissolution (Dokoumetzidis et al., 2006, pp. 256-261).

$$\frac{dM}{dt} = DS \times \frac{(C_s - C_b)}{h} \qquad [15]$$

where *M* is the amount of drug dissolved, *t* is time, *D* is the diffusion coefficient of the drug in liquid, *S* is the surface area of the drug particle, *h* is the thickness of the diffusion layer, while C_s and C_b represent drug solubility and concentration in the bulk medium at time *t*, respectively.

In addition to solubility, is important to consider other factors like the ionization constant and the salt form of the drug. The pK$_a$ values determine the stability, solubility and absorption of compounds under different environmental pH conditions.

This is highly important since the human body contains inherent pH gradients, which give rise to pH-dependent absorption profiles *in-vivo*.

Generally, the salt form has a higher dissolution rate than the free acid or base form. However, under certain pH conditions in the GI tract, the reverse may also be true. Perhaps a more obvious source of effect on dissolution is particle size. It is commonly recognized that reduction in particle size would increase surface area and enhance the rate of dissolution (Johnson and Swindell, 1996, pp. 1795-1798).

Biopharmaceutical factors

In drug absorption, drug permeability is of crucial importance. The transcellular permeability (P_m) of a compound is defined as:

$$P_m = \frac{K_p D_m}{L_m}$$ [16]

where K_p is the membrane-water partition coefficient, D_m membrane diffusivity and L_m membrane thickness (Li et al., 2005, pp. 1396-1417). In the case of weakly acidic compounds, ionization is suppressed at low pH values, resulting in a relatively high absorption rate. At high pH values, equilibrium is shifted towards the ionized form, resulting in decreased membrane permeability. Opposite conclusions can be deduced for compounds which constitute a weak base. It is also predicted that the pH value at which C_{50max} absorption occurs is approximately equal to the pK$_a$ value for the compound. Some limitations and deviations from the model, due to factors such as micro-environmental pH and solubility issues, have been observed.

The octanol–water partition coefficient (*P* or *log P*) of neutral or unionized species represents another parameter that is used to estimate the ability of compounds to pass through membranes for absorption. By utilizing computer and multiple linear regression, it has proven possible to evaluate structure-activity relationships based on lipophilicity. It has been demonstrated that a bell-shaped distribution exists between absorption and *log P* values, indicating that compounds with *log P* between 0 and 3 generally exhibit high permeability, and those with *log P* values less than−1.5 or greater than 4.5 possess lower membrane permeability.

Although the octanol–water partition coefficient is a good indicator of membrane permeability, it is not a sufficient parameter to predict *in-vivo* absorption. Other measures of membrane permeability have been developed, such as absorption potential (*AP*) that is defined as:

$$AP = \log\left(\frac{PF_{un}}{D_0}\right) \tag{17}$$

where P is the partition coefficient, F_{un} is the fraction of unionized drug at pH 6.5 and D_0 is the dose number equal to the ratio of dose concentration to solubility. Studies indicate that *AP* correlates well with the fraction of drug absorbed and polar surface area (*PSA*), which has demonstrated good correlation with the passive transport of molecules through membranes, marking it out as a potential parameter to include in an *in-vivo* absorption model.

Physiological factors

Physiological conditions can directly affect drug dissolution, as well as the rate and extent of absorption. The effect of pH becomes particularly important in the human body, where a pH gradient is given. These changes in pH profile can alter drug solubility, dissolution, stability and permeability. Moreover, the physiological environment is constantly adjusting and changing according to normal human activity such as food intake. In oral dosage forms, it is fundamental to consider the GI transit time, which affects the extent of drug release in the body. In order to obtain an accurate relationship between *in-vitro* data and *in-vivo* response, the mathematical model must account for such changes.

IVIVC models

There are four levels of IVIVC model indicated as A, B, C and multiple C reported in the literature (Buch et al., 2010, pp. 4427-4436; Amann et al., 2010, pp. 1730-1737; Ochoa et al., 2010, pp. 306-312).

Level A is based on point-to-point correlation between *in-vitro* and *in-vivo* profiles. This is generally considered as the highest level of correlation and facilitates prediction of the entire duration of the course of *in-vivo* concentration from the *in-vitro* dissolution profile. Level B compares a summary parameter from the mean *in-vitro* profile with a summary parameter from the mean *in-vivo* profile. This type of correlation is not considered useful. Level C establishes correlation at a single time point between a dissolution parameter and an *in-vivo* parameter.

An extension of this type of correlation is multiple Level C, which relates several *in-vitro* parameters to *in-vivo* parameters at multiple points in time. Multiple Level C correlations are regarded as more useful than Level C correlations.

Application of IVIVC models

Biopharmaceutical classification system (BCS)

BCS represents a means of categorizing drug compounds based on their solubility and permeability properties. Under the BCS, drug substances can be grouped into four main classes:

- Class 1 highly soluble and highly permeable
- Class 2 highly permeable but of low solubility
- Class 3 highly soluble but rather impermeable
- Class 4 limited in solubility and permeability

It is recognized that successful development and application of an IVIVC requires dissolution to be the rate-limiting step in the process of drug administration and absorption. In Class 1 compounds, no rate-limiting steps for drug absorption are presented, except in immediate release dosage forms. For Class 2 compounds, dissolution is the rate-limiting step in absorption, while, IVIVC is generally regarded as unlikely for Class 3 compounds but may be possible depending on the relative rates of dissolution. Regarding Class 4 compounds, IVIVC is highly unlikely. Classification according to the BCS will enable early determination of whether IVIVC can be developed for a certain drug candidate (Buch et al., 2010, pp. 4427-4436

Biowaivers

A biowaiver is an exemption granted by the FDA that allows *in-vivo* bioavailability and/or bioequivalent studies to be avoided.

A predictive and reliable IVIVC model can serve as a basis for biowaivers. For immediate release dosage forms, the successful development of IVIVC models may be limited to Class 2 and Class 3 compounds classified under the BCS. The situation for extended release (ER) dosage forms is more complex, since the factors considered in the BCS are insufficient to predict the rate and extent of dissolution for ER drugs.

Non-oral dosage form

Currently, regulatory guidance for IVIVC is mainly focused on oral dosage forms. However, similar principles for developing the IVIVC model can be applied to non-oral dosage forms, with certain modifications.

One of the most challenging aspects of developing IVIVC model in non-oral drug delivery systems concerns designing *in-vitro* studies to reflect as much as possible *in-vivo* behaviour. Several publications have attempted to correlate *in-vitro* pharmacokinetics of drugs like paclitaxel and dexamethasone loaded in stents (Finkelstein et al., 2003, pp. 777-784) with limited success. Another difficulty in the design of appropriate *in-vitro* studies is the lack of suitable dissolution media that reflect the *in-vivo* environment. This is particularly the case for implanted drug delivery devices and liposomal products.

Liposomal formulations have traditionally demonstrated poor correlation between *in-vitro* and *in-vivo* performance, possibly due to the physiological presence of a lipid membrane that causes the so-called 'sink' effect (Shabbits et al., 2002, pp. 161-170). So as to circumvent this problem, a novel drug release assay has been developed using excess multilamellar vesicles (Shabbits et al., 2002, pp. 161-170). This method demonstrated improved correlation between *in-vitro* data and *in-vivo* release of doxorubicin, verapamil and ceramide.

1.6 Chitosan and chitosan grafted-PLA as a carrier and coating agent

Chitosan is a non-toxic, semi-crystalline (Rinaudo, 2006, pp. 603-632), biodegradable (Bagheri-Khoulenjani, et al., 2009, pp. 773-778), and biocompatible (Sashiwa and Aiba, 2004, pp. 887-908) linear polysaccharide made of N-acetyl glucosamine and glucosamine units. It is obtained from chitin by deacetylation - under alkaline conditions at a high temperature - of the N-acetyl glucosamine units. When the degree of deacetylation exceeds 40 mol%, chitin is considered chitosan. The degree of deacetylation is highly important as charge density and the primary chitosan properties are strictly connected to it.

One of the major drawbacks of chitosan, in particular for biomedical applications, relates to its low solubility in water; it is only soluble in an acidic solution of pH below 6.5. Such solubility is strictly connected to the degree of deacetylation. The presence of free amino groups protonated at pH < 6.5 (the pK_a of amino groups ranges at 6 - 6.5) increases repulsion between the polymer chains facilitating the solubility.

In order to overcome this drawback, the form at low molecular weight with a degree of polymerization of less than 50 is preferred as it is much more soluble than at high molecular weight, even at physiological pH. Another way to improve the properties of chitosan, not only in terms of solubility, is via chemical modification pertaining to –OH and –NH_2 groups.

Chitosan derivatives

Chitosan derivatives are mostly obtained via chemical modification by introducing small functional groups such as alkyl or carboxymethyl to improve solubility in neutral and alkaline media without altering cationic properties (Alves and Mano, 2008, pp. 401-414). Introducing molecules with carboxylic groups gives rise to chitosan polyampholytic properties (Lu et al., 2007, pp. 3807-3818). Grafting represents one of the most common techniques for chemical modification, permitting formation of derivatives by covalent binding of low or high molecular weight molecules to the chitosan backbone (Alves and Mano, 2008, pp. 401-414). This can be conducted in hydroxyl groups on C_3 and C_6 on acetylated or deacetylated units, or carried out on the free amino groups.

Grafting improves water solubility, as well as antibacterial and antioxidant properties (Xie et al., 2002, pp. 35-40), but also enhances chelating, complexations, bacteriostatic and adsorption properties (Thanou et al., 2001, pp. 117-126), although properties like mucoadesivity, biocompatibility and biodegradability remain generally conserved.

Poly (lactic acid) (PLA) is a linear aliphatic thermoplastic polyester. PLA has been utilized in biomedical applications due to its biodegradability, biocompatibility and good mechanical properties. PLA can be linked to the CS backbone by a coupling reaction, in the presence of EDC and NHS, between the chitosan amino group and PLA carboxylic groups (Fig. 16).

EDC (1-Ethyl-3-(3-dimethylaminopropyl)-carbodiimide) is a zero-length crosslinking agent used to couple carboxyl or phosphate groups to primary amines. One of the main advantages of using EDC, instead of another carbodiimide, is its water solubility, which facilitates carrying out the reaction without the use of solvents. Moreover, reagents and by-products can be easily removed. The coupling reaction has to be conducted rapidly, as the reactive ester which is formed is unstable in aqueous solutions. In order to increase the stability of this active ester, N-hydroxysuccinimide (NHS) or N-hydroxysulfosuccinimide (S-NHS) can be used. The addition of S-NHS stabilizes the amine-reactive intermediate by converting it to an amine-reactive S-NHS ester.

The success of the reaction is strictly bound to two parameters - the pH of the media, which influences the hydrolysis of the intermediate products, and the EDC/NHS ratio. Excess reagent and crosslinking by-products are easily removed by washing with water.
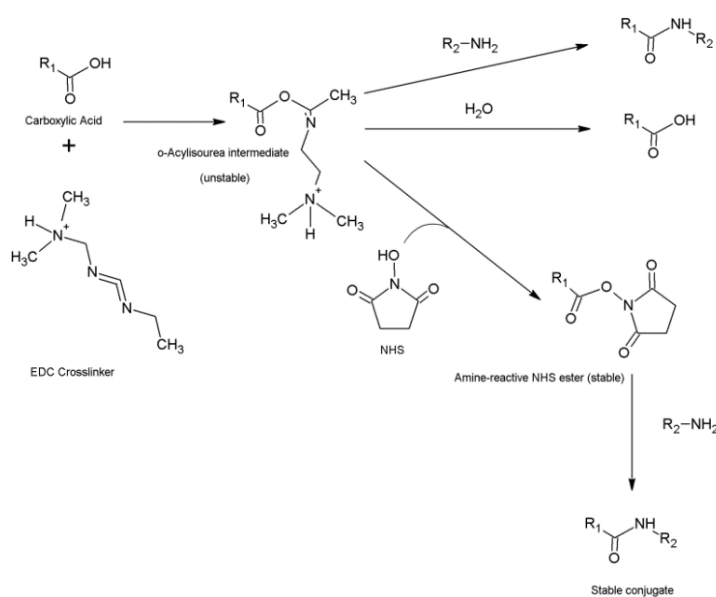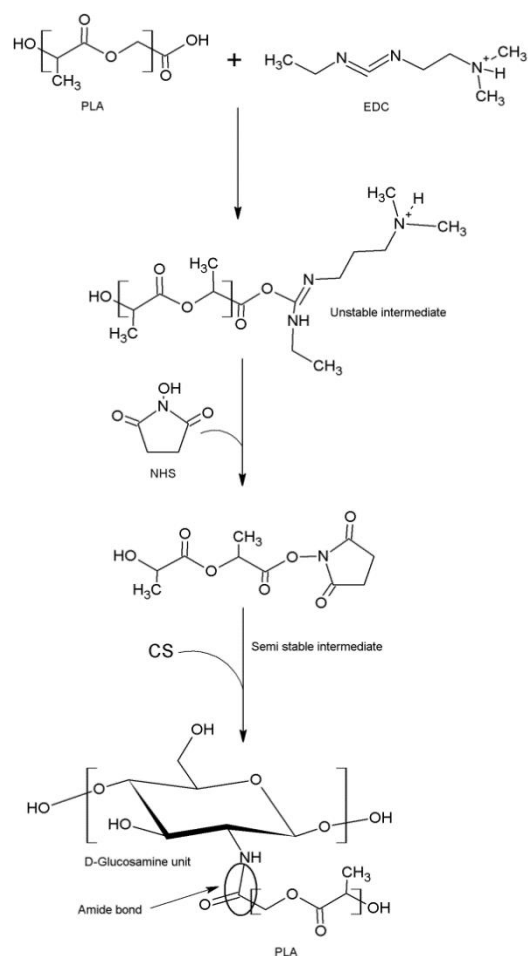

Fig.15 General reaction scheme for EDC and NHS

Fig.16 Reaction scheme for grafting PLA to the CS backbone
(Di Martino et al., 2015, pp. 912-921)

Chitosan as coating agent in drug delivery applications

In recent years, considerable attention has been paid to inorganic nanoparticles, in particular to iron oxide nanoparticles due to their unique magnetic properties such as superparamagnetic, low Curie temperature and high magnetic susceptibility, but also non-toxicity, biocompatibility and low cost of production, which make them interesting for biomedical applications (Wu et al., 2008). Numerous methods exist for preparing Fe_3O_4 nanoparticles, such as mechanical grinding, laser ablation, chemical co-precipitation, hydrolyzation and microemulsions (Chomoucka et al., 2010, pp. 144-149). Of these, chemical co-precipitation is the most common due to its simplicity, productivity and low cost, and it is possible to obtain fine, high-purity, stoichiometric particles made of a single and multicomponent.

Furthermore, by controlling certain process conditions, such as solution pH, reaction temperature, stirring rate, solute concentration and surfactant concentration, particles possessing the desired dimension and shape can be obtained (Zhao et al., 2009, pp. 68-78).

One of the major drawbacks of iron oxide nanoparticles is their tendency to aggregate when in colloidal suspension. So as to overcome this, the surface of the iron oxide nanoparticle is modified through creating a few atomic layers of organic (polymer) or inorganic (metal or oxide) coating, suitable for further functionalization with various bioactive molecules (Gupta and Gupta, 2005, pp. 3995-4021). A great many varieties of polymer with hydroxyl, carboxylate, carboxyl, styrene or vinyl alcohol groups have been used in the production of magnetic nanoparticles.

Chitosan represents an optimal choice as a coating polymer for iron nanoparticles intended for biomedical application as a consequence of its positive properties. In terms of the surface properties of iron oxide nanoparticles, chitosan can be adsorbed or linked chemically. In the case of adsorption, only electrostatic forces are involved and pH and ionic strength of the media constitute the main parameters for consideration. The presence of charged chitosan on the surface of the nanoparticles (NPs) increases the repulsion between the NPs, avoiding the formation of aggregates. Besides the improvement in stability, such a coating increases the dimension of the nanoparticles, which can shift from few nanometres to more than 200, depending on the M_w of chitosan and the conditions of preparation. However, at an ideal ratio of chitosan to iron weight, only a slight influence on the magnetic properties of iron oxide particles occurred.

Positive results have been obtained in the encapsulation of various bioactive compounds; in particular, anticancer drugs like doxorubicin, in a system based on iron oxides coated with chitosan, demonstrated greater efficiency than uncoated iron oxide nanoparticles (Javid et al., 2013, pp. 296-306).

AIMS OF THE WORK

In accordance with current trends in controlled drug delivery of bioactive molecules mediated by polymeric based nanoparticles, the aims of this PhD work can be summarized in the following major points:

- The development of a non-toxic and biocompatible set of amphiphilic polymers based on chitosan grafted by different PLA structures.

- Simultaneous encapsulation of environmentally sensible bioactive compounds.

- Modification of release profiles of loaded molecules with an emphasis on reducing the initial burst effect.

- Investigation of the role of PLA side chain structure on the encapsulation and release process.

- Development of analytical techniques relevant to the field of study in the laboratories of the Centre of Polymer Systems.

The results obtained herein shall be presented in scientific journals and at international conferences.

2. EXPERIMENTAL PART

2.1 Samples preparation and characterization methods

Determination of chitosan molecular weight

The molecular weight of the purchased chitosan was obtained by GPC analysis. The Waters chromatographic system, equipped with an aqueous gel column - the SHODEX OH pack SB-806 M HQ (8 mm × 300 mm), and the Shodex OHpak SB-G guard column, was used to record the molecular weight of chitosan. In order to construct a universal calibration curve, polysaccharide standards (Pullulan Polysaccharide, PL2090–0100 VARIAN) ranging from 180 to 708,000 g·mol were used. The sample of 1 mg/mL chitosan in mobile phase solvent was dissolved overnight and filtered through a 0.45 μm filter prior to analysis. Injection volume equalled to 50 μL, and analysis was performed using 0.2 M CH_3COOH/0.1 M CH_3COONa in mobile phase, while the flow rate measured 0.8 mL at temperature 30 °C. The data were processed using Empower software

Synthesis and characterization of low molecular weight PLA

Low molecular weight polylactic acid (PLA) was prepared via a polycondensation reaction using methanesulfonic acid (MSA) as the initiator, as described in a previous work (Kucharczyk et al. 2011, p. 1275-1285)). MSA is non-toxic and suitable for obtaining low molecular weight PLA. In brief, L-lactic acid was added into a double-necked flask (250 mL) equipped with a Teflon stirrer. The flask was placed in an oil bath heated under stirring and connected to distillation apparatus under reduced pressure. The dehydration step followed at 160 °C, at a reduced pressure of 15 kPa for 4 h. Afterwards, the reactor was disconnected from the vacuum pump and the initiator was added under stirring. The flask with dehydrated L-lactic acid and the initiator was reconnected to the vacuum source and the reaction continued for 24 h at 160 °C. The resulting product was cooled down at room temperature and dissolved in acetone. The polymer solution was precipitated into a mixture of chilled methanol/distilled water 1:1 (v/v). The product was filtered off, washed with methanol and dried at 45 °C for 48 h. This dissolving-precipitation procedure was repeated three times. Molecular weight of the resultant product was determined by gel permeation chromatography (Agilent PL-GPC220). PLA used in this work had following characteristics: $M_n = 8000$ g/mol, $M_w = 13800$ g/mol, intrinsic viscosity, $[\eta] = 0.2$ dl/g

Synthesis and characterization of carboxy modified PLA (PLACA)

Low molecular weight polylactide of up to 10^3 g/mol was synthesized by following a procedure previously described (Kucharczyk et al. 2011, p. 1275-1285). In brief, different proportions of L-lactic acid and citric acid (0, 2, 5 wt.% regarding lactic acid) were added into a double-necked flask (250 mL) equipped with a Teflon stirrer. The total mass of the mixture at the beginning of the reaction was 50 g (water not included). The flask was placed in an oil bath heated by a magnetic stirrer with heating, and connected to apparatus for distillation under reduced pressure. The dehydration step followed, at 160 °C and the reduced pressure of 15 kPa for 4 h. After that the reactor was disconnected from the vacuum pump and the initiator – methanesulfonic acid – was added under stirring. The flask with the initiator of dehydrated lactic acid–citric acid was reconnected to the vacuum source and reaction continued for 24 h at 160 °C. The resulting product was cooled down at room temperature and dissolved in acetone. The polymer solution was precipitated into a mixture of chilled methanol and distilled water at the ratio 1:1 (v/v). The product was filtrated, washed with methanol and dried at 45 °C for 48 h. This dissolving and precipitation procedure was repeated three times. The pH of the filtrate after polymer separation was checked to ensure that un-reacted citric acid was not present in the polymer.

In order to determine the concentration of terminal carboxyl groups, the acidic number (AN), which represents the amount of KOH (in mg) necessary to neutralize 1 g of substance, was calculated by titration in methanol–dichloromethane (1:1 v/v) with 0.01 M KOH ethanol solution, and bromothyol blue was used as an indicator. The presence of carboxylic groups was proven by UV–vis spectroscopy, carried out by dissolving samples in chloroform (1 mg/mL) in the range 200–400 nm on a Heλios Gamma UV–vis spectrometer (room temperature, 0.5 nm resolution in a quartz cuvette, path length 10 mm).

Synthesis of CS-g-PLA and CS-g-PLACA copolymer and characterization

CS-g-PLA and CS-g-PLACA were synthesized according to a procedure described previously (Li et al., 2012, p. 221-227). Briefly, 300 mg of chitosan was soaked in 30 mL of *N,N*-dimethyl formamide (DMF) – for 24 h, and then dissolved by adding 1% (w/v) acetic acid solution. 300 mg of PLA or PLACA, EDC and NHS (molar ratio PLA or PLACA: EDC: NHS = 1:1.5:3) was dissolved in 50 mL of chloroform; the solution was added to CS-DMF solution under vigorous stirring for 48 h at room temperature. The reaction was stopped by adjusting the solution to neutrality with 0.5 M NaOH solution. The final product was precipitated by adding excess ethanol, filtered and freeze-dried.

Fourier transform infrared spectroscopy-attenuated total reflectance (ATR-FTIR) analysis (Nicolet iS5 FTIR Spectrometer equipped with iD5 ATR accessory, Ge crystal, resolution 4 cm^{-1}, 64 scans) was performed on the freeze-dried samples to confirm that the coupling reaction between CS and PLA and PLACA occurred. ^{1}H NMR spectra were recorded on a Varian Unity Inova 400 MHz, using deuterium oxide (Aldrich) with the addition of 5% of deuterium hydrochloric acid and 1 μL of $(CH_3)_3COD$ for signal referencing (δ 1.23 ppm). Spectra were evaluated using 1st order spectral analysis.

Determination of free amino groups in CS and CS derivatives

The percentage of deacetylation degree (*N*) of CS and CS modified with PLA and PLACA was obtained by conductometric titration, as reported (De Alvarenga et al., 2010, p. 1155-1160). In brief, 200 mg of polymer (CS, CS-g-PLA, CS-g-PLACA2%, CS-g-PLACA5%) was dissolved in HCl 0.050 M solution and titrated by TitraLine Easy SI Analytics, Germany, using NaOH 0.160 M (0.6 mL of NaOH was added gradually). *N* (%) was calculated as follows:

$$N(\%) = \frac{C \times (V_2 - V_1) \times M}{m} \qquad [18]$$

where *C* is the concentration of NaOH solution (mol/L); V_1 and V_2 represent the volumes (mL) of NaOH solution required to reach the 1st and 2nd equivalence point, respectively; *M* represents the molar mass of the D-glucosamine unit of CS backbone; and *m* is the amount of polymer (mg) (De Alvarenga et al., 2010, p. 1155-1160).

The amount of free amino groups per polymer chain (*n*NH$_2$) was determined from the *N* value (Equation 20), considering the M_w of the CS equals 100×10^3 g/mol as indicated by the viscosity parameters obtained from the supplier. Knowing M_w of the D-glucosamine unit ($M_w = 179$ g/mol) the value of *n*NH$_2$ per single chain can be approximately calculated.

Nanoparticles preparation and characterization

Nanoparticles were prepared by Polyelectrolyte complexation method (PEC) using dextran sulphate as polyanion. CS-PLA derivatives were dissolved in aqueous solution containing 1% of acetic acid and subsequently filtered (pore size 0.45 μm) to remove any residue and dust. Different CS-PLA to polyanion weight ratio were used in the research work ranging from 0.2 to 5 in order to evaluate the influence of that ration on the nanoparticles properties like diameter, z-potential, stability, encapsulation and release capabilities. Aqueous solution containing determined amount of DS was added dropwise to CS-PLA solution under vigorous magnetic stirring. The obtained mixture was left under stirring for 30 minutes at 40° C. Afterwards, part of the solution was analysed by DLS to determine the nanoparticles diameter and z-potential while the rest centrifuged at 14000 rpm for 20 minutes and the pellet freeze and dried.

The effect of pH, DS concentration and temperature on the diameter of the nanoparticles (d_p, nm) and their ζ-potential (mV) and electrophoretic mobility (μ_e, μm cm/V s) were analysed through DLS (Nano ZS, Malvern Instrument) at 173° backscatter. Before measurement, the suspensions were sonicated in an ultrasound bath (50 MHz) for 20 min. Analyses were performed in triplicate on suspensions at different pH values (range from 2 to 9). The pH value was increased by adding NaOH solution of 0.1 M.

The μ_e values were obtained via the Smoluchowski equation (Equation 19), as it is suitable for nanoparticles of any shape dispersed in aqueous solution at any concentration. The Smoluchowski equation:

$$\mu_e = \frac{\epsilon_r \epsilon_0 \zeta}{\eta} \qquad\qquad [19]$$

where ϵ_r is the dielectric constant of the media, ϵ_0 is the permittivity of free space ($C^2\ N^{-1}\ m^{-2}$), η is the dynamic viscosity of the dispersion media (Pa s) and ζ is the zeta potential (mV).

Microscopic analysis

Microscopic analysis is widely used to investigate the morphology of the nanoparticles in dried form or in solution. The nanoparticles morphology and shape represent important parameter of nanoparticles for drug delivery applications as both of them influence the release rate of the loaded molecules and the cell-nanoparticles interactions.

TEM analysis (Tecnai G2 Spirit FEI) was preferred to SEM in the reported works as chitosan is highly sensible to freeze and dried treatments. For that reason, TEM analysis of nanoparticles in solutions were carried out.

Stability studies and temperature behaviour

Stability studies were carried out by dissolving the prepared formulations (1 mg/mL) in various simulated body fluids. Variations in the diameter and z-potential of the nanoparticles over time, at room temperature and 37 °C storage, were investigated by dynamic light scattering, DLS, (Nano ZS, from Malvern Instruments).

Temperature behaviour, in the range 0–60 °C, was analysed in order to understand how the prepared nanoparticles reacted when submitted to gradual warming. Measurements were taken on 2 mL of nanoparticle suspension (concentration 1 mg/mL) on a Nano ZS, from Malvern Instruments, UK, and temperature was increased automatically by 10 °C and stabilized for 2 minutes prior to measurement.

Water uptake studies

The swelling behaviour of polymeric nanoparticles is affected by the internal structure of the polymer network and the nature of the media (Bajpai et al., 2012,p. 9-17). Water intake capacity was analysed by gravimetric procedure in media with different pH levels (ranging from 2 to 11) and ionic strength (PBS-phosphate buffer solution; SGF-simulated gastric fluid; SIF-simulated intestinal fluid and PS-physiological solution) and reported as the swelling index (SI). SI determination was adhered to according to the procedure reported in a previous work (Bajpai et al., 2003, p. 347-357). Briefly, 0.2 g of nanoparticles were allowed to swell in a defined volume (20 mL) of media for 24 h.

Afterwards, the weight of the swollen nanoparticles was monitored continuously for up to 15 min, after which no gain was recorded once it was sure that equilibrium had been reached. SI was calculated as follows:

$$SI\ (\%) = \frac{W_s - W_d}{W_d} \qquad [20]$$

where W_s is the weight (mg) of the nanoparticles in the swelling state while W_d the weight (mg) in lyophilized form (powder).

All the simulated body fluids were prepared according to European Pharmacopeia standards.

The ionic strength of the media was calculated according to the followed Equation

$$I = 0.5\ \sum_1^j c_j z_j^2 \qquad [21]$$

where I is the ionic strength, J is the number of species in solution, c_J is the molar concentration of ion I and z_J is the charge of ion J.

Encapsulation efficiency and Loading capacity

Encapsulation efficiency (EE) and the loading capacity (LC) of nanoparticles was determined by UV−vis spectrophotometry (Perkins, Cary UV 300) at different wavelength according with the bioactive molecule; (480 nm for DOX, 325 for TMZ, 286 for 5FU and 280 for BSA. The concentration of the referred molecule was determined from the calibration curve of the free compound in solution. Calibration curve of the investigated compounds are:

A = 0.125c + 0.122; R^2 > 0.98 (TMZ)

A = 0.89c -0.83; R^2 > 0.98 (DOX)

A = 0.117c + 0.133; R^2 >0.98 (5FU)

A = 0.8 × $10^{-3}c$ + 0.0402, R^2 > 0.99 (BSA)

where *A* represents the absorbance and *c* the concentration of the loaded compound.

EE and *LC* values were obtained by the following equations:

$$EE\ (\%) = \frac{T_P - F_P}{T_P} \times 100 \qquad [22]$$

where T_P represents the total amount of protein loaded (mg) and F_P the amount of free protein detected in the supernatant (mg)

$$LC = \frac{T_P}{T_P + T_C} \qquad [23]$$

where T_P is the total amount of protein loaded (mg) and T_c is the mass of polymer (mg).

TMZ and 5FU loading (Referred to section 3.1)

TMZ (1 mg/mL; V = 1 mL) was dissolved in water and added to 1 mg/ml of aqueous solution containing ALG and PGA, separately. CS solution, 1 mg/mL, was prepared in CH₃COOH (1% v/v). The established volumes of mixtures containing ALG or PGA and TMZ were added dropwise to CS solution under vigorous stirring. In the case of double-loading, TMZ (0.5 mg/mL) and 5-FU (0.5 mg/mL) were dissolved in aqueous solution, separately. Both solutions were mixed and added to solution containing ALG or PGA.
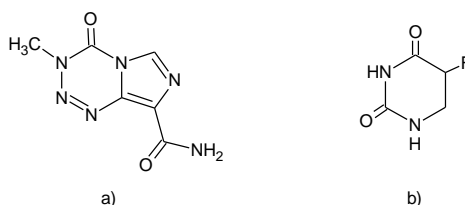

a)   b)

Fig. 17 Molecular structure of a) TMZ and b) 5FU

Doxorubicin and Temozolomide loading (Referred to Section 3.2)

DOX (1 mg/mL; $V = 1$ mL) was dissolved under stirring in CH₃COOH aqueous solution (pH 3.5). An aqueous solution of dextran sulphate was prepared (1 mg/mL; $V = 3$ mL) and added drop-wise to the solution containing the drug. The copolymer was dissolved in CH₃COOH aq. pH 3.5 to obtain a solution of 1 mg/mL ($V = 4$ mL). The mixture containing dextran sulphate and DOX ($V = 4$ mL) was added drop-wise to the copolymer solution under vigorous stirring.

Once a colloidal suspension had been obtained, the samples were centrifuged at $10,000 \times g$ (Hettich Zentrifuge – Universal 320) for 30 min. and the pellet freeze-dried. In the case of double-loading, DOX (1 mg/mL; $V = 1$ mL) was dissolved in CH_3COOH aqueous solution (pH 3.5), while TMZ (1 mg/mL; $V = 1$ mL) was dissolved in ethanol, and kept under mild stirring conditions for 30 min. till complete solubilisation had occurred. Both solutions were subsequently mixed. An aqueous solution of dextran sulphate was prepared (1 mg/mL; $V = 3$ mL) and added drop-wise under vigorous stirring to the mixture containing both drugs. The copolymer was dissolved in CH_3COOH aqueous solution (pH 3.5) to obtain a solution of 1 mg/mL ($V = 5$ mL). The mixture containing dextran sulphate, TMZ and DOX ($V = 5$ mL) was added drop-wise to the CS derived solution under vigorous stirring and slight heating. Once a colloidal suspension had been obtained, the samples were centrifuged at $10,000 \times g$ for 30 min. and the pellet freeze-dried (Cool Safe™ – Scanvan)

BSA loading (Referred to Section 3.3)

The nanoparticles loaded with BSA were formed upon incorporation of the DS solution containing BSA at the concentration of 0.5 mg/mL in CS-PLA derivatives solutions. The factors researched included the influence exerted on encapsulation efficiency by the kind of polymer used (CS or CS-g-PLA) and polymer concentration. DS and BSA concentrations were kept constant (1 mg/mL for DS and 0.5 mg/mL for BSA).

Drugs Stability studies (Referred to section 3.1)

In order to prove that no alteration to the structure of 5-FU and, in particular, TMZ occurred during release, LC–MS analysis (6530 Accurate-Mass Q-TOF LC/MS Agilent Technologies, ion mode positive, ionization ESI, collision energy 10 eV) was carried out on the drugs following release from the formulation after 24 h in preparation and physiological media. As a control, TMZ and 5-FU (10 µg/mL) were dissolved as a free drug in the tested media. Chromatographic separation was achieved using a column (ZORBAX Extended-C18, 2.1×50 mm, 1.8-Micron, 600 Bar, Agilent) as well as mobile phase 60% water (containing 0.1% of formic acid) and 40% methanol, at flow rate of 0.3 mL/min. The sample compartment was kept at 37 °C, while the column at 30 °C ± 1 °C and wavelength were monitored at 325 nm for TMZ and 286 nm for 5-FU. Injection volume was 2 µL.

In-vitro drug release studies

The release kinetic of the loaded molecules, separately or simultaneously, from the different CS-PLA nanoparticles was investigated in different simulated body fluids (simulated gastric and intestinal fluid), preparation media and phosphate buffer. In brief, 50 mg of each sample was suspended in 50 mL of the media and stored at 37 °C under oscillatory shake (GFL 3033 Incubator, Germany). At predetermined time intervals, an aliquot (1-3 mL) was withdrawn and the concentration, of the considered compound, released, at certain time was monitored by a UV–vis spectrophotometer at determined wavelength. The dissolution medium was replaced with fresh buffer to maintain the total volume

The amount of drug released (DR) was determined by the following equation:

$$DR\ (\%) = \frac{D_t}{D_0} \times 100 \tag{24}$$

where D_t (mg) represents the amount of drug released at the time t, and D_0 (mg) the amount of drug loaded. All studies were conducted in triplicate.

Each experiment was performed in triplicate. The calculated concentration (C) data were evaluated by applying a first-order equation (Equation 25) and regression processing by the least squares method, using the Solver sub-program of Microsoft® Office Excel 2003.

$$C = C_{max} \times (1 - e^{-k(t-t_{lag})}) \tag{25}$$

where C is the cumulative concentration (mg drug/mg polymer) of drug released at given time t (h), C_{max} represents the limit value of concentration that can be released from the tested system under given conditions (mg drug/mg polymer), t_{lag} represents the time

where no release is observed, and k the kinetic constant (h^{-1}), which represents the intensity of the release from the particles at the initial time (t). *In-vitro* release studies were focused to find a certain correlation among the nanoparticles properties like dimension, the effect of PLA side chains and interactions with the loaded compound and the external environment.

Statistical analysis

One-way ANOVA analysis was performed on all obtained date using the GraphPad Prism version 6.00, GraphPad Software, La Jolla California, USA, with consideration of $p < 0.05$ as statistically representative

3. RESULTS AND DISCUSSIONS

The results related to the presented topics are illustrated in the follow three sections. Each section consist of a brief introduction, results and discussion and conclusions. All presented results have been published in the reported journal.

The sections are entitled as follow:

- Polysaccharide-based nanocomplexes for co-encapsulation and controlled release of 5-Fluorouracil and Temozolomide (data published in European Journal of Pharmaceutices- In Press)

- Amphiphilic chitosan-grafted-functionalized polylactic acid based nanoparticles as a delivery system for doxorubicin and temozolomide co-therapy (data published in International Journal of Pharmaceutics, 474, 1–2, 20 2014, 134–145)

- Chitosan grafted low molecular weight polylactic acid for protein encapsulation and burst effect reduction (data published in International Journal of Pharmaceutics, 496, 2, 2015, 912-921

3.1 Polysaccharide-based nanocomplexes for co-encapsulation and controlled release of 5-Fluorouracil and Temozolomide

INTRODUCTION

Polysaccharide and derivatives has been extensively investigated for biomedical application, especially in drug delivery (Jayakumar et al., 2010, p. 142-150). Several bioactive compounds have been entrapped, adsorbed or chemically linked to PECs spacing from anticancer drugs like doxorubicin (Chen et al., 2011, p. 2586-2592; Di Martino and Sedlarik, 2014, p. 134-145), paclitaxel (Lee et al., 2008, p. 6442-6449), 5-Fluorouracile (Nagarwal et al., 2011, p. 272-278) to antibiotics and antimicrobic (De Campos et al., 2001, p. 159-168 ; Katiyar et al., 2014, p. 117-124); psycho active drugs (Varshosaz et al., 2015, p. 65-73); peptides and proteins; (Di Martino et al., 2015, p. 912-921 ; Dionisio et al., 2013, p. 102-113) nucleic acids (Bordi et al., 2013, p. 184-190; , Laroui et al., 2014, p. 41-53 and Li et al., 2014, p. 160) and the behaviour of the systems have been deeply investigated, as reported in literature (Wang et al., 2007, p. 336-343; Hu et al., 2011, p. 1128-1133; Hu et al.2010, p. 323-334) indicating the advantages of these systems compared to other drug delivery systems. In the last decade, in the clinical area a noticeable interest in multi-drug therapy is growing due to the positive results, in terms of therapeutic response, obtained in the treatment of various pathologies, in particular in anticancer therapies (Wang et al., 2007, p. 336-343).

A multidrug treatment can suppress the phenomena known as chemo-resistance, which is the main responsible of different failure in cancer therapy (Gottesman, 2002, p. 615-627).However, due to different pharmacokinetics, bio-distribution and membrane transport properties is difficult to make a combination therapy schedule, in particular in terms of dosage. The challenge is to combine nanotechnology with chemotherapy to obtain new nano-delivery systems or improve well known (Greco and Vicent, 2009, p. 1203-1213). Nowadays, a limited number of pharmaceutical formulations containing two or more drugs are approaching the clinical phase but no one of them belongs to nanoparticles or PECs based only on polysaccharides.

With these assumptions, the aim was to develop nanocarriers based on well-known polysaccharides; chitosan (CS), alginic acid (ALG) and polygalacturonic acid (PGA), able to carry simultaneously two widely used anticancer drugs, Temozolomide 9TMZ) and 5Fluorouracil (5FU) and release in controlled way and at different rate according to the external environment. Even if partial, this study represents a way how well known and simple systems could be used as support of new therapeutic protocols

Results and discussions

Nanocomplexes characterization

The molecular weight of chitosan used in the present work was obtained by GPC analysis. The weight average molecular weight $M_w = 290$ kg·mol^{-1}, number average molecular weight $M_n = 31$ kg·mol^{-1}, and molecular weight distribution $Đ(M_w/M_n) = 9.4$ that were obtained appear relative to the mass of pullulan standards and their hydrodynamic volume (elution volume). The hydrodynamic volume of chitosan molecules can be strongly affected by the ionic strength of the solvent (mobile phase), which can partially influence the resulting molecular weights (Kasaai et al., 2000, p. 2591-2598).

The ability of CS to form complexes with negatively charged molecules relies on the formation of inter- and intra-molecular physical cross linkages and electrostatic interactions mediated by polyanions. ALG and PGA carry negative charges at the preparation pH (pH 5.5), while CS contains amino groups that can undergo protonation. During the complexes formation process, the COO$^-$ are electrostatically attracted to the CS amino groups, thereby producing CS-ALG and CS-PGA PECs (Aydın and Pulat, 2012, p.42).

Unloaded complexes present diameters which fall in the range of 120–150 nm, and 100–130 nm for CS-ALG and CS-PGA, respectively. The lowest value was obtained at a polycation-polyanion weight ratio of 1 for all formulations. The loading process tends to increase the size, in particular when both drugs are simultaneously allocated. All formulations, whether loaded or unloaded, show diameters in the narrow range of 100–200 nm which is acceptable for drug delivery applications.

For drug-free complexes, the results are fully comparable with published data, whereas loaded systems show disagreement. In some cases an increase in dimension after loading is demonstrated, especially in uncharged polymers (Goycoolea et al., 2009, p. 1736-1743), while for others a decrease is described. In this instance the increase in size is probably connected with the hydrogen bonds and electrostatic and physical interactions between the polysaccharides, which are altered by the presence of the drugs.
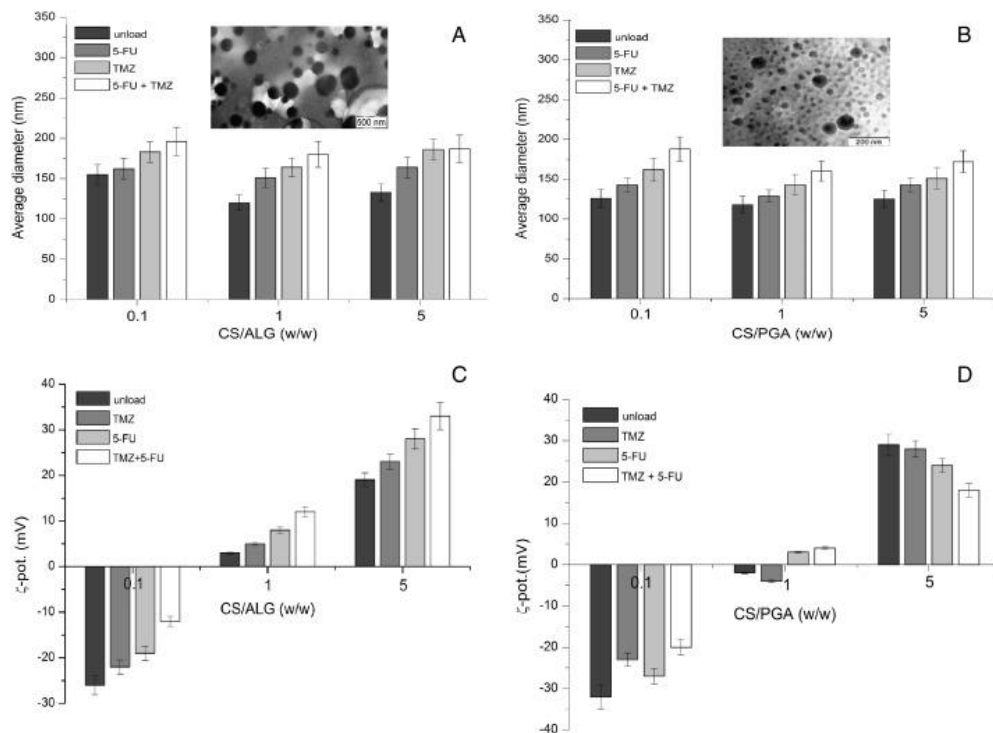
Fig. 18 TEM images and average diameter of nanoparticles A) CS-ALG and B) CS-PGA and z-potential C) CS-ALG and D) CS-PGA in preparation media (pH 5.5) at room temperature.

An important parameter is the ζ-potential, which gives information on the surface charge and colloidal stability of the system. The influence of the weight ratio of the polyelectrolytes and the presence of drug(s) on the ζ-potential values is reported in Fig.18.

Increasing the amount of CS instigates a shift in the ζ-potential of all formulations from negative to positive, with the isoelectric point (*pI*) being located in the range of 0.5–0.8 (w/w), depending on the system.

The influence of drug and weight ratio on ζ-potential is different in CS-ALG and CS-PGA. CS-ALG complexes show an increase in ζ-potential after loading the drug. The trend is linear, with a higher increment appearing when TMZ and 5-FU are present simultaneously in the system.

Different behaviour is shown for CS-PGA, where at w/w 1 the ζ-potential fluctuates at around 0 mV, and w/w 5 shows a decrease by up to 30% compared to the drug-free system. A rise in ζ-potential is expected when the amount of CS is raised, due to the higher number of positive charges in the system.

The hydrogen bonds and electrostatic and physical interactions between the drugs and polymers influence the structure, and subsequently the surface charge of the system.

TEM analysis (Fig.18 A, B) confirms the spherical shape of the complexes in solution, and the values for sizes are fully comparable with DLS. TEM investigation was carried out on the sample in solution to avoid freeze-drying procedures, as it could influence PEC morphology, in particular when a cryo-protectant or lyo-protectant is not used

Amount of drug entrapped in CS based nanocomplexes

5-FU and TMZ are encapsulated during the preparation process. Formation of the complexes depends on the concentrations of the free amino groups, which strengthen electrostatic interactions between the polyelectrolytes and the drug. Fig.19 reports the effect of the polysaccharide couple and its weight ratio (w/w) on single (A, B) and multiple (C, D) *EE*.
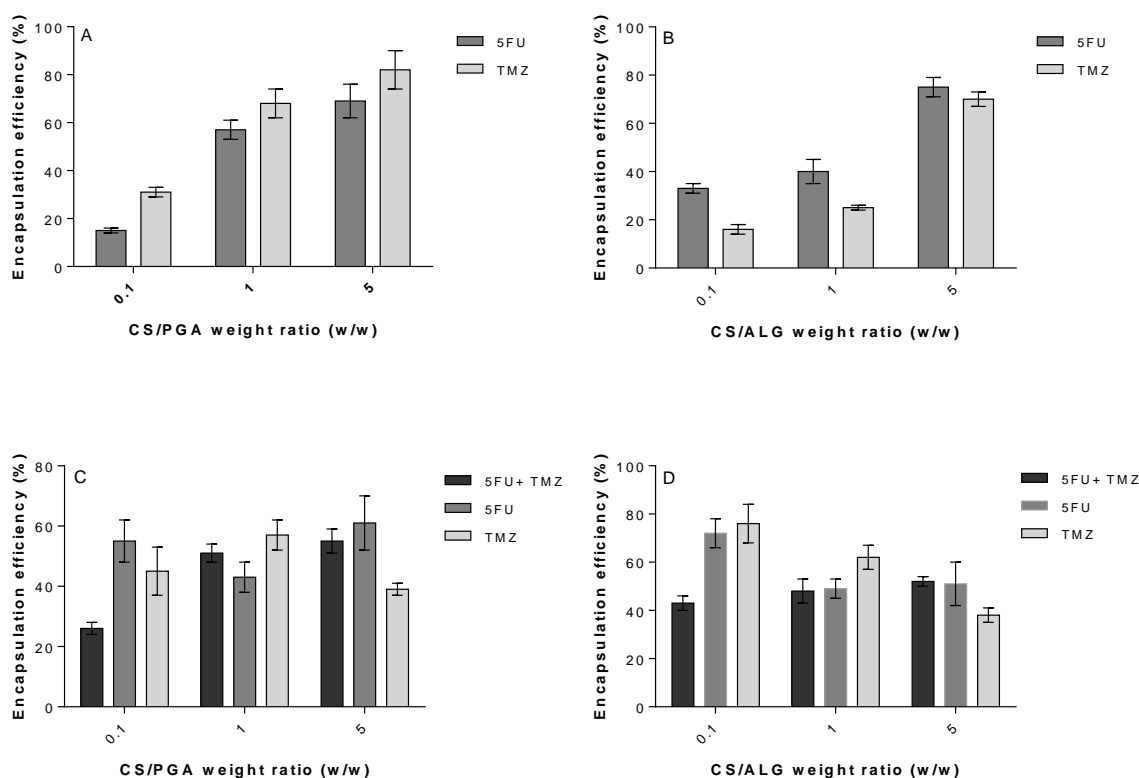

Fig. 19 Relationship between encapsulation efficiency and polycation/polyanion weight ratio. A, B) single loading and C, D) multiple loading

Increasing the CS concentration led to more effective encapsulation of 5-FU and TMZ. Moreover, 5-FU seems more affine for CS-ALG, while TMZ is for CS-PGA PECs.

The values shown in Fig.19 are comparable with prior reported data, where *EE* can reach values of up to 90%; in particular for TMZ when polymethacrylate-based nanoparticles are utilised (Howard et al., 2012, p. 1270-1279).

Fig. 19 C,D displays the co-encapsulation efficiency of TMZ and 5-FU in preparation media. Even if values are lower compared to single loading, the overall amount (5-FU + TMZ) entrapped tends to increase concurrent with a greater presence of CS, confirming the important role CS plays in the loading process. Except at w/w 5, where an excess of 5-FU is presented, in all formulations the amount of drug is well balanced, indicating that not particular completion or interference occurs between the given drugs during the loading process. Even though few studies have been published on multi-drug encapsulation in comparable systems, the data presented are in agreement and analogous with them, as reported in a previous work (Di Martino and Sedlarik, 2014, p. 134-145).

Release kinetic

Variation in pH in accordance with body compartments may allow a specific drug to be selectively delivered at a target site. Physical properties, such as the swelling/deswelling of stimuli responsive carriers as polysaccharides, vary according to the given environmental conditions, influencing the release of the drug to the designed site.

In order to evaluate the influence of pH on the release rate of 5-FU and TMZ, the loaded PECs were incubated in different release media (SGF, PM, PS and PB) and assessed by UV-Vis spectrophotometry. The percentage of swelling for the systems in all the studied media is given after 10 min of contact. The results are shown in Fig.20
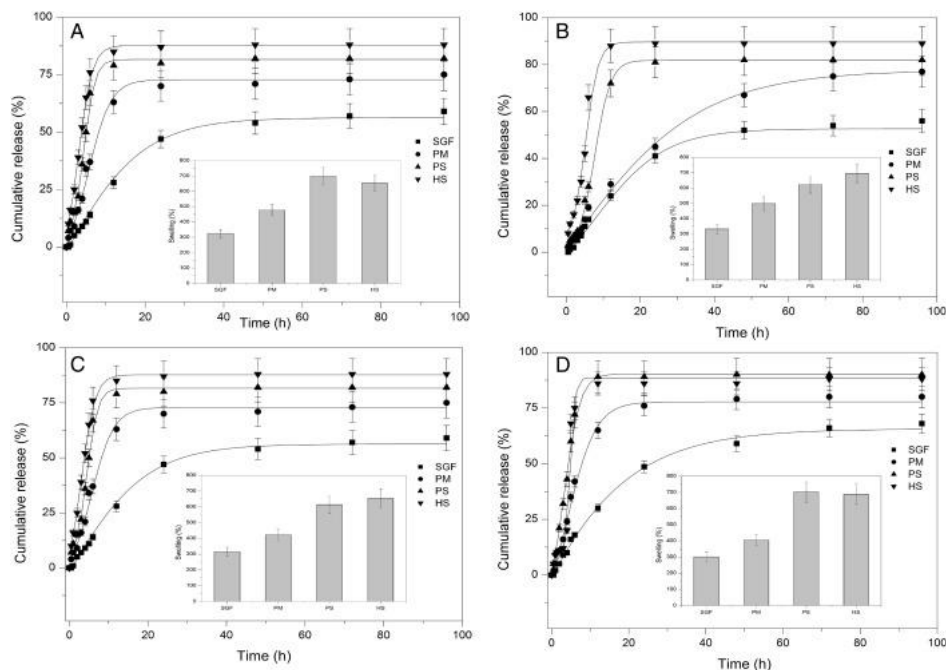
Fig. 20 Cumulative release of A) TMZ and B) 5-FU from CS-ALG, and C) TMZ and D) 5-FU from CS-PGA at 37 °C in different media. The inner pane indicates the percentage of swelling after soaking for 10 min in the relevant medium.

As can be seen from the charts reported in Fig. 20, the release rate tends to increase when pH moves from acidic to alkaline, reaching the highest value in HS and PS, with > 70% of the loaded drug released in < 12h in all formulations. Comparing the release data with the percentage of swelling a clear relationship is revealed. Increasing pH led to electrostatic interactions becoming weaker, thereby promoting the intake of the medium. The more swell that the system demonstrates, the faster the diffusion of the drug towards the surface and the external medium, with a subsequent increase in release rate. In acidic media, especially SGF, CS is fully protonated and stronger interactions occur with ALG or PGA, producing a compact structure which hinders the penetration of the medium and diffusion of the drugs.

These results prove the pH sensitivity of the systems presented, allowing for control of the release rate by changing the environment.

The release rate at the initial point in time is a critical juncture during the preparation of drug delivery systems. Despite the fact that fast release (burst) following contact with the media is utilised in certain drug administration strategies, the negative effects connected with such a burst can be pharmacologically dangerous and economically inefficient.

Both systems present an initial burst release of 5-FU and TMZ during a period of 6 h in all incubation media, ranging at 16–85% (Fig. 21). This could be related to i) some amounts of drugs localised on the surface, or ii) the degree of protonation of the CS amino groups. Another factor that may be responsible for the burst is the drying procedure. Freeze-drying ($-$ 110 °C) was applied on the samples presented in this work. During the drying process, migration of the loaded drugs might occur as the water moves towards the surface, resulting in heterogeneous distribution in the matrix and accumulation on the surface (Zhang et al., 2012, p. 1109-1125).

Fig. 21 clearly shows that burst intensity is pH dependent. This represents an advantage in controlled delivery applications, as it facilitates rapid release and permits pharmacological concentration merely in specific body compartments.
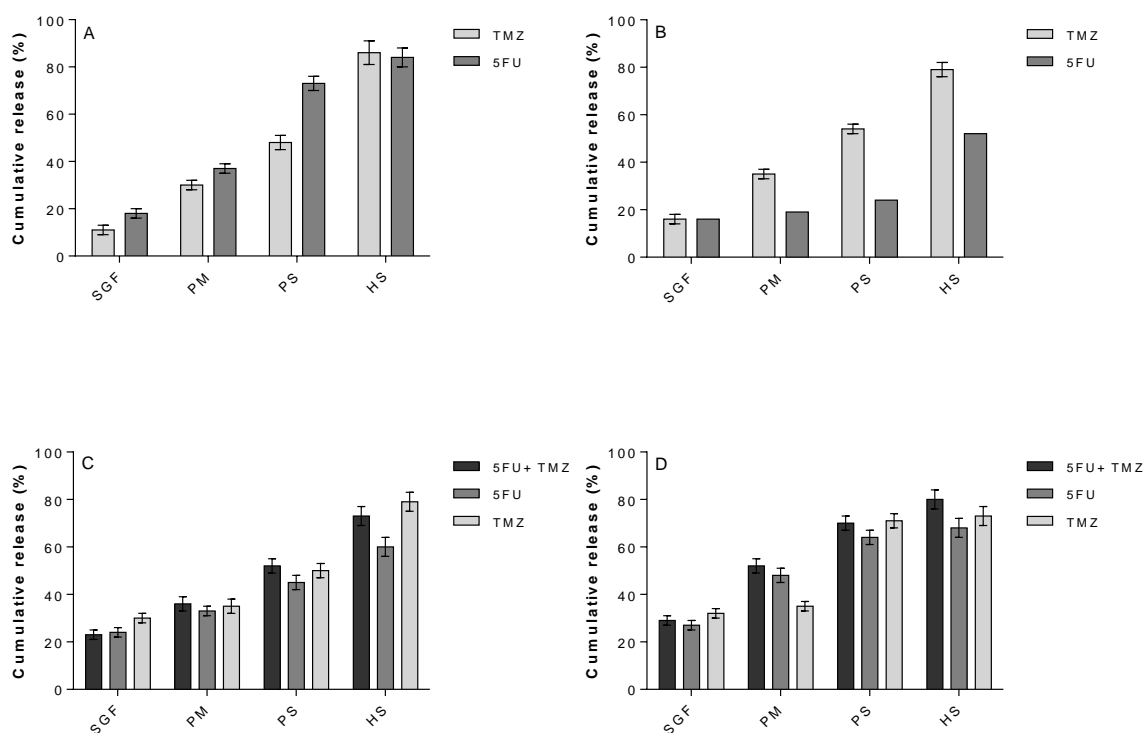

Fig. 21 Individual (A, B) and simultaneous (C, D) release intensity of TMZ and 5FU after 6 h of incubation in different media at 37 °C from CS-PGA (A, C) and CS-ALG (B, D)

A number of research papers have observed burst release from various polymeric materials like PLGA (Polylactide-co-Glycolide) (Chen and Zhou, 2010, p. 2011-2017), PLA, PNIPAM (Poly(*N*-isopropylacrylamid) (Moody and Wheelhouse, 2014, p. 797-838) and CS for various bioactive molecules (e.g. bovine serum albumin, 5-FU, g-Globulin, Heparin and Ampicillin) but few have attempted to explain it. However, some chemical modification - especially in polysaccharides, exhibited great reduction in the burst effect (Di Martino and Sedlarik, 2014, p. 134-145), particularly for TMZ.

Fig.22 and 23 display the co-release of TMZ and 5-FU from CS-ALG and CS-PGA
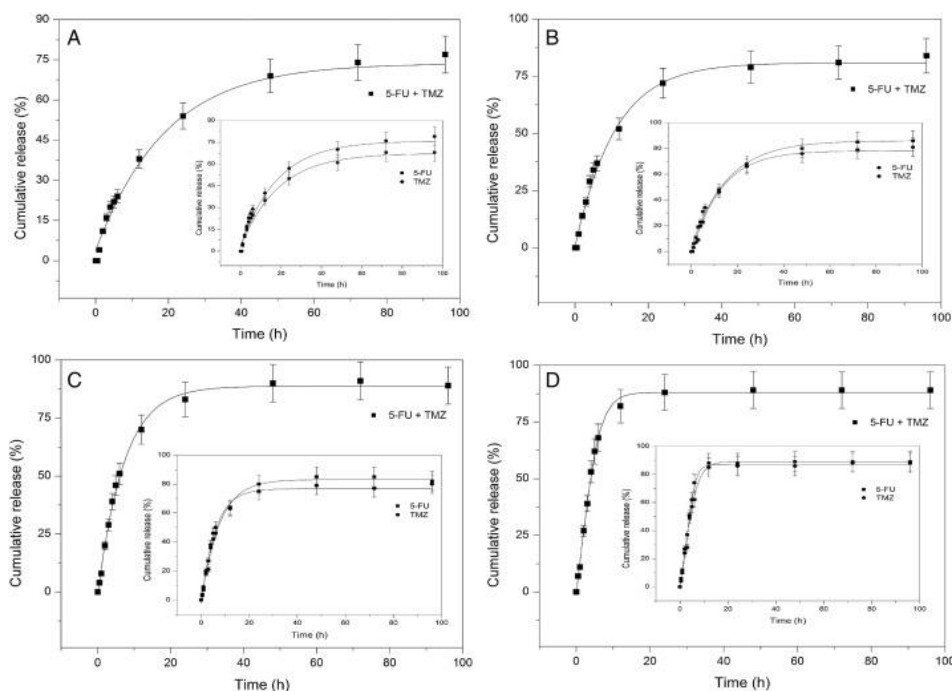

Fig. 22 TMZ and 5-FU co-release profiles from CS-AA in A) SGF, B) PM, C) PS and D) HS at 37 °C; the main chart represents total release (5-FU + TMZ), while the inner pane specifically indicates the trend of 5-FU and TMZ.
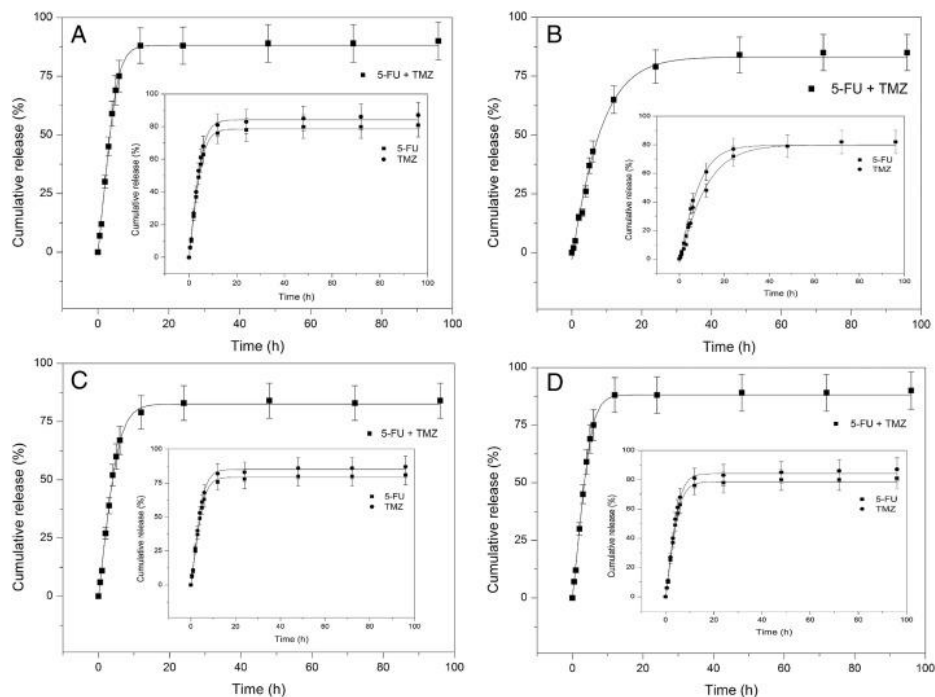
Fig. 23 TMZ and 5-FU co-release profiles from CS-PGA in A) SGF, B) PM, C) PS and D) HS at 37 °C; the main chart represents total release (5-FU + TMZ), while the inner pane specifically indicates the trend of 5-FU and TMZ.

In the release trends reported in Figures 22 and 23 (A, B, C, D) no particular differences arise between the CS-ALG and CS-PGA systems. The effect of pH is evident in all the formulations. In PS and HS, in < 12 h, > 70% of the drug(s) (TMZ + 5-FU) is released, while for PM and SGF is < 50%. Considering the release of the drugs separately (see the inner panel in Fig.23), no interference or synergic effect occurs and the values are comparable when the drugs are loaded singularly.

The data reported in Fig.22 confirmed the relationship between the intensity of the burst effect and pH of the medium in double-loaded systems. Even if the intensity is high, in particular in HS and PS, the amount of drug released is well-balanced, indicating that there is no interference or synergic effect, and the given drugs diffuse independently.

ANOVA analysis performed on the amount of TMZ and 5-FU released in the first 6 h, when loaded separately and simultaneously, reveals that - except in HS - insignificant differences arose between the amount of drugs released when singularly and simultaneously loaded, indicating that no interferences were present and the drugs maintained the same behaviour.

LC–MS analysis

Several studies and analytical methods have reported to determine the amount of TMZ and 5-FU or their metabolites in biological fluid, such as plasma and urine (Darkes et al., 2002). Moreover, techniques like LC–MS are highly useful, rapid and lack any particular sample preparation.

In accordance with published works (Darkes et al., 2002), TMZ yielded an ion at m/z 195 $[M + H]^+$ although Na and K adducts were also present at m/z 233 and m/z 217, respectively. Moreover, TMZ tended to form a dimer or occasionally a cluster through an H-bond between NH_2 and COOH groups. As reported in Fig. 24, TMZ dimers with the relative Na and K adducts appeared at m/z 389 $[M_d + H]^+$, m/z 411 $[M_d + Na]^+$, and m/z 427 $[M_d + K]^+$.
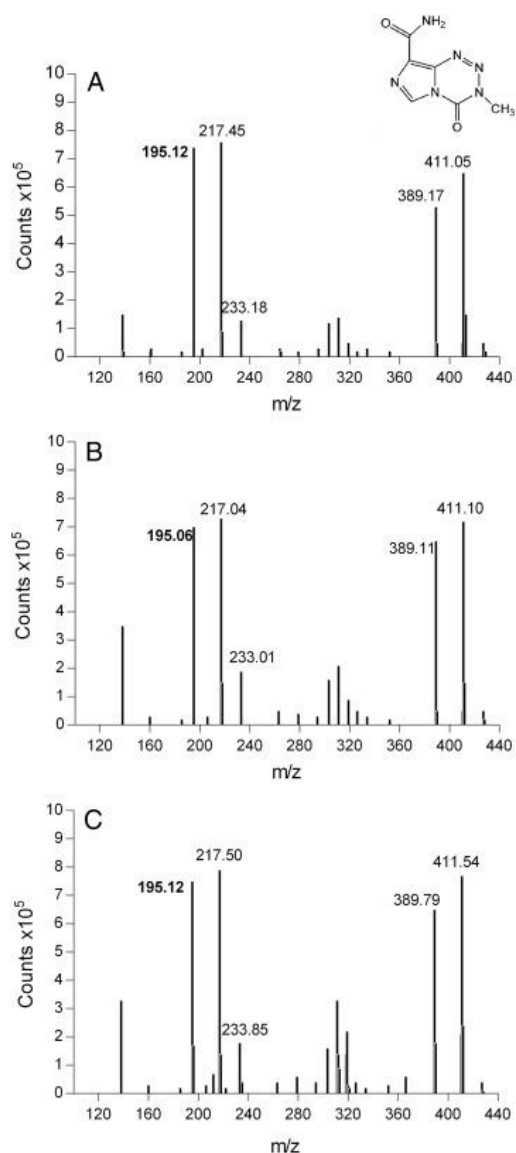

Fig. 24 MS spectra of A) TMZ (control) and TMZ after release in B) physiological and C) preparation media at different time.

TMZ is a prodrug and shows good stability in acidic media, whereas in physiological pH it is spontaneously hydrolysed, through the effect of water at C_4, to the active form 5-(3-methyltriazen-1-yl)imidazole-4-carboxamide (MTIC) (MTIC M_w 168.15 Da). Subsequently, MTIC degrades to 5-aminoimidazole-4-carboxamide (AIC) (M_w 126.12) and a methyldiazonium ion (Friedman et al., 2000, p. 2585-2597).

As hydrolysis occurred in less than 2 h in physiological conditions, it represents a primary drawback of TMZ, thereby limiting therapeutic efficacy.

As can be seen from the MS spectra of the TMZ control (Fig. 24 A), and after release in physiological (Fig.24 B and C) and preparation media (time 24 h), no peaks related to the hydrolysis products were visible. The given results indicate that both formulation CS-ALG and CS-PGA clearly protect TMZ from the external environment and could prolong residential time in biological fluid.

As described (Derissen et al., 2015, p. 58-66), in accordance with the molecular structure of 5-FU, the following representative ions were detected at m/z 131 relative to 5-FU, $[M + H]^+$, with Na and HCOOH adducts also present at m/z 153 and 175, respectively (Fig. 25). Comparing the MS spectra of 5-FU control and after release ($t = 24$ h) from both systems, no differences were demonstrated, indicating no alteration in the chemical structure
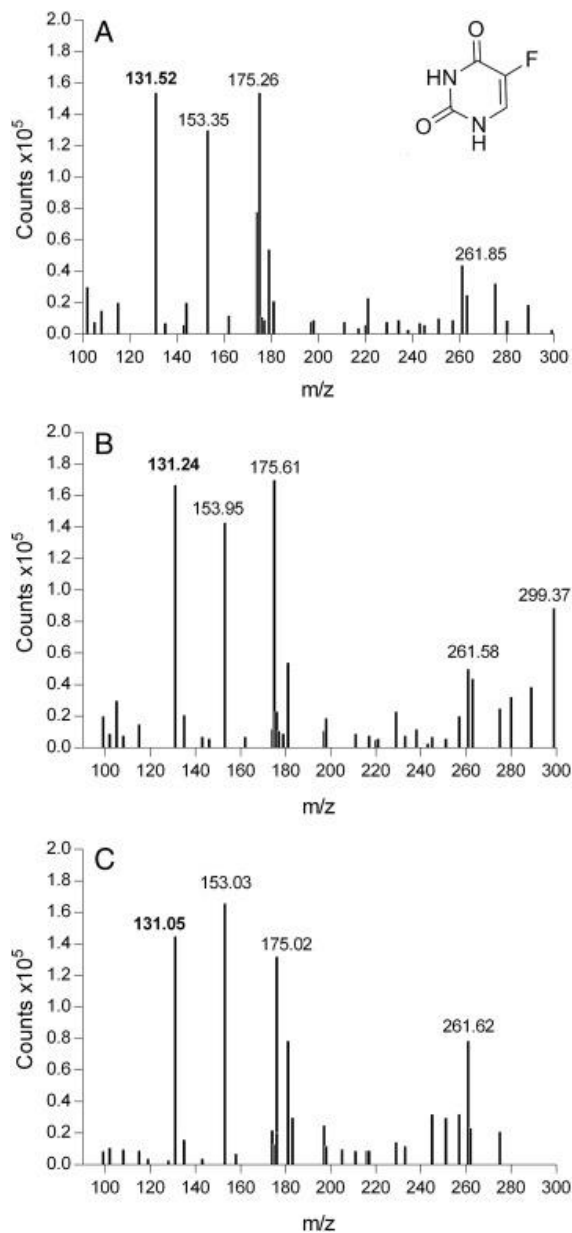
Fig. 25 MS spectra of A) 5-FU (control) and 5-FU after release in B) physiological and C) preparation media at different time.

The loaded drugs gave a stable result when loaded simultaneously in the same system, as no new peaks related to any sub-products were observed (Fig. 26).
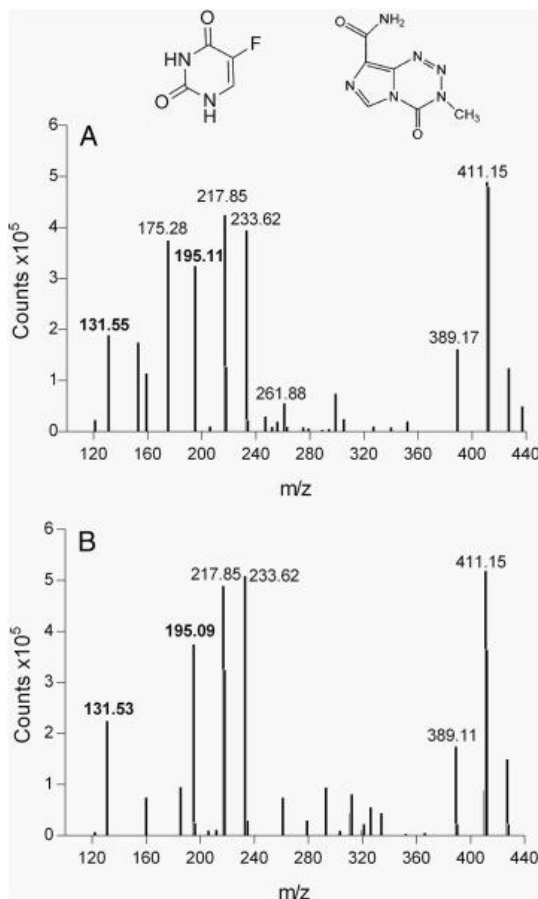
Fig. 26 MS spectra of TMZ and 5-FU co-released from A) physiological and B) preparation media.

Taking into consideration the co-encapsulation and co-release kinetics with the MS results, it is clearly indicated that the prepared systems are able to load and release more drugs simultaneously without any interference occurring between them. In other words, the drugs present the same behaviour as when loaded separately.

The MS spectra reported herein were referred to CS-ALG-based complexes at the weight ratio used for release studies. Spectra are not shown concerning the drugs released pertaining to any CS-PGA complexes formed, as no variation with reported data were observed.

Conclusions

The study is focuses on CS-based PECs for simultaneous encapsulation and controlled delivery of antineoplastic drugs. Such systems possess important properties, as follows: i) mild preparation conditions without the necessity for high temperature or organic solvents; ii) valuable drug-loading capacity, providing continuous and sustainable release from hours to days and in particular protection of the encapsulated drug; and iii) pH sensitive behaviour.

PECs exhibit dimension and ζ-potential in the range of 100–200 nm and from -30 to $+35$ mV, respectively. The amount of drugs entrapped is displaced between 20 and 80% of the total amount, depending on the weight ratio between the used polysaccharides. An excess of CS leads to superior encapsulation of the drugs singularly or simultaneously.

In vitro release of the drugs exhibited sustained (up to one week) and controlled release in connection with the pH of the media. The opportunity to modulate the burst intensity and release rate by changing the pH or the ratio between the polysaccharides indicates that these systems benefit from high versatility, with the possibility to facilitate controlled release in various body fluid compartments. The absence of any interference between TMZ and 5-FU during loading and especially the release process stands out as important findings, suggesting polysaccharide-based PECs would make interesting candidates for multi-drug controlled delivery. Moreover, no structural alteration occurred in 5-FU or, particularly, in TMZ after release, thereby demonstrating the protective role exhibited by the system.

It was found that PECs based on CS-ALG and CS-PGA do not present significant differences in terms of particle dimensions and ζ-potential. However, significantly different values of encapsulation efficiencies and release kinetics were observed depending on the drug used and their weight ratio. It clearly shows an importance of the polyanion chemical structure in complex with CS to drug(s) encapsulation ability.

3.2 Chitosan grafted PLA and carboxy functionalized PLA for doxorubicin and temozolomide co-therapy

INTRODUCTION

Drug delivery is the method or process of administering a pharmaceutical compound to achieve a therapeutic effect in human or animals (Tiwari et al., 2012, p.2). A drug delivery system (DDS) is defined as a formulation or device that enables introduction of the bioactive compound in the body and improves its efficacy and safety by controlling the rate, time, and place of release of the drugs in the body (Mainardes et al., 2006, p. 275-285). Several DDS have been formulated and investigated; these include liposomes, microspheres, gels, nanoparticles and others. Among them, nanoparticles provide several advantages in terms of drug targeting, delivery and release compared to the others. In the design of nanoparticles as drug delivery systems the main goals are to improve stability in the biological environment, to mediate bio-distribution of active compounds, and to further drug loading, targeting, transport, release and interaction with biological barriers. The cytotoxicity of nanoparticles or their degradation products remains a major problem, and improvements in biocompatibility are the main concerns of future research.

Nanoparticles made from natural or artificial polymers have been applied as drug delivery systems with great success and they show potential for many biomedical applications. Drugs may be bound in the form of a solid solution, or through dispersion, or be physically adsorbed or chemically attached. Polymeric nanoparticles are, generally, prepared by following three methods: (i) dispersion of preformed polymers; (ii) polymerization of monomers; and (iii) ionic gelation or coacervation of hydrophilic polymers.

In this paper an amphiphilic co-polymer was synthesized by grafting PLA and PLA modified with citric acid (PLACA) at different ratios to the CS backbone. Nanoparticles loaded with DOX and TMZ have been prepared via the polyelectrolyte complexation method (PEC) which represents a simple, low-cost and solvent-free procedure to prepare nanoparticles. Moreover, is possible to manipulate the diameter of particles by changing the ratio of polycation and polyanion. Obtained nanoparticles were characterized, in terms of dimension and ζ-potential at different pH levels and temperatures by light scattering analysis, as well as regarding stability in physiological conditions and temperature behaviour (range 0–60 °C). The encapsulation efficiency and release kinetic studies were carried out via UV–vis spectrophotometry, since DOX and TMZ absorb at 480 and 325 nm respectively. Satisfactory results regarding the diameter of particles and ζ-potential boosted high encapsulation efficiency and sustained drug release without an

initial burst, which suggested that CS grafted with PLA modified with citric acid was a suitable carrier for co-therapy of DOX and TMZ.

Results and discussions

PLA and carboxy enriched PLA characterization

In Table 10 the acidic number (AN), λ_{max} and the M_w, obtained through GPC analysis, of PLA and PLA with different amounts of citric acid (PLACA) are reported.

Table 10 Acid number (AN), λ_{max}, M_w determined by GPC of PLA, PLACA2% and PLACA5%

Sample	AN (mg KOH/g PLA)	λ_{max}(nm)	M_w (g/mol)	PDI
PLA	21.4 ± 0.3	236	47,000	2.1
PLACA2%	32.7 ± 0.2	239	27,000	2.5
PLACA5%	45.2 ± 0.2	241	5000	4.1

As can been seen, the highest M_w was achieved for PLA (47,000 g/mol). Increasing the amount of citric acid diminishes M_w values. In addition, the polydispersity (M_w/M_n) of the polycondensates increases from 2.1 (for PLA) to 4.1 (for PLACA5%). The incorporation of citric acid in the structure of a product through a condensation reaction can be proven by determining the carboxyl groups, which should be in excess if a reaction has taken place during product formation. The titration method can provide such information in the form of AN as presented above. The values of AN, shown in Table 10 are in accordance with assuming the occurrence of a condensation reaction between lactic acid and citric acid molecules. Despite the previously mentioned assumption of carboxyl absence in pure PLA, a low AN value was observed. It can be ascribed to the presence of a residual monomer (Kucharczyk et al., 2011, p. 1275-1285). In addition, the indicator – bromothyol blue – has an equivalence point of above pH 7. The rising citric acid content causes an increase in AN.

UV–vis analysis of the samples can support the idea of COOH attachment on PLA chains. Generally, PLA displays maximum absorbency at the wavelength (λ_{max}) 240 nm (Leu and Chow, 2011, p. 40-47). For the authors of the paper presented here, pure PLA showed $\lambda_{max} = 236$ nm. The increasing content of citric acid led to slight shift of λ_{max} towards higher values. The sample with 5% of citric acid content showed $\lambda_{max} = 241$ nm. It is noticeable that absorption at λ_{max} is heightened with an accordant rise in the content of citric acid. It could be considered that this phenomenon is a consequence of PLA functionalization (Kucharczyk et al., 2011, p. 1275-1285).

FTIR-ATR analysis

ATR-FTIR analysis was performed to prove the occurrence of a reaction between CS amino groups and PLA and PLACA carboxylic groups as reported
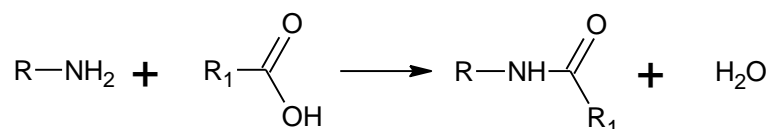

Fig. 27 Schematic representation of amide bond formation between CS amino groups and COOH group in PLA

where *R* an *R$_1$* represent D-glucosamine unit and the PLA or PLCA chains, respectively.

As previously described (Li et al. 2012, p. 221-227) the reaction between CS amino groups and PLA carboxylic groups, as occurs in the presence of EDC and NHS, leads to the formation of an amide bond between the CS chains and PLA or PLACA. Fig. 28 shows the ATR-FTIR spectra of CS, PLA, PLACA2% and PLACA5%.
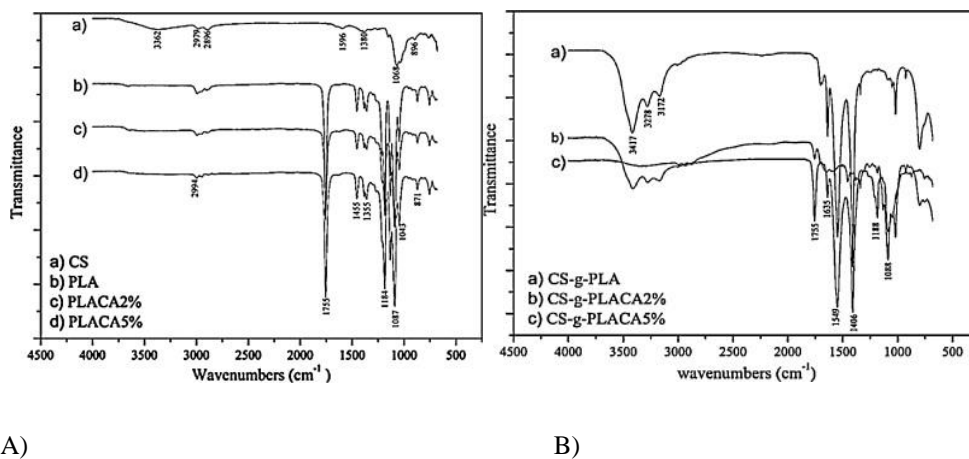
Fig. 28 ATR-FTIR spectra of A) CS and various PLA and B) the obtained products

In accordance with results reported the previous work (Li et al., 2012), the representative peaks of the CS backbone are as follows: 3362 cm^{-1} (OH stretch), 2979 cm^{-1} (CH), 1596 cm^{-1} (NH$_2$ deformation) and 1068 cm^{-1} (COC). The PLA and PLACA representative peaks are at 2994 cm^{-1} (CH stretch of methyl), 1755 cm^{-1} (C=O stretch), 1455 cm^{-1} (CH bend of methyl) and 1184 and 1087 cm^{-1} (CO stretch). Due to the chemical similarity of lactic acid (LA) and citric acid (CA), the differences between PLA and PLACA spectra are difficult to analyse (Kucharczyk et al., 2011, p. 1275-1285). The only difference can be found in the intensity of the peak related to C=O stretching, which is slightly more intense for CS-g-PLACA5% (Fig. 28). Compared to the individual components presented in Fig. 27 A, the ATR-FTIR spectra of the grafting-reaction products show new peaks observed at 1455 cm^{-1} (methyl asymmetric deformation of PLA and PLACA), 1635 cm^{-1} (the amide bond), and 1755 cm^{-1} (the carbonyl group of the branched PLA and PLACA) (Li et al. 2012, p. 221-227)). The spectra of CS-g-PLA and CS-g-PLACA (Fig. 27 B) shows peaks at 3412 cm^{-1} (NH stretching), 3278 cm^{-1} and 3172 cm^{-1} (OH stretching) which are connected through the presence of CS.

Physicochemical characterization of nanoparticles

Study approaches include preparing four sets of particles, i.e. without the drug, with DOX or TMZ and with both drugs at different polymer to DS ratio (0.05, 0.1, 0.2, 0.5 and 1). As expected from the literature (Yousefpour et al., 2011, p. 1977-1990), all drug loaded nanoparticles exhibited an increase in diameter in comparison with the drug free particles. This was probably due to electrostatic interferences of the drugs with the polymer chains, which took place during formation of the nanoparticles as a drug, where loaded at that time.

As can been seen in Fig. 29, the presence of -COOH influenced the ζ-potential as well diameter values. CS-g-PLACA5% showed a favourable trend as only a slight increase in diameter occurred when one or both drugs were loaded. This can be explained by electrostatic interactions occurring in the system. Due to both drugs carrying a positive charge and the greater presence of COOH groups in ionic form (COO$^-$) in CS-g-PLACA5%, an expansion of the systems is prevented as clearly happens in CS-g-PLA. ζ-potential values (12–34 mV) indicated that the nanoparticles are relatively stable, and positive values suggest that chitosan chains are located externally (Honary and Zahir, 2013, p. 265-273). The presence of drugs in the nanoparticles also influences the ζ-potential values. In particular, there is a decrease in various extents where observed in accordance with the chemical structure of the polymer used. The results in Fig. 29 reveal that CS-g-PLACA systems are more sensitive to drug loading in comparison to CS-g-PLA, confirming the influence of COOH groups on the properties of the co-polymer.
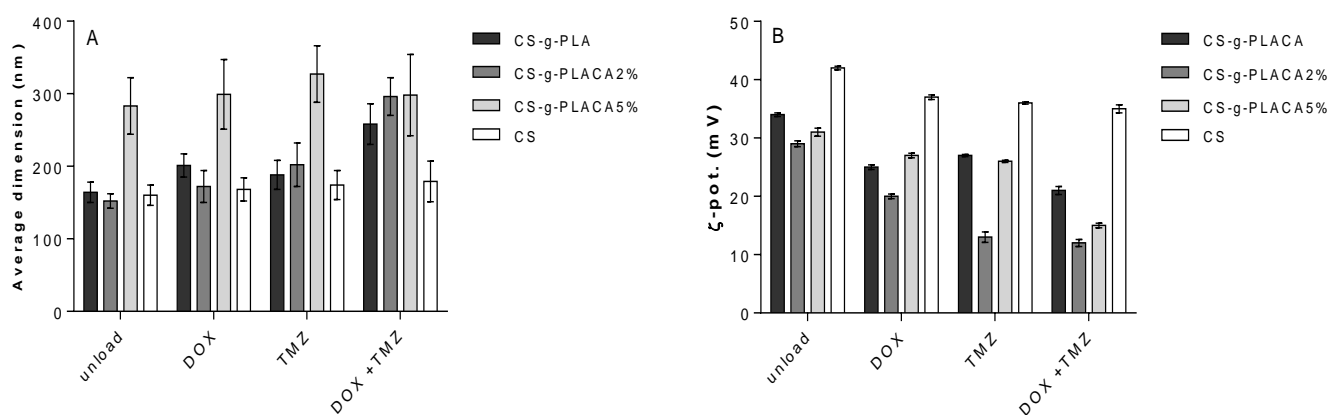

Fig. 29 A) Average dimension and B) z-potential of all prepared formulations, loaded and unloaded compared with unmodified chitosan (CS).

The relationship between polymer/DS ratio (w/w) versus average diameter, ζ-potential and the μ_e of nanoparticles is reported in Fig.30 A, B, C.
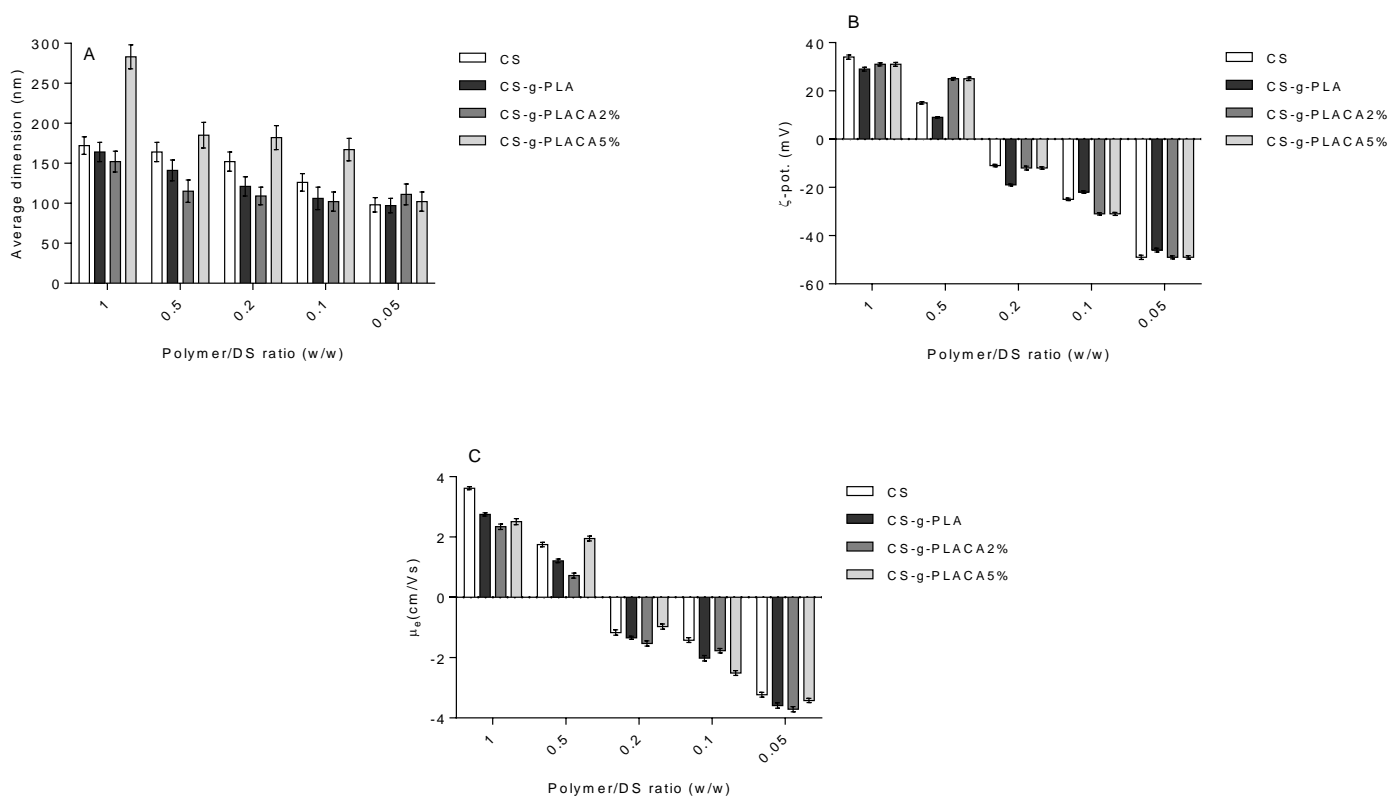
Fig. 30 Relationship between polymer/DS ratio (w/w) and average dimension (nm), ζ-potential and the μ_e of nanoparticles in preparation media pH 5.5

It was found that the lower the polymer/DS ratio, the lower the values of diameter, ζ-potential and μ_e that were obtained (Fig. 30). When DS concentration increases, its molecules can fill the inter- and intra-molecular spaces between the polymer chain, forming ionic interactions and neutralizing the positive charges located on the CS backbone, thereby causing ζ-potential and μ_e reduction. When the number of negative charges exceeds the number of positive charges, a shift from positive to negative ζ-potential and μ_e values takes place as long as the number of negative charges start to predominate. The *pI* (isoelectric point) of the systems falls to around 0.3 polymer/DS ratio, except in CS-g-PLACA2% where it is at around 0.4. As the charge on the CS backbone is reduced, the CS chains start to fold, giving a more compact structure characterized by lower diameter values (Chen et al., 2007, p. 131-139). In the case of CS-g-PLA and CS-g-PLACA, reduction in ζ-potential and me values occur, thereby increasing DS concentration due to a lack of free amino groups not involved in the amide bond with PLA and PLACA

Encapsulation efficiency (EE)

Drug loading in nanoparticles is achieved in two ways, by incorporating the drug at the time of producing the particles or by adsorbing the drug after forming the particles by incubating them in the drug solution. Thus, it is evident that a large amount of drug can be entrapped by the incorporation method when compared with the adsorption technique (Reis et al., 2006, p. 8-21). DOX and TMZ were loaded during the production process of the nanoparticles, leading to higher encapsulation and co-encapsulation efficiencies, as represented in Fig. 31 and Table 10.
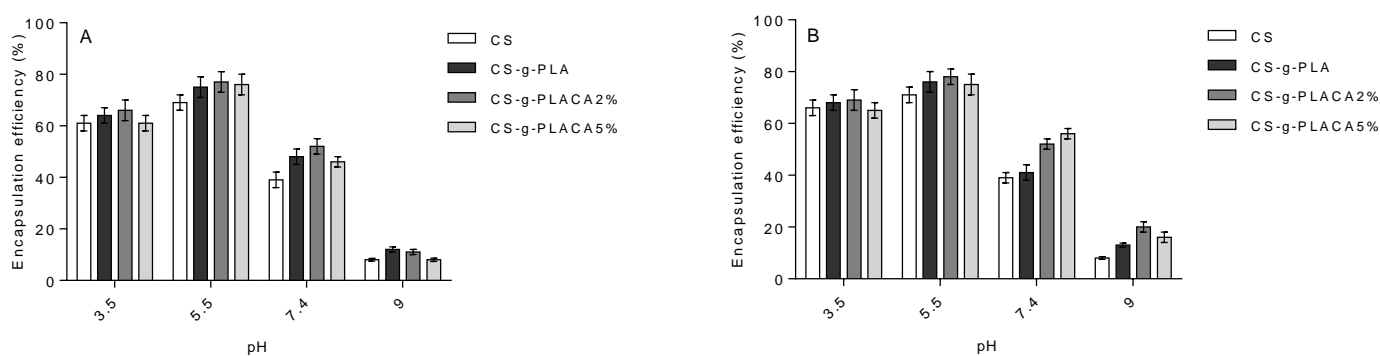

Fig. 31 Effect of pH on A) DOX and B) TMZ encapsulation efficiency in all formulation

CS-g-PLACA shows the highest EE values for both drugs investigated at all the pH values analyzed. These results indicate that the presence of COO^- helps to keep the drug within the nanoparticles through electrostatic interactions. Generally, it can be observed that increasing pH values cause a reduction in *EE* of all the samples at a given pH. However, the *EE* of CS-g-PLACA samples is higher in comparison with systems based on pure PLA. The exception can be observed in DOX containing the CS-g-PLACA5% particle system. It may be explained by the bulky structure of DOX.

Table 11 displays the EE when drugs are simultaneously loaded. As can been seen in all cases, the amount of DOX encapsulated is higher than TMZ. The difference is significant especially at neutral and alkaline pH levels. To summarize, the difference in the quantity of DOX and TMZ encapsulated indicates the influence of the different molecular structures and charges of both drugs. These results are in agreement with previously published works where drug–polymer electrostatic interactions have been described (Dadsetan et al., 2013, p. 5438-5446). In fact, considering the pK_a value of CS amino groups, they tend to be in neutral form at pH values higher than 6.5, resulting in a lack of polymer and polymer–drug interactions.

Temperature behaviour

In this section, the effect of thermal treatment on diameter was analysed. Only a few studies exist on the temperature effect on polymers used as drug delivery systems (Morris et al., 2011, p. 1430-1434; Sershen et al., 2000, p. 293-298). Indeed, it represents a parameter that should not be underestimated, since a subtle change in temperature can cause various rearrangements of the polymer chains, influencing the entire system including the release kinetic of the present bio-active compound. Temperature behaviour was analysed in the range 0–60 °C over six steps.
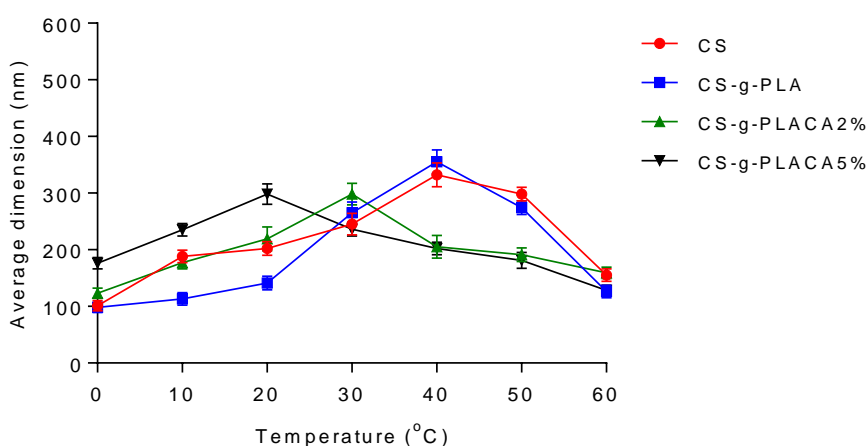

Fig. 32 Relationship between average dimension of nanoparticles and temperature

As shown in Fig. 32, increasing the temperature causes an upward trend in diameter. However, each composition is characterized by a critical temperature ($T_{crit.}$), where diameter reached the maximum value. Reduction in diameter was observed above $T_{crit.}$, probably due to a reduction in hydrogen bonds amongst CS chains and water molecules, causing a de-swelling in the system. Systems containing CS-g-PLACA showed $T_{crit.}$ in the temperature range 20–30 °C, while those comprising CS-g-PLA were found at approximately 10 °C higher. These results indicate that the presence of COO⁻ influences the thermal properties of the carrier, as they can interact with the free amino groups, avoiding the formation of the hydrogen bond with the water molecules in the release environment. One of the consequences related to this behaviour (swelling and de-swelling) might be the rapid release of the drug in correspondence with the temperature at which the $T_{crit.}$ value of diameter is located (Martinez-Ruvalcaba et al., 2009, p. 25-32

Table 11 Co-encapsulation efficiencies (%) of DOX and TMZ at different pH values of release media.

pH	CS	CS-g-PLA	CS-g-PLACA2%	CS-g-PLACA5%
3.5	18% (DOX+TMZ)	20% (DOX +TMZ)	32 % (DOX + TMZ)	36 % (DOX + TMZ)
	55% (DOX)	53% (DOX)	60% (DOX)	69% (DOX)
	45% (TMZ)	47 % (TMZ)	40% (TMZ)	31% (TMZ)
5.5	31% (DOX +TMZ)	33% (DOX +TMZ)	35% (DOX +TMZ)	31% (DOX +TMZ)
	49% (DOX)	58% (DOX)	64% (DOX)	61% (DOX)
	51% (TMZ)	42%(TMZ)	36%(TMZ)	39%(TMZ)
7.4	14% (DOX +TMZ)	13% (DOX +TMZ)	23% (DOX +TMZ)	26% (DOX +TMZ)
	46% (DOX)	53% (DOX)	62% (DOX)	70% (DOX)
	54% (TMZ)	47%(TMZ)	38%(TMZ)	30%(TMZ)
9	3% (DOX +TMZ)	4% (DOX +TMZ)	6% (DOX +TMZ)	4% (DOX +TMZ)
	45% (DOX)	60% (DOX)	69% (DOX)	73% (DOX)
	55% (TMZ)	40% (TMZ)	31% (TMZ)	27% (TMZ)

Release kinetic

The release profiles of drugs from the nanoparticles depend on several parameters, such as the nature of the delivery system (the chemical structure of polymer), the drug encapsulated and environmental factors such as pH, temperature, ionic strength and the chemical composition of the release media.

In this work, the in-vitro DOX and TMZ release and co-release profile were studied in phosphate buffer (pH 7.4) at 37 °C.

The kinetic parameters and coefficient of determination (R^2) values obtained by statistical regression analysis (Equation 24) of experimentally obtained data (Fig. 33 and Fig. 34). The parameters of Equation 24 clearly describe the release profile of the systems investigated. Generally, C_{max} represents the maximum limit value of the drug content released from the particles. The kinetic parameter k reveals the intensity of the drug release at the initial stage of the process. Systems possessing burst effect show typically high k values. Some of the systems are characteristic of a certain time period between introducing the nanoparticles into the release media and actually delivering the incorporated drug. This phenomenon, known as a lag phase, is represented by the parameter t_{lag} in Equation 24 In the case of the single-loaded system, the release efficiency, represented by C_{max} approaches 0.9 mg drug/mg polymer in all systems. The values of k show the significant effect of both DOX and TMZ release rate over 24 h. While CS-g-PLA based nanoparticles demonstrate a typical burst effect, where the release of 50% of DOX (t_{50}), was observed even after 5 h, the CS-g-PLACA system reaches this level only after 24 h (CS-g-PLACA2%) and 20 hours (CS-g-PLACA5%). This trend was more pronounced for TMZ release. In addition, a lag phase period ($t_{lag} \approx 3$–4 h) was observed for CS-g-PLACA comprising samples. The higher the level of the COOH functionalization, the more obvious the suppression of the burst effect is observable. This is probably due to electrostatic interactions between the COO^- groups and the positive charged molecules of the drug, slowing diffusion towards the surface of the nanoparticles and, subsequently, in the media (Fu and Kao, 2010, p. 429-444). Moreover, the absence of an initial burst indicates that the whole amount of drug was located inside the structure of the nanoparticles, meaning that it was protected from the outer environment. These results demonstrate that CS-g-PLACA systems behave in contrast with most results presented in the literature regarding the release of DOX or TMZ from polymeric nanoparticles, where a burst effect of even higher than 50% of the loaded drug in a few hours is recorded (Zhang and Gao, 2007, p. 122-128; Lin et al., 2005, p. 143-151; Jiang et al., 2013, p. 542-548).
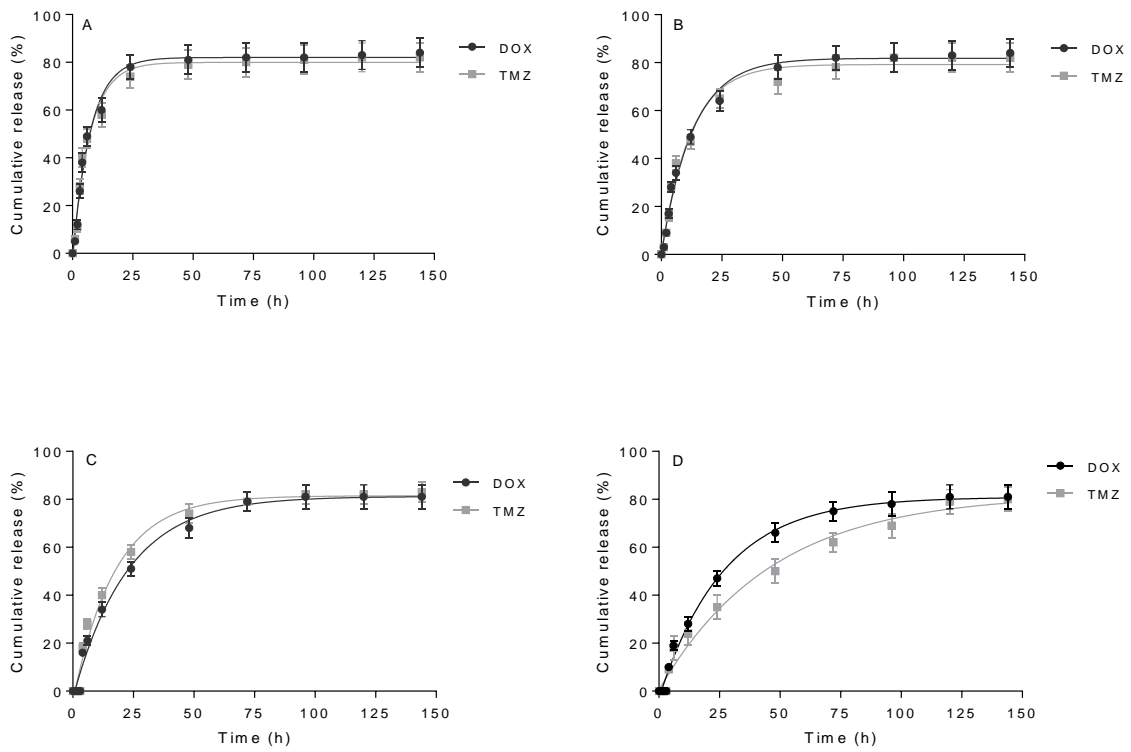
Fig. 33 Cumulative co-release rate in PBS pH 7.4 at 37 °C of DOX and TMZ from A) CS, B) CS-g-PLA; C) CS-g-PLACA2% and D) CS-g-PLACA5%
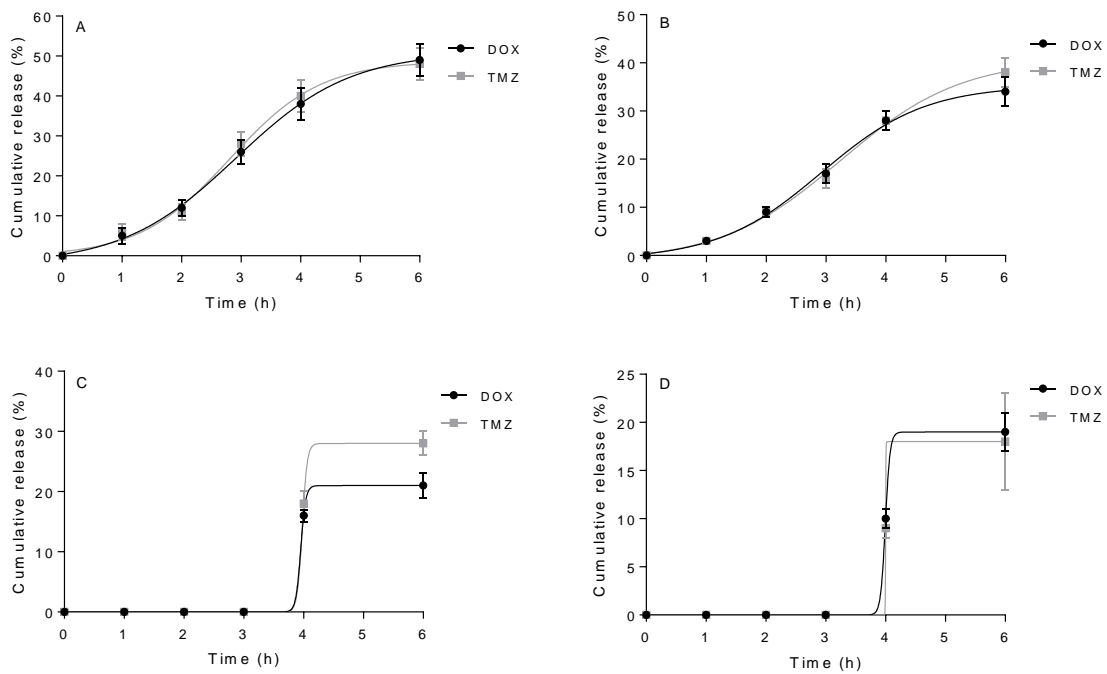

Fig. 34 First 6h Cumulative co-release rate in PBS pH 7.4 at 37 °C of DOX and TMZ from A) CS, B) CS-g-PLA; C) CS-g-PLACA2% and D) CS-g-PLACA5%.

Similar behaviour is found for the co-release of DOX and TMZ in PBS (Table 11). No burst effect and a lag phase of around 2–3 h were observed (Fig. 34). CS-g-PLACA systems confirmed the influence of COO$^-$ groups on the release mechanism. The effect of the extent of functionalization on the release kinetic is visible as t_{50} values. However, t_{50} release was reached after 12 h. A rapid initial release occurred as regards the CS-g-PLA system ($k = 0.24$ and 0.21 for DOX and TMZ, respectively. In both cases, CS-g-PLA and CS-g-PLACA, DOX and TMZ are released with a well-balanced trend, comparable with that obtained for the single drug. It indicates that no interference occurred between the drugs during the release.

Table 12 The parameters of release kinetic regression (Equation 24) for the single release of DOX and TMZ from CS-g-PLA and CS-g-PLACA systems (t_{50} represents time where 50% of the drug loaded is released).

	C_{max} (mg drug/mg polymer)	k (h^{-1})	t_{lag} (h)	R^2	t_{50} (h)
DOX					
CS	0.9	0.15	0	0.99	4
CS-g-PLA	0.9	0.11	0	0.98	5
CS-g-PLACA2%	0.9	0.035	3	0.86	24
CS-g-PLACA5%	0.9	0.037	4	0.94	20
TMZ					
CS	0.9	0.59	0	0.99	2
CS-g-PLA	0.9	0.54	0	0.95	2
CS-g-PLACA2%	0.9	0.055	4	0.96	12
CS-g-PLACA5%	0.9	0.041	4	0.82	72

Table 13 The parameters of co-release kinetic regression (Equation 24) for the release of DOX and TMZ from CS-g-PLA and CS-g-PLACA systems.

		C_{max} (mg drug/mg polymer)	k (h^{-1})	t_{lag} (h)	R^2	t_{50} (h)
CS	DOX	0.9	0.36	-	0.95	-
	TMZ	0.9	0.39	-	0.99	
CS-g-PLA	DOX	0.9	0.24	-	0.88	3
	TMZ	0.9	0.21	-	0.86	3
CS-g-PLACA2%	DOX	0.9	0.079	3	0.92	12
	TMZ	0.9	0.062	3	0.96	12
CS-g-PLACA5%	DOX	0.85	0.061	2	0.91	15
	TMZ	0.9	0.036	3	0.95	24

Conclusions

Polymeric nanoparticles made from the amphiphilic polymers CS-g-PLA and CS-g-PLACA loaded with DOX and TMZ were obtained through the polyelectrolyte complexation method. Results show that the presence of -COOH groups along the PLA side chains influence the dimension and temperature behaviour of the particles as well as the encapsulation efficiency and release rate of the drugs.

Nanoparticles shown diameter in range 150-300 nm and ζ-potential between 12–34 mV and high encapsulation and co-encapsulation efficiency of the selected drugs, DOX and TMZ, at neutral and acidic pH (more than 50 μg/g polymer) and a good release rate characterized by the absence of an initial burst. In CS-g-PLACA the release took place after 4–5 h, suggesting that carboxylic groups play an important role in the release mechanism, as well as that the drugs are located in the core of the system and are well protected from the external medium. Furthermore, the ratio of how DOX and TMZ are released when loaded in the same system is completely balanced, suggesting that CS-g-PLACA is a suitable candidate as a carrier for DOX and TMZ co-administration.

3.3 Chitosan grafted low molecular weight PLA for protein encapsulation and burst reduction

INTRODUCTION

Drugs based on proteins, peptides and oligonucleotides tend to attract the greatest attention due to their potential to treat chronic diseases. However, conditions inherent to the human body always limit the therapeutic applications of such substances (Terbojevich et al., 1996, p. 63-68).

One potential way to overcome such limitation is to control the delivery by carriers. Various carriers have been researched for peptide and oligonucleotide encapsulation and delivery (Tiwari et al., 2012, p.2). Many systems are based on micelles of different types, although polymeric nanoparticles have proven of interest as delivery systems due to their ability to penetrate physiological barriers, as well as protecting the loaded substances and targeting them to specific cells (Singh and Lillard, 2008, p. 2239-2252).

Naturally occurring polymers, especially polysaccharides have gained large attention within the scope of obtaining nanocarriers capable of releasing therapeutic molecules to the target sites.

This section deals with the preparing an amphiphilic pH sensitive co-polymer, synthetized via a grafting reaction of low molecular weight PLA to CS, as the carrier for controlled release of the model protein bovine serum albumin (BSA). Nanoparticle were prepared and characterized in terms of diameter, ζ-potential and their relation with polymer concentration was also investigated. BSA was loaded into the nanoparticles during their preparation; encapsulation and release kinetics were evaluated as a function of polymer concentration in physiological solution and simulated gastric fluid at 37 °C. Unmodified CS was used as a control to understand the influence of the PLA side chains on the properties of the carrier.

Results and discussions

CS-g-PLA characterization

FTIR–ATR (Fig. 35) analysis was performed to prove the occurrence of a reaction between CS amino groups and PLA carboxylic groups as indicated in Fig.34.
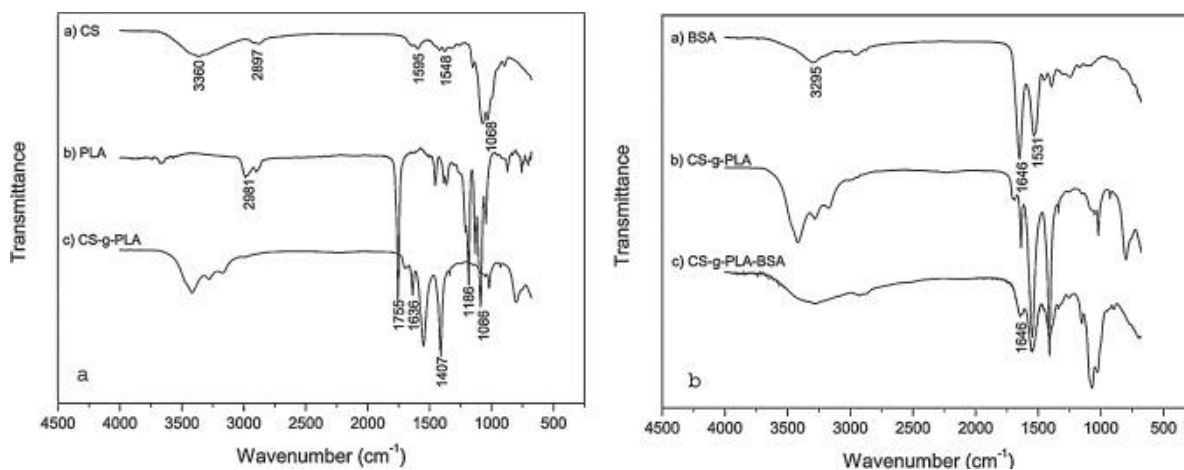

Fig. 35 ATR-FTIR spectra of A) the obtained polymer and B) nanoparticles formulation loaded and unloaded with BSA

The representative peaks (Dang and Leong, 2006) of CS backbone are: 3360 cm^{-1} (OH stretching), 2897 cm^{-1} (-CH), 1595 cm^{-1} (NH$_2$ deformation), 1548 cm^{-1} (NH bending), and 1068 cm^{-1} (COC) while for PLA are: 2981 cm^{-1} (CH stretching of methyl), 1755 cm^{-1} (C=O stretching), 1186 and 1086 cm^{-1} (CO stretching). CS-g-PLA spectra show a new peak at 1636 cm^{-1}, ascribed to the amide bond between CS and PLA, while the peak at 1407 cm^{-1} (CN stretching) is more intense in CS-g-PLA than in the unmodified sample (Liu et al., 2010, p. 301-305; Schwach et al., 1997, p. 3431-3440).

Fig. 35 B shows the FTIR-ATR spectra of the BSA, CS-g-PLA and CS-g-PLA-BSA nanoparticles. Considering the main peaks related to BSA (Schwach et al., 1997, p. 3431-3440) at 3295 cm^{-1} (OH stretching), 1646 cm^{-1} (C=O stretching) and at 1531 cm^{-1} (amide II coupling and bending NH, and CN stretching). The spectra for CS-g-PLA-BSA nanoparticles confirm the presence of BSA (1646 cm^{-1}), while no new chemical bonds were formed between CS-g-PLA and BSA, merely electrostatic interactions occurred.

The ^{1}H NMR spectra presented in Fig. 36 are in accordance with results reported in previous works (Schwach et al., 1997, p. 3431-3440) chemical shifts for chitosan appear at 3.55–3.72 ppm (H-3, H-4, H-5, and H-6), 2.98 ppm (H-2), and 1.85 ppm (NH-CO). The chemical shifts for CS-g-PLA are at 4.81–4.83 ppm (CH of lactyl unit), 4.62 ppm (CH of hydroxylated lactyl unit), 3.60–3.85 ppm (H-3, H-4, H-5, and H-6), 3.15 ppm (H-2), 2.01 ppm (NH-CO), 1.51 ppm (CH$_3$ of lactyl units), and 3.12 ppm; the H-2 proton signal of *N*-alkylation of chitosan confirms the bonding between chitosan and lactic acid.
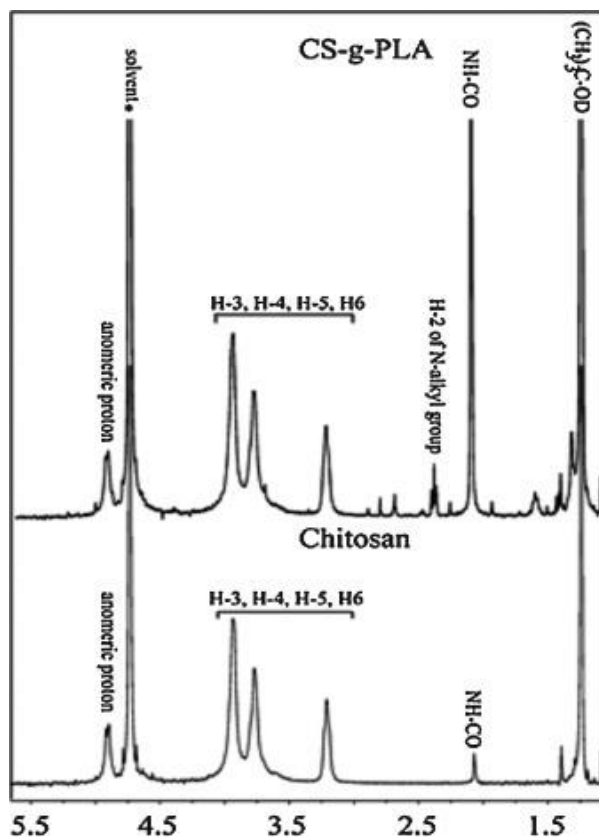

Fig. 36 ^{1}H NMR spectra of CS and CS-g-PLA.

Quantitative evaluation of CS and CS-g-PLA free amino groups

Occurrence of the reaction between CS and PLA can be also supported by quantitative evaluation of free amino groups present on the CS backbone before and after conjugation with PLA.

The N in unmodified CS and CS-g-PLA was determined by conductometric titration, as reported in a previous work (De Alvarenga et al., 2010, p. 1155-1160). The relationship between conductance (mS/cm) and NaOH volume is reported in Fig. 37
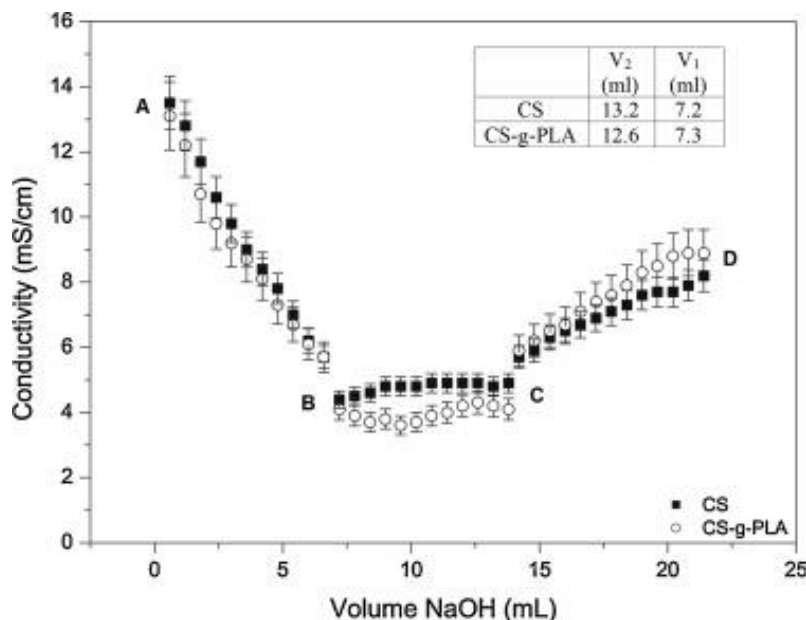

Fig. 37 Relationship between CS and CS-g-PLA solution conductivity (mS/cm) and volume (mL) of NaOH 0.160 M.

It is noticeable that the relationship between conductance and NaOH volume can be described in three main phases. In the first (Fig.37 A and B), a decrease in conductance connected with neutralizing acidic HCl solution is observed. The second (Fig. 37 B and C), refers to neutralizing the protonated amino groups of CS, while the last corresponds to the excess of the base (Fig. 37 C and D). The volume (V_1 and V_2) of the base necessary to neutralize the free amino groups on the CS and CS-g-PLA backbones was obtained by intersecting the three lines passing through points   AB-BC-CD. Once the two volumes were obtained, the N value was calculated, as indicated in Equation 25 (De Alvarenga et al., 2010, p. 1155-1160). Volume ($V_2 - V_1$) is reduced when CS is grafted with PLA N of pure CS confirms the value reported by the manufacturer (Sigma–Aldrich). Reduction in N could also be considered as additional proof that a reaction between CS amino groups and PLA carboxylic groups had occurred.

The number of free amino groups (F_{NH2}) obtained by the N value reinforced that a reaction between CS and PLA had taken place. The amount of free amino groups along each CS chain equals 469, which also represents the number of positive charges. Meanwhile, for CS-g-PLA the F_{NH2} is 395, around 16% lower due to the presence of PLA chains.

Swelling studies

Fig. 38 displays the effect of pH on the SI of CS and CS-g-PLA based nanoparticles.

It is known that pH represents one of the main factors influencing the swelling behaviour of a system, and swelling properties directly influence the release rate of the loaded molecules (Pasparakis and Bouropoulous, 2006, p. 34-42; Chatri et al., 2011, p. 876-882).
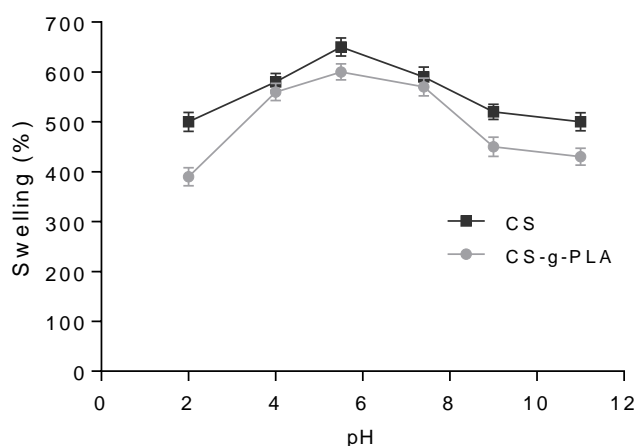

Fig. 38 Effect of pH on the swelling properties of CS and CS-g-PLA

The swelling trend is sharp in CS, the maximum value being at pH 5.5 (SI = 670%), while in CS-g-PLA a range of pH exists (between pH 4 and 6) where SI equals approximately 600%, indicating that the presence of PLA makes the system less sensible to pH variation.

Based on the pK_a value of CS amino groups and sulphate groups presented in DS, the species involved in the electrostatic interactions are NH_3^+, NH_2, SO_3^- and SO_3H in the given pH of the media. In acidic condition, the swelling is controlled by the amino groups.

As the CS amino groups are weak, bases (pK_a 6.2) in the acidic media are protonated (NH_3^+), causing an increase in charge density along the polymer chains. Electrostatic repulsion between NH_3^+ groups heightens osmotic pressure inside the nanoparticles. The difference in osmotic pressure between the internal and external solutions of the network is balanced by the swelling phenomena (Kucharczyk et al., 2011, p. 1275-1285). In highly acidic conditions (pH $\approx$2), the presence of Cl^- ions (due to HCl utilized from the acidified solution) can shield the charges present on the amino groups, preventing efficient repulsion and subsequently lowering the SI (Fig. 38). The same effect occurs in alkaline media, where the screening effect of Na^+ ions (from NaOH solutions used to increase pH) reduces the SI value.

The results presented in Fig. 39 indicate that the presence of solute diminishes the osmotic pressure of the external solution, thereby altering swelling intensity (Pasparakis and Bouropoulous, 2006, p. 34-42). CS-g-PLA based nanoparticles are not only less sensitive to pH but also to ionic strength than CS based nanoparticles. The ionic strength (I) of the used media is: SGF, $I = 0.095$ mol/L; PBS, $I = 0.100$ mol/L; PS, $I = 0.166$; SIF, $I = 0.120$ mol/L.
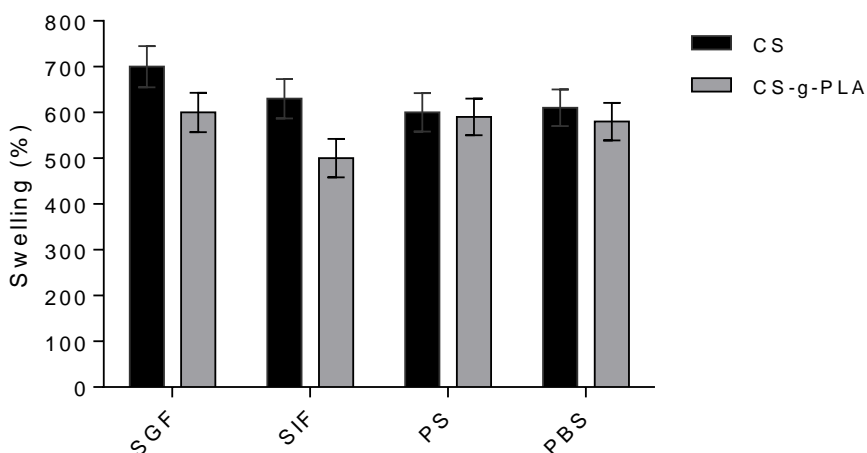

Fig. 39 Effect of different media composition on the swelling properties of CS and CS-g-PLA

Effect of polymer concentration on BSA encapsulation efficiency and loading capacity

In Fig. 40 A and B, the influence of polymer concentration on encapsulation efficiency (*EE*) and loading capacity (LC) of BSA at pH 5.5 is displayed.
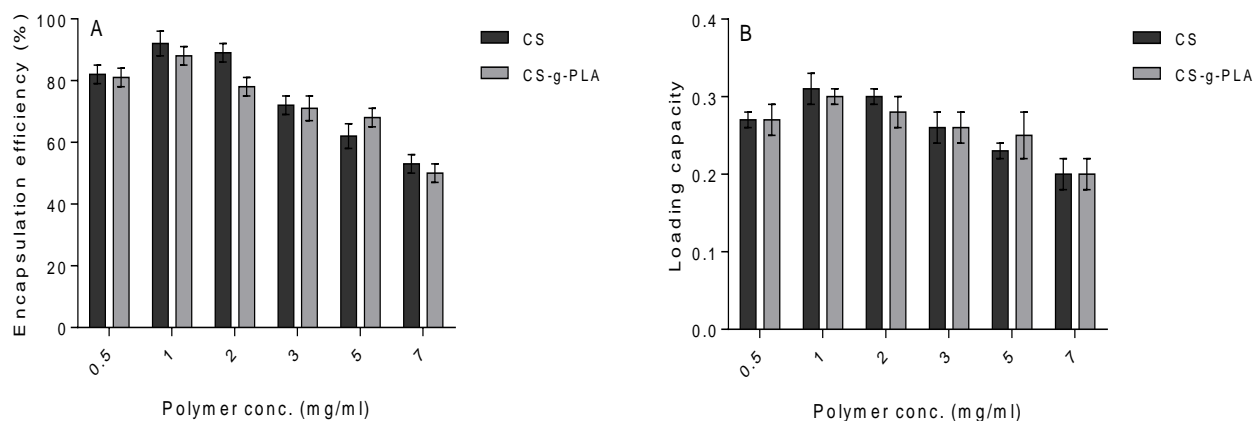

Fig. 40 Influence of polymer concentration on encapsulation efficiency (EE) and loading capacity (LC) of BSA in preparation media pH 5.5

EE decreases from 92% to 53% in CS and from 88% to 50% in CS-g-PLA when polymer concentration increases from 0.5 mg/mL to 7 mg/mL. Most of this decrease could be explained by an increase in solution viscosity (Lee and Chen, 2001, p. 2487-2496). It has been reported that higher viscosity associated with an increase in polymer concentration could hinder encapsulation of BSA molecular movement around the polymer chain (Jiang and Schwendeman, 2001, p. 878-885).

Maximum EE and LC are observed at 1 mg/mL polymer concentration; precisely 92% and 88% in CS and CS-g-PLA, respectively.

Generally, CS based systems show slightly higher EE and LC values than modified CS; except at 5 mg/mL, which is due to more intense electrostatic interactions between negatively charged BSA molecules under preparation conditions (pH 5.5). This can be proven by the N and F_{NH2} values of CS and CS-g-PLA.

The influence of polymer concentration on BSA loading parameters (*EE* and *LC*) does not concur with values presented in other works (Mehta et al., 1996, p. 249-257).

The relationship (among EE, LC and polymer concentration) is connected not only with the characteristics of the carrier (chemical structure), but also with the methodologies used for preparing the nanoparticles. In the case of the W/O emulsion technique, an increase in EE and LC occurs when polymer concentration increases. Indeed, the contribution of high polymer concentration to encapsulation efficiency could be interpreted in two ways.

Firstly, increasing polymer concentration means the polymer precipitates faster, preventing diffusion of the encapsulated molecule. Secondly, high concentration increases the viscosity of the solution, causing a delay in diffusion of the drug within the polymer droplets (Fernandez et al., 2011, p. 1628-1651).

In the case of the PEC (polyelectrolytes complexation) technique, encapsulation is related to electrostatic interactions between the given polymer and the loaded molecule. Increasing the amount of polymer means that the phenomena of repulsion between the chains strengthens, resulting in a less compact structure. If the loaded molecule is water soluble and the preparation media is represented by water, outward diffusion of the loaded molecule from the nanoparticles is more rapid.

However, some results regarding the EE and LC relationship with polymer concentration are comparable with those reported in this paper (Akbuga and Bergisadi, 1999 and Izumrudov et al., 2013). In this case, it seems that viscosity of the solution represents the main parameter potentially influencing EE and LC.

BSA release kinetics from CS and CS-g-PLA nanoparticles

Studies regarding protein encapsulation in CS and its nanoparticle-based derivatives are conducted with the purpose of achieving a desirable release profile for a given protein molecule, in terms of kinetics and total release (Lee and Chen, 2001, p. 2487-2496). Protein release from CS-based nanoparticle systems is characterized by an initial burst, when 30–70% of the loaded protein can be released within the first 3–6 h, which is followed by slow release over a few days (Kim et al., 2003, p. 371-383). Information on detailed controlling parameters and exact conditions to modulate the release profile of a protein are still incomplete, and often does not concur in reported studies (Calvo et al., 1997, p. 125-132 ; Calvo et al., 1997, p. 1431-1436).

A portion of the published results concluded that the chemical structure of the protein, CS (in particular CS-derivative polymers), and release medium properties such as pH and ionic strength were major factors influencing the release process (Chang and Lin, 2000, p. 163-169).

Table 14 Kinetic parameters referred to BSA release from CS and CS-g-PLA at pH 2 and 7.4

pH 2	C_{max} (%)	k (h^{-1})	R^2	t_{50} (h)
CS	90	0.23	0.97	14
CS-g-PLA	88	0.035	0.98	58
pH 7.4				
CS	90	0.54	0.94	3
CS-g-PLA	88	0.16	0.97	20

Table 14 displays the kinetic parameters and the coefficient of determination (R^2) obtained by statistical regression analysis of the experimentally obtained data (Fig. 41). The parameters C_{max}, k and t_{50} of Equation 25 clearly describe the release profile of the systems investigated. The parameter C_{max} represents the maximum concentration of the protein that can be released from the nanoparticles under the given experimental conditions. The kinetic constant k reveals the intensity of drug release at the initial stage. The value k gives information on the occurrence and intensity of burst phenomena. Systems with burst effect are typically characterized by a high k value. In both systems, release performance is represented by C_{max} and insubstantial differences are detected. The main differences between CS and CS-g-PLA are represented by k and t_{50} values, in particular in SGF. CS nanoparticles demonstrate a moderate burst effect, where the release of 50% of BSA (t_{50}) occurs over 14 h in SGF. A more intense burst effect is presented in PBS, where the same amount of BSA is released in only 3 h.
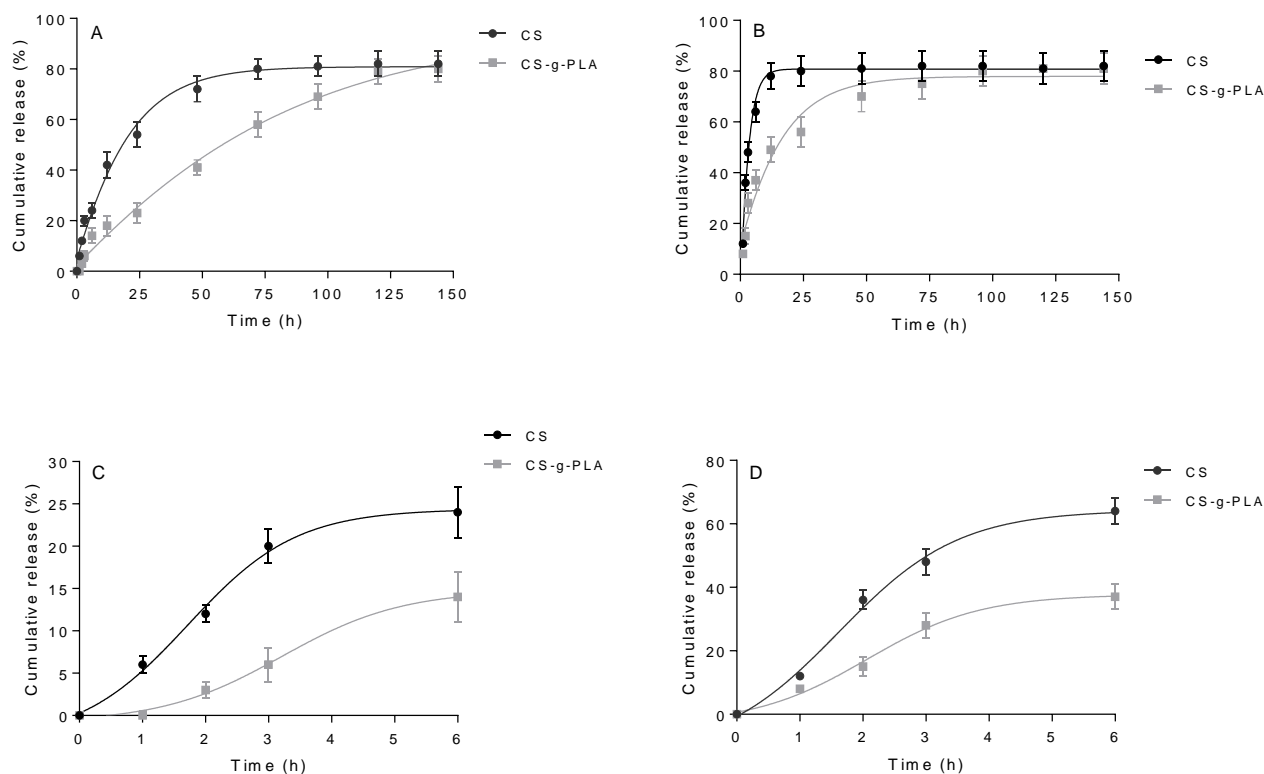
Fig. 41 Release trend of BSA from CS and CS-g-PLA in different medis; A) pH 2 and B) pH 7.4. BSA released in the first 6h after media contact in reported in panel C) pH 2 and D) pH 7.4

The release rate of BSA from CS in both tested media is characterized by two phases in which similar curves (Fig. 41) are presented. In the first one, which goes up to 24 h, almost 50% and 70% of loaded BSA is released in SGF and PBS, respectively. A second phase characterized by a gradual release takes place, where around 85% of BSA is released either in simulated gastric fluid, rather than in PBS (Fig.40).

Compared with unmodified CS, BSA release from CS-g-PLA in SGF shows reduction in the burst-effect phenomena characterized by $k = 0.035$, when around 30% of the encapsulated BSA is released in the first 24 h (Fig. 41). Over the next 150 h the release rate is more or less constant. Afterwards, a stationary phase takes place in which 90% of loaded BSA is released. A different trend can be seen in PBS media. In this case, the initial tendency of release is characterized by $k = 0.16$, which is higher than in SGF, but still lower than the value belonging to CS in PBS. The release curve in PBS (Fig.41) is characterized by two main phases: the first one, extending over 24 h, shows almost 50% of encapsulated BSA is released; afterwards, in the second phase, a slow and constant release is visible, the remaining amount of loaded protein being released over the next few hours.

117

Both polymeric systems are characterized by slower release in SGF compared with PBS. This could be down to two things. Firstly, CS free amino groups are protonated in acid media (SGF), permitting electrostatically interaction with BSA negatively charged amino acid residues thereby slowing release. In accordance with the pK_a value of amino groups ($pK_a = 6.5$), they are not protonated in PBS and less interaction with BSA molecules is discernible. Secondly, BSA can be denatured in SGF due to the effect of pH, hence it forms aggregate and becomes insoluble, and subsequently diffusion proceeds gradually through the nanoparticle structure (Bhattarai et al., 2006, p.181 ; Fu and Kao, 2010, p. 429-444).

The slower release rate from CS-g-PLA systems is likely due to the presence of PLA side chains, which make the inner structure of the nanoparticles more compact, causing retarded diffusion of the BSA molecules. Moreover, hydrophobic interaction between PLA chains and BSA might also influence the release rate.

These results suggest that influence is exerted on BSA release kinetics not only by the release medium, but also by carrier structure, as is observable from the reduced intensity of the burst effect. In the case of CS-g-PLA based nanoparticles, the reduction in burst effect might be due to the hydrogen bonding between the amino groups of CS and carboxylic groups in the PLA side chains; hence the same obtain a more compact structure that diminishes the diffusion of BSA molecules (Calvo et al., 1997, p. 125-132).

The BSA release from CS concurs with results reported in the literature (Katas et al., 2013, p.2013; Janes et al., 2001, p. 83-97). In fact, the release of BSA from polycation-polyanion systems is dominated by a large initial burst, in which up to 60% of the loaded compound is released in the first hours, followed by steady continuation (Amidi et al., 2006, p. 107-116). However, the reduction in the burst phenomena in the CS-g-PLA system suggests that the conjugation of CS with PLA causes a drop in the release rate, especially in the initial phase. This is important in terms of the massive release of bioactive molecules entrapped in the nanoparticles, which could alter the parameters of pharmacodynamics and pharmacokinetics.

Conclusions

In this study, nanoparticles made from CS and PLA grafted to CS backbone (CS-g-PLA) were prepared for encapsulation and controlled release of the model protein BSA.

The nanoparticles were synthetized via the polyelectrolyte complexation method using DS in mild acidic solution (pH 5.5). Particle diameter, the ζ-potential, and swelling behaviour of the systems were influenced by polymer concentration and the pH of the media. In acidic media, a reduction in particle dimension occurred when polymer concentration increased, while in PBS a decrease followed by an increase was obtained. TEM analysis confirmed the spherical shape and nano dimensions of the particles, even in the presence of aggregates. The amount of BSA entrapped was around 0.250–0.450 mg BSA/mg polymer in relation with CS and CS-g-PLA concentration. Increasing polymer concentration caused a decrease in the encapsulation efficiency that arose due to an increase in solution viscosity.

In vitro release studies of BSA from CS and CS-g-PLA nanoparticles in PBS pH 7.4 and SGF (pH 2), exhibited a sustained (up to one week) and controlled release in connection with the pH of the media. Reduction in the burst effect phenomena in the CS-g-PLA nanoparticles can be ascribed to the hydrophobic contribution of the PLA chains, as well as to the presence of -COOH groups that influence the release mechanism of BSA.

SUMMARY REMARKS

Polymeric nanoparticles as drug delivery systems represent a promising strategy in biomedical field. Compare to conventional drug delivery systems they display several advantages as increase the bioavailability, solubility, stability of different class of drugs in particular that which are difficult to administrate orally. Moreover, the use of nanoparticles as drug carriers increases the targeting, reduce the administration frequency and the dosage, resulting in a better patient compliance and side effect diminution.

Nowadays, great interest is growing in the multidrug encapsulation and delivery the effective dose at the target site at determined time. The aim is to ameliorate the multi-therapy approach for different diseases by administration of a single carrier which is able to release various bioactive compounds without interactions among them.

In this view, a set of amphiphilic polymers based on chitosan and different polylactic acid have been prepared to develop nanoparticles able to encapsulate, simultaneously, and release in a controlled way bioactive compounds, in particular anticancer drugs and one model protein.

All the amphiphilic polymers were obtained by coupling reaction between chitosan amino groups and carboxylic groups of PLA. FTIR-ATR and ^{1}H-NMR analysis confirmed the occurrence of the reaction for all formulations.

Nanoparticles were prepared by polyelectrolytes complexation which is a simple, solve free and low cost method with high reproducibility. According to the PLA side chain and the preparation conditions, nanoparticles displayed a diameter in the range 100-250 nm, ζ-potential in range 15-35 mV and high stability in preparation and physiological like media up to one month at room temperature and in cooling conditions (4°C).

Microscopic analysis demonstrates that almost all prepared nanoparticles presented a spherical shape in solutions while presence of aggregates were detected in the dried form.

All set of prepared nanoparticles were able to accommodate up to 0.8 mg of drug or protein per mg of carrier in preparation media. A direct influence of pH and ionic strength on the encapsulation efficiency was revealed. High encapsulation values have been obtained in case of multidrug encapsulation as well, with a distribution of the drugs close to 1:1.

Results demonstrate that the presence of PLA side chain, in particular in case of carboxy enriched PLA enables a higher encapsulation, in particular when more than one drug is loaded.

The effect of PLA on the release kinetic of all the loaded drug and protein was evident, in particular a noticeable reduction of the initial burst compare to unmodified chitosan was observed. In particular, in case of carboxy enriched PLA where the release took place after 4-5 hours following contact with the media.

The release of the loaded drugs and protein was strictly dependant to the pH of the release media. Obtained data demonstrate the possibility to increase or reduce the release rate by changing the pH of the environment. Increasing the pH, a faster release was observed. It allows to modulate the release according to the environment around the target site. Moreover, in case of multiple encapsulation no interferences occurred during the release between the drugs which presented a release trend comparable to the individual release.

MS analysis of the drug release from the nanoparticles proved that no changed in structure occurred. It indicates the ability of the prepared carriers to interact only physically with the loaded compounds and protect them from the external environment. It is particularly important in case of protein or some anticancer drugs like TMZ which are highly sensible to the external environment.

All the obtained data were subjected to statistical analysis to confirm the correlations among the PLA side chain structure and the nanoparticles properties in solution, encapsulation efficiency and in particular the release kinetic.

CONTRIBUTION TO SCIENCE AND PRACTICE

The presented thesis provides a review of the polymeric based nanoparticles for encapsulation and controlled release of bioactive molecules. All the procedure used during the experimental work were adopted or developed according to scientific works published in high impact factor journals.

The contribution of the reported work can be summarizing as follow:

-preparation of a set of amphiphilic polymers based on chitosan and various type of polylactic acid;

-development of nanoparticles based on the prepared polymer and evaluation of the physical-chemical properties, in relations to the chemical structure of PLA, and the influence of the external environment;

- single and simultaneous loading of bioactive molecules with different molecular weight, chemical structure and biological properties;

- Detailed evaluation of the influence of the external media, in particular simulated body fluid, on the release kinetics of the loaded molecules from the nanoparticles prepared.

REFERENCES

Ajima, K., Murakami, T., Mizoguchi, Y., Tsuchida, K., Ichihashi, T., Iijima, S., and Yudasaka, M. (2008). Enhancement of in vivo anticancer effects of cisplatin by incorporation inside single-wall carbon nanohorns. *Acs Nano*, *2*(10), 2057-2064.

Alves, N. M., and Mano, J. F. (2008). Chitosan derivatives obtained by chemical modifications for biomedical and environmental applications. *International journal of biological macromolecules*, *43*(5), 401-414.

Amann, L. C., Gandal, M. J., Lin, R., Liang, Y., and Siegel, S. J. (2010). In vitro–in vivo correlations of scalable PLGA-risperidone implants for the treatment of schizophrenia. *Pharmaceutical research*, *27*(8), 1730-1737.

Amidi, M., Romeijn, S. G., Borchard, G., Junginger, H. E., Hennink, W. E., and Jiskoot, W. (2006). Preparation and characterization of protein-loaded N-trimethyl chitosan nanoparticles as nasal delivery system. *Journal of Controlled Release*, *111*(1), 107-116.

Arhewoh, I. M., Okhamafe, A. O. (2004). An overview of site-specific delivery of orally administered proteins/peptides and modelling considerations.

Arifin, D. Y., Lee, L. Y., Wang, C. H. (2006). Mathematical modeling and simulation of drug release from microspheres: Implications to drug delivery systems. *Advanced drug delivery reviews*, *58*(12), 1274-1325.

Arsawang, U., Saengsawang, O., Rungrotmongkol, T., Sornmee, P., Wittayanarakul, K., Remsungnen, T., Hannongbua, S. (2011). How do carbon nanotubes serve as carriers for gemcitabine transport in a drug delivery system?. *Journal of Molecular Graphics and Modelling*, *29*(5), 591-596.

Aydin, R., Pulat, M. (2012). 5-Fluorouracil encapsulated chitosan nanoparticles for pH-stimulated drug delivery: evaluation of controlled release kinetics. *Journal of Nanomaterials*, *2012*, 42.

Bagheri-Khoulenjani, S., Taghizadeh, S. M., Mirzadeh, H. (2009). An investigation on the short-term biodegradability of chitosan with various molecular weights and degrees of deacetylation. *Carbohydrate Polymers*, *78*(4), 773-778.

Bajpai, A. K., Bajpai, J., Shukla, S. (2003). Release dynamics of tetracycline from a loaded semi-interpenetrating polymeric material of polyvinyl alcohol and poly (acrylamide-co-styrene). *Journal of Materials Science: Materials in Medicine*, *14*(4), 347-357.

Bajpai, A. K., Gupta, R. (2011). Magnetically mediated release of ciprofloxacin from polyvinyl alcohol based superparamagnetic nanocomposites. *Journal of Materials Science: Materials in Medicine*, *22*(2), 357-369.

Bajpai, J., Maan, G. K., Bajpai, A. K. (2012). Preparation, characterization and water uptake behavior of polysaccharide based nanoparticles: swelling behavior of nanoparticles. *Prog. Nanotech. Nanomater*, *1*, 9-17.

Beg, S., Rizwan, M., Sheikh, A. M., Hasnain, M. S., Anwer, K., Kohli, K. (2011). Advancement in carbon nanotubes: basics, biomedical applications and toxicity. *Journal of pharmacy and pharmacology*, *63*(2), 141-163.

Berger, J., Reist, M., Mayer, J. M., Felt, O., Gurny, R. (2004). Structure and interactions in chitosan hydrogels formed by complexation or aggregation for biomedical applications. *European Journal of Pharmaceutics and Biopharmaceutics*, *57*(1), 35-52.

Bhattarai, N., Ramay, H. R., Chou, S. H., Zhang, M. (2006). Chitosan and lactic acid-grafted chitosan nanoparticles as carriers for prolonged drug delivery. *International journal of nanomedicine*, *1*(2), 181.

Bhirde, A. A., Patel, S., Sousa, A. A., Patel, V., Molinolo, A. A., Ji, Y., Rusling, J. F. (2010). Distribution and clearance of PEG-single-walled carbon nanotube cancer drug delivery vehicles in mice. *Nanomedicine*, *5*(10), 1535-1546.

Bielawski, K., Bielawska, A., Muszyńska, A., Popławska, B., Czarnomysy, R. (2011). Cytotoxic activity of G3 PAMAM-NH 2 dendrimer-chlorambucil conjugate in human breast cancer cells. *environmental toxicology and pharmacology*, *32*(3), 364-372.

Bigucci, F., Luppi, B., Cerchiara, T., Sorrenti, M., Bettinetti, G., Rodriguez, L., Zecchi, V. (2008). Chitosan/pectin polyelectrolyte complexes: selection of suitable preparative conditions for colon-specific delivery of vancomycin. *European journal of pharmaceutical sciences*, *35*(5), 435-441.

Bilensoy, E., Sarisozen, C., Esendağlı, G., Doğan, A. L., Aktaş, Y., Şen, M., Mungan, N. A. (2009). Intravesical cationic nanoparticles of chitosan and polycaprolactone for the delivery of Mitomycin C to bladder tumors. *International journal of pharmaceutics*, *371*(1), 170-176.

Bois, F. Y. (2010). Physiologically based modelling and prediction of drug interactions. *Basic & clinical pharmacology & toxicology*, *106*(3), 154-161.

Boppana, R., Kulkarni, R. V., Setty, C. M., Kalyane, N. V. (2010). Carboxymethylcellulose-aluminum hydrogel microbeads for prolonged release of simvastatin. *Acta Pharmaceutica Sciencia*, *52*, 137-143.

Bordi, F., Chronopoulou, L., Palocci, C., Bomboi, F., Di Martino, A., Cifani, N., Sennato, S. (2014). Chitosan–DNA complexes: effect of molecular parameters on the efficiency of delivery. *Colloids and Surfaces A: Physicochemical and Engineering Aspects*, *460*, 184-190.

Brown, S. C., Kamal, M., Nasreen, N., Baumuratov, A., Sharma, P., Antony, V. B., Moudgil, B. M. (2007). Influence of shape, adhesion and simulated lung mechanics on amorphous silica nanoparticle toxicity. *Advanced Powder Technology*, *18*(1), 69-79.

Calvo, P., Remunan-Lopez, C., Vila-Jato, J. L., Alonso, M. J. (1997). Novel hydrophilic chitosan-polyethylene oxide nanoparticles as protein carriers. *Journal of Applied Polymer Science*, *63*(1), 125-132.

Calvo, P., Remuñan-López, C., Vila-Jato, J. L., Alonso, M. J. (1997). Chitosan and chitosan/ethylene oxide-propylene oxide block copolymer nanoparticles as novel carriers for proteins and vaccines. *Pharmaceutical research*, *14*(10), 1431-1436.

Casey, A., Herzog, E., Davoren, M., Lyng, F. M., Byrne, H. J., Chambers, G. (2007). Spectroscopic analysis confirms the interactions between single walled carbon nanotubes and various dyes commonly used to assess cytotoxicity. *Carbon*, *45*(7), 1425-1432.

Chang, J. S., Chang, K. L. B., Hwang, D. F., Kong, Z. L. (2007). In vitro cytotoxicitiy of silica nanoparticles at high concentrations strongly depends on the metabolic activity type of the cell line. *Environmental Science & Technology*, *41*(6), 2064-2068.

Chang, K. L. B., Lin, J. (2000). Swelling behavior and the release of protein from chitosan–pectin composite particles. *Carbohydrate polymers*, *43*(2), 163-169.

Chen, J., Zhou, M. (2010). Determination of eniluracil and 5-fluorouracil in human plasma by LC-MS/MS. *Bioanalysis*, *2*(12), 2011-2017.

Chen, K. J., Chiu, Y. L., Chen, Y. M., Ho, Y. C., & Sung, H. W. (2011). Intracellularly monitoring/imaging the release of doxorubicin from pH-responsive nanoparticles using Förster resonance energy transfer. *Biomaterials*, *32*(10), 2586-2592.

Chen, S., Zhu, J., Cheng, J. (2007). Preparation and in vitro evaluation of a novel combined multiparticulate delayed-onset sustained-release formulation of diltiazem hydrochloride. *Die Pharmazie-An International Journal of Pharmaceutical Sciences*, *62*(12), 907-913.

Chen, Y., Mohanraj, V. J., Wang, F., Benson, H. A. (2007). Designing chitosan-dextran sulfate nanoparticles using charge ratios. *AAPS PharmSciTech*, *8*(4), 131-139.

Chhatri, A., Bajpai, J., Bajpai, A. K., Sandhu, S. S., Jain, N., Biswas, J. (2011). Cryogenic fabrication of savlon loaded macroporous blends of alginate and polyvinyl alcohol (PVA). Swelling, deswelling and antibacterial behaviors. *Carbohydrate Polymers*, *83*(2), 876-882.

Chithrani, B. D., Chan, W. C. (2007). Elucidating the mechanism of cellular uptake and removal of protein-coated gold nanoparticles of different sizes and shapes. *Nano letters*, *7*(6), 1542-1550.

Cho, M., Cho, W. S., Choi, M., Kim, S. J., Han, B. S., Kim, S. H., Jeong, J. (2009). The impact of size on tissue distribution and elimination by single intravenous injection of silica nanoparticles. *Toxicology letters*, *189*(3), 177-183.

Chomoucka, J., Drbohlavova, J., Huska, D., Adam, V., Kizek, R., Hubalek, J. (2010). Magnetic nanoparticles and targeted drug delivering. *Pharmacological Research*, *62*(2), 144-149.

Chouhan, R., Bajpai, A. K. (2009). An in vitro release study of 5-fluoro-uracil (5-FU) from swellable poly-(2-hydroxyethylmethacrylate)(PHEMA) nanoparticles. *Journal of Materials Science: Materials in Medicine*, *20*(5), 1103-1114.

Ciofani, G., Danti, S., D'Alessandro, D., Moscato, S., Menciassi, A. (2010). Assessing cytotoxicity of boron nitride nanotubes: interference with the MTT assay. *Biochemical and biophysical research communications*, *394*(2), 405-411.

Cocero, M. J., Martín, Á., Mattea, F., Varona, S. (2009). Encapsulation and co-precipitation processes with supercritical fluids: fundamentals and applications. *The Journal of Supercritical Fluids*, *47*(3), 546-555.

Coelho, J. F., Ferreira, P. C., Alves, P., Cordeiro, R., Fonseca, A. C., Góis, J. R., Gil, M. H. (2010). Drug delivery systems: Advanced technologies potentially applicable in personalized treatments. *The EPMA journal*, *1*(1), 164-209.

Cooper, C. L., Dubin, P. L., Kayitmazer, A. B., Turksen, S. (2005). Polyelectrolyte–protein complexes. *Current Opinion in Colloid & Interface Science*, *10*(1), 52-78.

Costa, P., & Lobo, J. M. S. (2001). Modeling and comparison of dissolution profiles. *European journal of pharmaceutical sciences*, *13*(2), 123-133.

Csaba, N., Caamaño, P., Sánchez, A., Domínguez, F., Alonso, M. J. (2005). PLGA: poloxamer and PLGA: poloxamine blend nanoparticles: new carriers for gene delivery. *Biomacromolecules*, *6*(1), 271-278.

Csajka, C., Verotta, D. (2006). Pharmacokinetic–pharmacodynamic modelling: history and perspectives. *Journal of pharmacokinetics and pharmacodynamics*, *33*(3), 227-279.

Dadsetan, M., Taylor, K. E., Yong, C., Bajzer, Ž., Lu, L., Yaszemski, M. J. (2013). Controlled release of doxorubicin from pH-responsive microgels. *Acta biomaterialia*, *9*(3), 5438-5446.

Danhier, F., Ansorena, E., Silva, J. M., Coco, R., Le Breton, A., Préat, V. (2012). PLGA-based nanoparticles: an overview of biomedical applications. *Journal of controlled release*, *161*(2), 505-522.

Danhof, M., de Lange, E. C., Della Pasqua, O. E., Ploeger, B. A., Voskuyl, R. A. (2008). Mechanism-based pharmacokinetic-pharmacodynamic (PK-PD) modeling in translational drug research. *Trends in pharmacological sciences*, *29*(4), 186-191.

Dash, S., Murthy, P. N., Nath, L., Chowdhury, P. (2010). Kinetic modeling on drug release from controlled drug delivery systems. *Acta Pol Pharm*, *67*(3), 217-23.

de Alvarenga, E. S., de Oliveira, C. P., Bellato, C. R. (2010). An approach to understanding the deacetylation degree of chitosan. *Carbohydrate Polymers*, *80*(4), 1155-1160.

De Campos, A. M., Sánchez, A., Alonso, M. J. (2001). Chitosan nanoparticles: a new vehicle for the improvement of the delivery of drugs to the ocular surface. Application to cyclosporin A. *International journal of pharmaceutics*, *224*(1), 159-168.

de Vos, P., Faas, M. M., Spasojevic, M., Sikkema, J. (2010). Encapsulation for preservation of functionality and targeted delivery of bioactive food components. *International Dairy Journal*, *20*(4), 292-302.

Derissen, E. J., Hillebrand, M. J., Rosing, H., Schellens, J. H., Beijnen, J. H. (2015). Development of an LC–MS/MS assay for the quantitative determination of the intracellular 5-fluorouracil nucleotides responsible for the anticancer effect of 5-fluorouracil. *Journal of pharmaceutical and biomedical analysis*, *110*, 58-66.

Dhawan, A., Sharma, V. (2010). Toxicity assessment of nanomaterials: methods and challenges. *Analytical and bioanalytical chemistry*, *398*(2), 589-605.

Di Crescenzo, A., Velluto, D., Hubbell, J. A., Fontana, A. (2011). Biocompatible dispersions of carbon nanotubes: a potential tool for intracellular transport of anticancer drugs. *Nanoscale*, *3*(3), 925-928.

Di Martino, A., Kucharczyk, P., Zednik, J., Sedlarik, V. (2015). Chitosan grafted low molecular weight polylactic acid for protein encapsulation and burst effect reduction. *International journal of pharmaceutics*, *496*(2), 912-921.

Di Martino, A., Sedlarik, V. (2014). Amphiphilic chitosan-grafted-functionalized polylactic acid based nanoparticles as a delivery system for doxorubicin and temozolomide co-therapy. *International journal of pharmaceutics*, *474*(1), 134-145.

Di Pasqua, A. J., Wallner, S., Kerwood, D. J., Dabrowiak, J. C. (2009). Adsorption of the PtII anticancer drug carboplatin by mesoporous silica.*Chemistry & biodiversity*, *6*(9), 1343-1349.

Dionísio, M., Cordeiro, C., Remuñán-López, C., Seijo, B., da Costa, A. M. R., Grenha, A. (2013). Pullulan-based nanoparticles as carriers for transmucosal protein delivery. *European Journal of Pharmaceutical Sciences*, *50*(1), 102-113.

Dobrovolskaia, M. A., Mcneil, S. E. Immunological properties of engineered nanomaterials. Nature Nanotech. 2, 469–478 (2007). *Excellent perspective regarding formal guidelines for the testing of nanomaterials. Article ChemPort*.

Dokoumetzidis, A., Papadopoulou, V., Macheras, P. (2006). Analysis of dissolution data using modified versions of Noyes–Whitney equation and the Weibull function. *Pharmaceutical research*, *23*(2), 256-261.

Errico, C., Bartoli, C., Chiellini, F., Chiellini, E. (2009). Poly (hydroxyalkanoates)-based polymeric nanoparticles for drug delivery. *BioMed Research International*, *2009*.

Fernandez-Fernandez, A., Manchanda, R., McGoron, A. J. (2011). Theranostic applications of nanomaterials in cancer: drug delivery, image-guided therapy, and multifunctional platforms. *Applied biochemistry and biotechnology*, *165*(7-8), 1628-1651.

Finkelstein, A., McClean, D., Kar, S., Takizawa, K., Varghese, K., Baek, N., Eigler, N. L. (2003). Local drug delivery via a coronary stent with programmable release pharmacokinetics. *Circulation*, *107*(5), 777-784.

Fortner, J. D., Lyon, D. Y., Sayes, C. M., Boyd, A. M., Falkner, J. C., Hotze, E. M., Colvin, V. L. (2005). C60 in water: nanocrystal formation and microbial response. *Environmental Science & Technology*, *39*(11), 4307-4316.

Freitas, M. N., Marchetti, J. M. (2005). Nimesulide PLA microspheres as a potential sustained release system for the treatment of inflammatory diseases.*International journal of pharmaceutics*, *295*(1), 201-211.

Friedman, H. S., Kerby, T., Calvert, H. (2000). Temozolomide and treatment of malignant glioma. *Clinical Cancer Research*, *6*(7), 2585-2597.

Fu, Y., Kao, W. J. (2010). Drug release kinetics and transport mechanisms of non-degradable and degradable polymeric delivery systems. *Expert opinion on drug delivery*, *7*(4), 429-444.

Gaihre, B., Khil, M. S., Lee, D. R., Kim, H. Y. (2009). Gelatin-coated magnetic iron oxide nanoparticles as carrier system: drug loading and in vitro drug release study. *International Journal of Pharmaceutics*, *365*(1), 180-189.

Galindo-Rodriguez, S., Allémann, E., Fessi, H., Doelker, E. (2004). Physicochemical parameters associated with nanoparticle formation in the salting-out, emulsification-diffusion, and nanoprecipitation methods. *Pharmaceutical research*, *21*(8), 1428-1439.

Ganachaud, F., Katz, J. L. (2005). Nanoparticles and Nanocapsules Created Using the Ouzo Effect: Spontaneous Emulsification as an Alternative to Ultrasonic and High-Shear Devices. *ChemPhysChem*, *6*(2), 209-216.

Goycoolea, F. M., Lollo, G., Remunán-López, C., Quaglia, F., Alonso, M. J. (2009). Chitosan-alginate blended nanoparticles as carriers for the transmucosal delivery of macromolecules. *Biomacromolecules*, *10*(7), 1736-1743.

Gulson, B., Wong, H. (2006). Stable isotopic tracing: A way forward for nanotechnology. *Environmental health perspectives*, 1486-1488.

Gupta, A. K., Gupta, M. (2005). Synthesis and surface engineering of iron oxide nanoparticles for biomedical applications. *Biomaterials*, *26*(18), 3995-4021.

He, Q., Liu, J., Sun, X., Zhang, Z. R. (2004). Preparation and characteristics of DNA-nanoparticles targeting to hepatocarcinoma cells. *World J Gastroenterol*, *10*(5), 660-663.

Hewakuruppu, Y. L., Dombrovsky, L. A., Chen, C., Timchenko, V., Jiang, X., Baek, S., Taylor, R. A. (2013). Plasmonic "pump–probe" method to study semi-transparent nanofluids. *Applied optics*, *52*(24), 6041-6050.

Honary, S., Zahir, F. (2013). Effect of zeta potential on the properties of nano-drug delivery systems-a review (Part 2). *Tropical Journal of Pharmaceutical Research*, *12*(2), 265-273.

Hornig, S., Bunjes, H., Heinze, T. (2009). Preparation and characterization of nanoparticles based on dextran–drug conjugates. *Journal of colloid and interface science*, *338*(1), 56-62.

Howard, M. D., Lu, X., Jay, M., Dziubla, T. D. (2012). Optimization of the lyophilization process for long-term stability of solid–lipid nanoparticles. *Drug development and industrial pharmacy*, *38*(10), 1270-1279.

Hu, C. M. J., Aryal, S., Zhang, L. (2010). Nanoparticle-assisted combination therapies for effective cancer treatment. *Therapeutic delivery*, *1*(2), 323-334.

Hu, X., Tang, Y., Wang, Q., Li, Y., Yang, J., Du, Y., Kennedy, J. F. (2011). Rheological behavior of chitin in NaOH/urea aqueous solution. *Carbohydrate Polymers*, *83*(3), 1128-1133.

Huang, H. C., Barua, S., Sharma, G., Dey, S. K., Rege, K. (2011). Inorganic nanoparticles for cancer imaging and therapy. *Journal of controlled Release*,*155*(3), 344-357.

Huang, L., Wang, Z., Sun, J., Miao, L., Li, Q., Yan, Y., Zhao, D. (2000). Fabrication of ordered porous structures by self-assembly of zeolite nanocrystals. *Journal of the American Chemical Society*, *122*(14), 3530-3531.

Il'ina, A. V., Varlamov, V. P. (2005). Chitosan-based polyelectrolyte complexes: a review. *Applied Biochemistry and Microbiology*, *41*(1), 5-11.

Janes, K. A., Calvo, P., Alonso, M. J. (2001). Polysaccharide colloidal particles as delivery systems for macromolecules. *Advanced drug delivery reviews*, *47*(1), 83-97.

Javid, A., Ahmadian, S., Saboury, A. A., Kalantar, S. M., Rezaei-Zarchi, S. (2013). Chitosan-Coated Superparamagnetic Iron Oxide Nanoparticles for Doxorubicin Delivery: Synthesis and Anticancer Effect Against Human Ovarian Cancer Cells. *Chemical biology & drug design*, *82*(3), 296-306.

Jayakumar, R., Prabaharan, M., Nair, S. V., Tamura, H. (2010). Novel chitin and chitosan nanofibers in biomedical applications. *Biotechnology advances*,*28*(1), 142-150.

Jelvehgari, M., Montazam, S. H. (2012). Comparison of microencapsulation by emulsion-solvent extraction/evaporation technique using derivatives cellulose and acrylate-methacrylate copolymer as carriers. *Jundishapur Journal of Natural Pharmaceutical Products*, *7*(4), 144.

Jhaveri, S. J., Hynd, M. R., Dowell-Mesfin, N., Turner, J. N., Shain, W., Ober, C. K. (2008). Release of nerve growth factor from HEMA hydrogel-coated substrates and its effect on the differentiation of neural cells. *Biomacromolecules*, *10*(1), 174-183.

Jia, G., Wang, H., Yan, L., Wang, X., Pei, R., Yan, T., Guo, X. (2005). Cytotoxicity of carbon nanomaterials: single-wall nanotube, multi-wall nanotube, and fullerene. *Environmental science & technology*, *39*(5), 1378-1383.

Jiang, T., Li, Y. M., Lv, Y., Cheng, Y. J., He, F., Zhuo, R. X. (2013). Amphiphilic polycarbonate conjugates of doxorubicin with pH-sensitive hydrazone linker for controlled release. *Colloids and Surfaces B: Biointerfaces*,*111*, 542-548.

Jiang, W., Schwendeman, S. P. (2001). Stabilization and controlled release of bovine serum albumin encapsulated in poly (D, L-lactide) and poly (ethylene glycol) microsphere blends. *Pharmaceutical research*, *18*(6), 878-885.

Johnson, K. C., Swindell, A. C. (1996). Guidance in the setting of drug particle size specifications to minimize variability in absorption. *Pharmaceutical research*, *13*(12), 1795-1798.

Ju, R. T., Nixon, P. R., Patel, M. V. (1995). Drug release from hydrophilic matrices. 1. New scaling laws for predicting polymer and drug release based on the polymer disentanglement concentration and the diffusion layer. *Journal of pharmaceutical sciences*, *84*(12), 1455-1463.

Kachrimanis, K., Malamataris, S. (2000). Release of ibuprofen from spherical crystal agglomerates prepared using the solvent-change technique in the presence of Eudragit polymers and from corresponding compacts. *STP pharma sciences*, *10*(5), 387-393.

Kale, S. N., Jadhav, A. D., Verma, S., Koppikar, S. J., Kaul-Ghanekar, R., Dhole, S. D., Ogale, S. B. (2012). Characterization of biocompatible NiCo 2 O 4 nanoparticles for applications in hyperthermia and drug delivery.*Nanomedicine: Nanotechnology, Biology and Medicine*, *8*(4), 452-459.

Kasaai, M. R., Arul, J., Charlet, G. (2000). Intrinsic viscosity–molecular weight relationship for chitosan. *Journal of Polymer Science Part B: Polymer Physics*, *38*(19), 2591-2598.

Katas, H., Raja, M. A. G., Lam, K. L. (2013). Development of chitosan nanoparticles as a stable drug delivery system for protein/siRNA. *International journal of biomaterials*, *2013*.

Katiyar, S., Pandit, J., Mondal, R. S., Mishra, A. K., Chuttani, K., Aqil, M., Sultana, Y. (2014). In situ gelling dorzolamide loaded chitosan nanoparticles for the treatment of glaucoma. *Carbohydrate polymers*, *102*, 117-124.

Kievit, F. M., Wang, F. Y., Fang, C., Mok, H., Wang, K., Silber, J. R., Zhang, M. (2011). Doxorubicin loaded iron oxide nanoparticles overcome multidrug resistance in cancer in vitro. *Journal of controlled release*, *152*(1), 76-83.

Kim, J. H., Li, Y., Kim, M. S., Kang, S. W., Jeong, J. H., Lee, D. S. (2012). Synthesis and evaluation of biotin-conjugated pH-responsive polymeric micelles as drug carriers. *International journal of pharmaceutics*, *427*(2), 435-442.

Kim, T. H., Park, Y. H., Kim, K. J., Cho, C. S. (2003). Release of albumin from chitosan-coated pectin beads in vitro. *International journal of pharmaceutics*, *250*(2), 371-383.

Kong, B., Seog, J. H., Graham, L. M., Lee, S. B. (2011). Experimental considerations on the cytotoxicity of nanoparticles. *Nanomedicine*, *6*(5), 929-941.

Koo, O. M., Rubinstein, I., Onyuksel, H. (2005). Role of nanotechnology in targeted drug delivery and imaging: a concise review. *Nanomedicine: Nanotechnology, Biology and Medicine*, *1*(3), 193-212.

Kucharczyk, P., Poljansek, I., Sedlarik, V., Kasparkova, V., Salakova, A., Drbohlav, J., Saha, P. (2011). Functionalization of polylactic acid through direct melt polycondensation in the presence of tricarboxylic acid. *Journal of Applied Polymer Science*, *122*(2), 1275-1285.

Kumar, A., Boruah, B. M., Liang, X. J. (2011). Gold nanoparticles: promising nanomaterials for the diagnosis of cancer and HIV/AIDS. *Journal of Nanomaterials*, *2011*, 22.

Kumar, N., Langer, R. S., Domb, A. J. (2002). Polyanhydrides: an overview. *Advanced drug delivery reviews*, *54*(7), 889-910.

Kumar, R., Roy, I., Ohulchanskky, T. Y., Vathy, L. A., Bergey, E. J., Sajjad, M., Prasad, P. N. (2010). In vivo biodistribution and clearance studies using multimodal organically modified silica nanoparticles. *ACS nano*, *4*(2), 699-708.

Kunjachan, S., Rychlik, B., Storm, G., Kiessling, F., Lammers, T. (2013). Multidrug resistance: Physiological principles and nanomedical solutions. *Advanced drug delivery reviews*, *65*(13), 1852-1865.

Lankalapalli, S., Kolapalli, V. M. (2009). Polyelectrolyte complexes: a review of their applicability in drug delivery technology. *Indian journal of pharmaceutical sciences*, *71*(5), 481.

Laroui, H., Viennois, E., Xiao, B., Canup, B. S., Geem, D., Denning, T. L., Merlin, D. (2014). Fab'-bearing siRNA TNFα-loaded nanoparticles targeted to colonic macrophages offer an effective therapy for experimental colitis. *Journal of Controlled Release*, *186*, 41-53.

Laub, P. B., Gallo, J. M. (1996). NCOMP—A windows-based computer program for noncompartmental analysis of pharmacokinetic data. *Journal of pharmaceutical sciences*, *85*(4), 393-395.

Lee, E. J., Ribeiro, C., Longo, E., Leite, E. R. (2006). Growth kinetics of tin oxide nanocrystals in colloidal suspensions under hydrothermal conditions. *Chemical physics*, *328*(1), 229-235.

Lee, E., Lee, J., Lee, I. H., Yu, M., Kim, H., Chae, S. Y., Jon, S. (2008). Conjugated chitosan as a novel platform for oral delivery of paclitaxel. *Journal of medicinal chemistry*, *51*(20), 6442-6449.

Lee, T. H., Wang, J., Wang, C. H. (2002). Double-walled microspheres for the sustained release of a highly water soluble drug: characterization and irradiation studies. *Journal of controlled release*, *83*(3), 437-452.

Leu, Y. Y., & Chow, W. S. (2011). Kinetics of water absorption and thermal properties of poly (lactic acid)/organomontmorillonite/poly (ethylene glycol) nanocomposites. *Journal of Vinyl and Additive Technology*, *17*(1), 40-47.

Li, J., Kong, M., Cheng, X. J., Dang, Q. F., Zhou, X., Wei, Y. N., Chen, X. G. (2012). Preparation of biocompatible chitosan grafted poly (lactic acid) nanoparticles. *International journal of biological macromolecules*, *51*(3), 221-227.

Li, S., He, H., Parthiban, L. J., Yin, H., Serajuddin, A. (2005). IV-IVC considerations in the development of immediate-release oral dosage form. *Journal of pharmaceutical sciences*, *94*(7), 1396-1417.

Li, T., Wang, G. D., Tan, Y. Z., Wang, H. J. (2014). Inhibition of lymphangiogenesis of endothelial progenitor cells with VEGFR-3 siRNA delivered with PEI-alginate nanoparticles. *International journal of biological sciences*, *10*(2), 160..

Liggins, R. T., Burt, H. M. (2001). Paclitaxel loaded poly (L-lactic acid) microspheres: properties of microspheres made with low molecular weight polymers. *International journal of pharmaceutics*, *222*(1), 19-33.

Limbach, L. K., Li, Y., Grass, R. N., Brunner, T. J., Hintermann, M. A., Muller, M., Stark, W. J. (2005). Oxide nanoparticle uptake in human lung fibroblasts: effects of particle size, agglomeration, and diffusion at low concentrations. *Environmental science & technology*, *39*(23), 9370-9376.

Lin, M., Meng, S., Zhong, W., Cai, R., Du, Q., Tomasik, P. (2009). Novel drug-loaded gelatin films and their sustained-release performance. *Journal of Biomedical Materials Research Part B: Applied Biomaterials*, *90*(2), 939-944.

Lin, W. C., Yu, D. G., Yang, M. C. (2005). pH-sensitive polyelectrolyte complex gel microspheres composed of chitosan/sodium tripolyphosphate/dextran sulfate: swelling kinetics and drug delivery properties. *Colloids and surfaces B: Biointerfaces*, *44*(2), 143-151.

Lisunova, M. O., Lebovka, N. I., Melezhyk, O. V., Boiko, Y. P. (2006). Stability of the aqueous suspensions of nanotubes in the presence of nonionic surfactant. *Journal of colloid and interface science*, *299*(2), 740-746.

Liu, Z., Jiao, Y., Wang, Y., Zhou, C., Zhang, Z. (2008). Polysaccharides-based nanoparticles as drug delivery systems. *Advanced drug delivery reviews*, *60*(15), 1650-1662.

Losic, D., Yu, Y., Aw, M. S., Simovic, S., Thierry, B., Addai-Mensah, J. (2010). Surface functionalisation of diatoms with dopamine modified iron-oxide nanoparticles: toward magnetically guided drug microcarriers with biologically derived morphologies. *Chemical Communications*, *46*(34), 6323-6325.

Lu, G., Kong, L., Sheng, B., Wang, G., Gong, Y., Zhang, X. (2007). Degradation of covalently cross-linked carboxymethyl chitosan and its potential application for peripheral nerve regeneration. *European Polymer Journal*, *43*(9), 3807-3818.

Luo, X., Matranga, C., Tan, S., Alba, N., Cui, X. T. (2011). Carbon nanotube nanoreservior for controlled release of anti-inflammatory dexamethasone. *Biomaterials*, *32*(26), 6316-6323.

Luo, Y., Wang, Q. (2014). Recent development of chitosan-based polyelectrolyte complexes with natural polysaccharides for drug delivery. *International journal of biological macromolecules*, *64*, 353-367.

Madhusudhan, B., Ravikumara, N. R., Nagaraj, T. S., Aditya, N. P., HIREMAT, S., Raina, G. (2009). Preparation and evaluation of nimesulide-loaded ethylcellulose and methylcellulose nanoparticles and microparticles for oral delivery. *Journal of biomaterials applications*.

MaHam, A., Tang, Z., Wu, H., Wang, J., Lin, Y. (2009). Protein-Based Nanomedicine Platforms for Drug Delivery. *Small*, *5*(15), 1706-1721.

Mahmoudi, M., Simchi, A., Imani, M., Shokrgozar, M. A., Milani, A. S., Häfeli, U. O., Stroeve, P. (2010). A new approach for the in vitro identification of the cytotoxicity of superparamagnetic iron oxide nanoparticles. *Colloids and Surfaces B: Biointerfaces*, *75*(1), 300-309.

Mao, H. Q., Roy, K., Troung-Le, V. L., Janes, K. A., Lin, K. Y., Wang, Y., Leong, K. W. (2001). Chitosan-DNA nanoparticles as gene carriers: synthesis, characterization and transfection efficiency. *Journal of controlled release*, *70*(3), 399-421.

Mara Mainardes, R., Cristina Cocenza Urban, M., Oliveira Cinto, P., Vinicius Chaud, M., Cesar Evangelista, R., Palmira Daflon Gremiao, M. (2006). Liposomes and micro/nanoparticles as colloidal carriers for nasal drug delivery. *Current drug delivery*, *3*(3), 275-285.

Martinez-Ruvalcaba, A., Sanchez-Diaz, J. C., Becerra, F., Cruz-Barba, L. E., Gonzalez-Alvarez, A. (2009). Swelling characterization and drug delivery kinetics of polyacrylamide-co-itaconic acid/chitosan hydrogels. *Express Polym Lett*, *3*(1), 25-32.

Mehta, R. C., Thanoo, B. C., Deluca, P. P. (1996). Peptide containing microspheres from low molecular weight and hydrophilic poly (d, l-lactide-co-glycolide). *Journal of Controlled Release*, *41*(3), 249-257.

Meng, X., Seton, H. C., Lu, L. T., Prior, I. A., Thanh, N. T., Song, B. (2011). Magnetic CoPt nanoparticles as MRI contrast agent for transplanted neural stem cells detection. *Nanoscale*, *3*(3), 977-984.

Mishra, B., Patel, B. B., Tiwari, S. (2010). Colloidal nanocarriers: a review on formulation technology, types and applications toward targeted drug delivery. *Nanomedicine: Nanotechnology, biology and medicine*, *6*(1), 9-24.

Molpeceres, J., Aberturas, M. R., Guzman, M. (2000). Biodegradable nanoparticles as a delivery system for cyclosporine: preparation and characterization. *Journal of microencapsulation*, *17*(5), 599-614.

Moody, C. L., Wheelhouse, R. T. (2014). The medicinal chemistry of imidazotetrazine prodrugs. *Pharmaceuticals*, *7*(7), 797-838.

Morris, G. A., Castile, J., Smith, A., Adams, G. G., Harding, S. E. (2011). The effect of prolonged storage at different temperatures on the particle size distribution of tripolyphosphate (TPP)–chitosan nanoparticles. *Carbohydrate polymers*, *84*(4), 1430-1434.

Mourya, V. K., Inamdar, N. N. (2008). Chitosan-modifications and applications: opportunities galore. *Reactive and Functional polymers*, *68*(6), 1013-1051.

Murthy, T. E. G. K., Chowdary, K. P. R. (2005). Formulation and evaluation of ethyl cellulose-coated diclofenac sodium microcapsules: Influence of solvents. *Indian journal of pharmaceutical sciences*, *67*(2), 216-219.

Nagarwal, R. C., Nath Singh, P., Kant, S., Maiti, P., Pandit, J. K. (2011). Chitosan nanoparticles of 5-fluorouracil for ophthalmic delivery: characterization, in-vitro and in-vivo study. *Chemical and Pharmaceutical Bulletin*, *59*(2), 272-278.

Nair, L. S., Laurencin, C. T. (2007). Biodegradable polymers as biomaterials. *Progress in polymer science*, *32*(8), 762-798.

Nan, A., Bai, X., Son, S. J., Lee, S. B., Ghandehari, H. (2008). Cellular uptake and cytotoxicity of silica nanotubes. *Nano letters*, *8*(8), 2150-2154.

Nemmar, A., Hoylaerts, M. F., Hoet, P. H., Dinsdale, D., Smith, T., Xu, H., Nemery, B. (2002). Ultrafine particles affect experimental thrombosis in an in vivo hamster model. *American journal of respiratory and critical care medicine*, *166*(7), 998-1004.

Oberdörster, G., Sharp, Z., Atudorei, V., Elder, A., Gelein, R., Lunts, A., Cox, C. (2002). Extrapulmonary translocation of ultrafine carbon particles following whole-body inhalation exposure of rats. *Journal of Toxicology and Environmental Health Part A*, *65*(20), 1531-1543.

Ochoa, L., Igartua, M., Hernández, R. M., Gascón, A. R., Solinis, M. A., Pedraz, J. L. (2011). Novel extended-release formulation of lovastatin by one-step melt granulation: in vitro and in vivo evaluation. *European Journal of Pharmaceutics and Biopharmaceutics*, *77*(2), 306-312.

Pan, Y., Neuss, S., Leifert, A., Fischler, M., Wen, F., Simon, U., Jahnen-Dechent, W. (2007). Size-dependent cytotoxicity of gold nanoparticles. *Small*, *3*(11), 1941-1949.

Parhi, P., Mohanty, C., Sahoo, S. K. (2012). Nanotechnology-based combinational drug delivery: an emerging approach for cancer therapy. *Drug discovery today*, *17*(17), 1044-1052.

Park, M. V., Annema, W., Salvati, A., Lesniak, A., Elsaesser, A., Barnes, C., Piersma, A. H. (2009). In vitro developmental toxicity test detects inhibition of stem cell differentiation by silica nanoparticles. *Toxicology and applied pharmacology*, *240*(1), 108-116.

Pasparakis, G., Bouropoulos, N. (2006). Swelling studies and in vitro release of verapamil from calcium alginate and calcium alginate–chitosan beads. *International journal of pharmaceutics*, *323*(1), 34-42.

Patil, P., Chavanke, D., Wagh, M. (2012). A review on ionotropic gelation method: novel approach for controlled gastroretentive gelispheres. *International journal of pharmaceutics and Pharmaceutical Science*, *4*(4), 27-32.

Peters, S. A. (2008). Evaluation of a generic physiologically based pharmacokinetic model for lineshape analysis. *Clinical pharmacokinetics*, *47*(4), 261-275.

Poland, C. A., Duffin, R., Kinloch, I., Maynard, A., Wallace, W. A., Seaton, A., Donaldson, K. (2008). Carbon nanotubes introduced into the abdominal cavity of mice show asbestos-like pathogenicity in a pilot study. *Nature nanotechnology*, *3*(7), 423-428.

Poletto, F. S., Jäger, E., Ré, M. I., Guterres, S. S., Pohlmann, A. R. (2007). Rate-modulating PHBHV/PCL microparticles containing weak acid model drugs. *International journal of pharmaceutics*, *345*(1), 70-80.

Popovici, R. F., Seftel, E. M., Mihai, G. D., Popovici, E., Voicu, V. A. (2011). Controlled drug delivery system based on ordered mesoporous silica matrices of captopril as angiotensin-converting enzyme inhibitor drug. *Journal of pharmaceutical sciences*, *100*(2), 704-714.

Prajapati, V. K., Awasthi, K., Gautam, S., Yadav, T. P., Rai, M., Srivastava, O. N., Sundar, S. (2011). Targeted killing of Leishmania donovani in vivo and in vitro with amphotericin B attached to functionalized carbon nanotubes. *Journal of antimicrobial chemotherapy*, dkr002.

Rao, J. P., Geckeler, K. E. (2011). Polymer nanoparticles: preparation techniques and size-control parameters. *Progress in Polymer Science*, *36*(7), 887-913.

Reis, C. P., Neufeld, R. J., Ribeiro, A. J., Veiga, F. (2006). Nanoencapsulation I. Methods for preparation of drug-loaded polymeric nanoparticles. *Nanomedicine: Nanotechnology, Biology and Medicine*, *2*(1), 8-21.

Rinaudo, M. (2006). Chitin and chitosan: properties and applications. *Progress in polymer science*, *31*(7), 603-632.

Rothen-Rutishauser, B. M., Kiama, S. G., Gehr, P. (2005). A three-dimensional cellular model of the human respiratory tract to study the interaction with particles. *American journal of respiratory cell and molecular biology*, *32*(4), 281-289.

Rothstein, S. N., Federspiel, W. J., Little, S. R. (2009). A unified mathematical model for the prediction of controlled release from surface and bulk eroding polymer matrices. *Biomaterials*, *30*(8), 1657-1664.

Safari, J., Zarnegar, Z. (2014). Advanced drug delivery systems: Nanotechnology of health design A review. *Journal of Saudi Chemical Society*, *18*(2), 85-99.

Sahoo, S., Sasmal, A., Nanda, R., Phani, A. R., Nayak, P. L. (2010). Synthesis of chitosan–polycaprolactone blend for control delivery of ofloxacin drug. *Carbohydrate Polymers*, *79*(1), 106-113.

Saraogi, G. K., Gupta, P., Gupta, U. D., Jain, N. K., Agrawal, G. P. (2010). Gelatin nanocarriers as potential vectors for effective management of tuberculosis. *International journal of pharmaceutics*, *385*(1), 143-149.

Sashiwa, H., Aiba, S. I. (2004). Chemically modified chitin and chitosan as biomaterials. *Progress in Polymer Science*, *29*(9), 887-908.

Sayed, F. N., Jayakumar, O. D., Sudakar, C., Naik, R., Tyagi, A. K. (2011). Possible weak ferromagnetism in pure and M (Mn, Cu, Co, Fe and Tb) doped NiGa2O4 nanoparticles. *Journal of nanoscience and nanotechnology*, *11*(4), 3363-3369.

Schaer, M., Crittin, M., Kasmi, L., Pierzchala, K., Calderone, C., Digigow, R. G., Sienkiewicz, A. (2014). Multi-functional magnetic photoluminescent photocatalytic polystyrene-based micro-and nano-fibers obtained by electrospinning. *Fibers*, *2*(1), 75-91.

Schmaljohann, D. (2006). Thermo-and pH-responsive polymers in drug delivery. *Advanced drug delivery reviews*, *58*(15), 1655-1670.

Schönhoff, M. (2003). Layered polyelectrolyte complexes: physics of formation and molecular properties. *Journal of Physics: Condensed Matter*, *15*(49), R1781.

Schwach, G., Coudane, J., Engel, R., Vert, M. (1997). More about the polymerization of lactides in the presence of stannous octoate. *Journal of Polymer Science Part A: Polymer Chemistry*, *35*(16), 3431-3440.

Sershen, S. R., Westcott, S. L., Halas, N. J., West, J. L. (2000). Temperature-sensitive polymer–nanoshell composites for photothermally modulated drug delivery. *Journal of biomedical materials research*, *51*(3), 293-298.

Shabbits, J. A., Chiu, G. N., Mayer, L. D. (2002). Development of an in vitro drug release assay that accurately predicts in vivo drug retention for liposome-based delivery systems. *Journal of Controlled Release*, *84*(3), 161-170.

Shi, H. G., Farber, L., Michaels, J. N., Dickey, A., Thompson, K. C., Shelukar, S. D., Kaufman, M. J. (2003). Characterization of crystalline drug nanoparticles using atomic force microscopy and complementary techniques. *Pharmaceutical research*, *20*(3), 479-484.

Shin, U. S., Yoon, I. K., Lee, G. S., Jang, W. C., Knowles, J. C., Kim, H. W. (2011). Carbon nanotubes in nanocomposites and hybrids with hydroxyapatite for bone replacements. *Journal of tissue engineering*, 674287.

Shoaib, M. H., Tazeen, J., Merchant, H. A., Yousuf, R. I. (2006). Evaluation of drug release kinetics from ibuprofen matrix tablets using HPMC. *Pakistan Journal of Pharmaceutical Sciences*, *19*(2), 119-124.

Siepmann, J., Peppas, N. A. (2012). Modeling of drug release from delivery systems based on hydroxypropyl methylcellulose (HPMC). *Advanced drug delivery reviews*, *64*, 163-174.

Siepmann, J., Elkharraz, K., Siepmann, F., Klose, D. (2005). How autocatalysis accelerates drug release from PLGA-based microparticles: a quantitative treatment. *Biomacromolecules*, *6*(4), 2312-2319.

Simeonova, M., Velichkova, R., Ivanova, G., Enchev, V., Abrahams, I. (2003). Poly (butylcyanoacrylate) nanoparticles for topical delivery of 5-fluorouracil. *International journal of pharmaceutics*, *263*(1), 133-140.

Singh, P., Gupta, U., Asthana, A., Jain, N. K. (2008). Folate and folate− PEG− PAMAM Dendrimers: synthesis, characterization, and targeted anticancer drug delivery potential in tumor bearing mice. *Bioconjugate chemistry*, *19*(11), 2239-2252.

Sinha, V. R., Kumria, R. (2001). Polysaccharides in colon-specific drug delivery. *International journal of pharmaceutics*, *224*(1), 19-38.

Slowing, I. I., Vivero-Escoto, J. L., Wu, C. W., Lin, V. S. Y. (2008). Mesoporous silica nanoparticles as controlled release drug delivery and gene transfection carriers. *Advanced drug delivery reviews*, *60*(11), 1278-1288.

Stone, V., Johnston, H., Schins, R. P. (2009). Development of in vitro systems for nanotoxicology: methodological considerations. *Critical reviews in toxicology*, *39*(7), 613-626.

Sunderland, C. J., Steiert, M., Talmadge, J. E., Derfus, A. M., Barry, S. E. (2006). Targeted nanoparticles for detecting and treating cancer. *Drug Development Research*, *67*(1), 70-93.

Sze, A., Erickson, D., Ren, L., Li, D. (2003). Zeta-potential measurement using the Smoluchowski equation and the slope of the current–time relationship in electroosmotic flow. *Journal of colloid and interface science*, *261*(2), 402-410.

Ta, H. T., Dass, C. R., Dunstan, D. E. (2008). Injectable chitosan hydrogels for localised cancer therapy. *Journal of Controlled Release*, *126*(3), 205-216.

Tao, S. L., Lubeley, M. W., Desai, T. A. (2003). Bioadhesive poly (methyl methacrylate) microdevices for controlled drug delivery. *Journal of controlled release*, *88*(2), 215-228.

Teeguarden, J. G., Hinderliter, P. M., Orr, G., Thrall, B. D., Pounds, J. G. (2007). Particokinetics in vitro: dosimetry considerations for in vitro nanoparticle toxicity assessments. *Toxicological Sciences*, *95*(2), 300-312.

Terbojevich, M., Cosani, A., Muzzarelli, R. A. A. (1996). Molecular parameters of chitosans depolymerized with the aid of papain. *Carbohydrate Polymers*, *29*(1), 63-68.

Thanou, M., Verhoef, J. C., Junginger, H. E. (2001). Oral drug absorption enhancement by chitosan and its derivatives. *Advanced drug delivery reviews*,*52*(2), 117-126.

Tiwari, G., Tiwari, R., Sriwastawa, B., Bhati, L., Pandey, S., Pandey, P., Bannerjee, S. K. (2012). Drug delivery systems: An updated review.*International journal of pharmaceutical investigation*, *2*(1), 2.

Tolnai, G., Csempesz, F., Kabai-Faix, M., Kálmán, E., Keresztes, Z., Kovács, A. L., Hórvölgyi, Z. (2001). Preparation and characterization of surface-modified silica-nanoparticles. *Langmuir*, *17*(9), 2683-2687.

Tomaro-Duchesneau, C., Saha, S., Malhotra, M., Kahouli, I., Prakash, S. (2012). Microencapsulation for the therapeutic delivery of drugs, live mammalian and bacterial cells, and other biopharmaceutics: current status and future directions. *Journal of pharmaceutics*, *2013*.

Tripisciano, C., Costa, S., Kalenczuk, R. J., Borowiak-Palen, E. (2010). Cisplatin filled multiwalled carbon nanotubes–a novel molecular hybrid of anticancer drug container. *The European Physical Journal B*, *75*(2), 141-146.

Trommelen, A. M., Crosby, E. J. (1970). Evaporation and drying of drops in superheated vapors. *AIChE Journal*, *16*(5), 857-867.

Varshosaz, J., Tavakoli, N., Moghaddam, F., & Ghassami, E. (2015). Polyelectrolyte complexes of chitosan for production of sustained release tablets of bupropion hcl. *Farmacia*, *63*(1), 65-73.

Vauthier, C., Labarre, D., Ponchel, G. (2007). Design aspects of poly (alkylcyanoacrylate) nanoparticles for drug delivery. *Journal of drug targeting*,*15*(10), 641-663.

Vemavarapu, C., Mollan, M. J., Lodaya, M., Needham, T. E. (2005). Design and process aspects of laboratory scale SCF particle formation systems. *International journal of pharmaceutics*, *292*(1), 1-16.

Vergnaud, J. M. (1993). *Controlled drug release of oral dosage forms*. CRC Press.

Vickers, A. E., Rose, K., Fisher, R., Saulnier, M., Sahota, P., Bentley, P. (2004). Kidney slices of human and rat to characterize cisplatin-induced injury on cellular pathways and morphology. *Toxicologic pathology*, *32*(5), 577-590.

Wang, J., Ding, J., Jin, N., Zhou, Y., Li, X., Tang, M., Wang, X. M. (2010). Pharmacokinetic parameters and tissue distribution of magnetic Fe. *International Journal of Nanomedicine*, *5*, 861-866.

Wang, Q., Dong, Z., Du, Y., Kennedy, J. F. (2007). Controlled release of ciprofloxacin hydrochloride from chitosan/polyethylene glycol blend films. *Carbohydrate polymers*, *69*(2), 336-343.

Wei, L., Hu, N., Zhang, Y. (2010). Synthesis of polymer—mesoporous silica nanocomposites. *Materials*, *3*(7), 4066-4079.

Weinbreck, F., De Vries, R., Schrooyen, P., De Kruif, C. G. (2003). Complex coacervation of whey proteins and gum arabic. *Biomacromolecules*, *4*(2), 293-303.

Win, P. P., Shin-Ya, Y., Hong, K. J., Kajiuchi, T. (2003). Formulation and characterization of pH sensitive drug carrier based on phosphorylated chitosan (PCS). *Carbohydrate Polymers*, *53*(3), 305-310.

Wong, H. M., Wang, J. J., Wang, C. H. (2001). In vitro sustained release of human immunoglobulin G from biodegradable microspheres. *Industrial & engineering chemistry research*, *40*(3), 933-948.

Wörle-Knirsch, J. M., Pulskamp, K., Krug, H. F. (2006). Oops they did it again! Carbon nanotubes hoax scientists in viability assays. *Nano letters*, *6*(6), 1261-1268.

Wu, W., He, Q., Jiang, C. (2009). Magnetic iron oxide nanoparticles: synthesis and surface functionalization strategies. *ChemInform*, *40*(24), i.

Wunder, A., Müller-Ladner, U., Stelzer, E. H., Funk, J., Neumann, E., Stehle, G., Fiehn, C. (2003). Albumin-based drug delivery as novel therapeutic approach for rheumatoid arthritis. *The Journal of immunology*, *170*(9), 4793-4801.

Xie, W., Xu, P., Wang, W., Liu, Q. (2002). Preparation and antibacterial activity of a water-soluble chitosan derivative. *Carbohydrate polymers*, *50*(1), 35-40.

Yamada, T., Onishi, H., Machida, Y. (2001). Sustained release ketoprofen microparticles with ethylcellulose and carboxymethylethylcellulose. *Journal of controlled Release*, *75*(3), 271-282.

Yang, J., Park, S. B., Yoon, H. G., Huh, Y. M., Haam, S. (2006). Preparation of poly ε-caprolactone nanoparticles containing magnetite for magnetic drug carrier. *International journal of pharmaceutics*, *324*(2), 185-190.

Yoo, J. W., Chambers, E., Mitragotri, S. (2010). Factors that control the circulation time of nanoparticles in blood: challenges, solutions and future prospects. *Current pharmaceutical design*, *16*(21), 2298-2307.

Yordanov, G. G., Dushkin, C. D. (2010). Preparation of poly (butylcyanoacrylate) drug carriers by nanoprecipitation using a pre-synthesized polymer and different colloidal stabilizers. *Colloid and Polymer Science*, *288*(9), 1019-1026.

Yousefpour, P., Atyabi, F., Vasheghani-Farahani, E., Movahedi, A. A., Dinarvand, R. (2011). Targeted delivery of doxorubicin-utilizing chitosan nanoparticles surface-functionalized with anti-Her2 trastuzumab. *International Journal of Nanomedicine*, *6*, 1977-1990.

Zhang, D., Tian, A., Xue, X., Wang, M., Qiu, B., Wu, A. (2012). The effect of temozolomide/poly (lactide-co-glycolide)(PLGA)/nano-hydroxyapatite microspheres on glioma U87 cells behavior. *International journal of molecular sciences*, *13*(1), 1109-1125.

Zhang, H., Gao, S. (2007). Temozolomide/PLGA microparticles and antitumor activity against glioma C6 cancer cells in vitro. *International journal of pharmaceutics*, *329*(1), 122-128.

Zhang, L., Radovic-Moreno, A. F., Alexis, F., Gu, F. X., Basto, P. A., Bagalkot, V., Farokhzad, O. C. (2007). Co-delivery of hydrophobic and hydrophilic drugs from nanoparticle–aptamer bioconjugates. *ChemMedChem*, *2*(9), 1268-1271.

Zhao, Q., Qian, J., An, Q., Gao, C., Gui, Z., Jin, H. (2009). Synthesis and characterization of soluble chitosan/sodium carboxymethyl cellulose polyelectrolyte complexes and the pervaporation dehydration of their homogeneous membranes. *Journal of Membrane Science*, *333*(1), 68-78.

Zhu, C., Jung, S., Luo, S., Meng, F., Zhu, X., Park, T. G., Zhong, Z. (2010). Co-delivery of siRNA and paclitaxel into cancer cells by biodegradable cationic micelles based on PDMAEMA–PCL–PDMAEMA triblock copolymers. *Biomaterials*, *31*(8), 2408-2416.

Zientek, L. R., Thompson, B. (2009). Matrix summaries improve research reports: Secondary analyses using published literature. *Educational Researcher*, *38*(5), 343-352.

LIST OF TABLES

LIST OF FIGURES

Fig. 1 Representation of marked liposome based formulation Doxil®.

Fig. 2 Representation of molecular modelling of dendrimer.

Fig. 3 SEM micrograph of standard gold nanoparticles.

Fig. 4 TEM micrograph of Iron oxides nanoparticles.

Fig. 5 Schematic representation of a) SWCNT and b) MWCNT.

Fig. 6 TEM micrograph of mesoporous silica nanoparticles.

Fig. 7 Schematic representation of polyelectrolytes complexes formation.

Fig. 8 Schematic representation of the single emulsification-extraction/ evaporation technique.

Fig. 9 Schematic representation of EC microparticles preparation using double-emulsification called the W/O1/O2 method.

Fig. 10 Schematic representation of a) reservoir system; b) dissolved drug system and c) dispersed drug system.

Fig. 11 Schematic representation of concentration profile in a sphere of dispersed drug system in perfect sink conditions.

Fig. 12 Schematic illustration of polymer matrix disentanglement as a function of polymer concentration in a swelling-controlled drug system.

Fig. 13 Graphical representation of most used mathematical model for release kinetic

Fig. 14 Dose responsive curve.

Fig. 15 General reaction scheme of EDC and NHS

Fig. 16 Reaction scheme of grafting PLA to CS backbone.

Fig. 17 Molecular structure of a) TMZ and b) 5FU.

Fig. 18 TEM images and average diameter of nanoparticles A) CS-ALG and B) CS-PGA and z-potential C) CS-ALG and D) CS-PGA in preparation media (pH 5.5) at room temperature.

Fig. 19 Relationship between encapsulation efficiency and polycation/polyanion weight ratio. A, B) single loading and C, D) multiple loading

Fig. 20 Cumulative release of A) TMZ and B) 5-FU from CS-ALG, and C) TMZ and D) 5-FU from CS-PGA at 37 °C in different media. The inner pane indicates the percentage of swelling after soaking for 10 min in the relevant medium.

Fig. 21 Individual (A, B) and simultaneous (C, D) release intensity of TMZ and 5FU after 6 h of incubation in different media at 37 °C from CS-PGA (A, C) and CS-ALG (B, D)

Fig. 22 TMZ and 5-FU co-release profiles from CS-AA in A) SGF, B) PM, C) PS and D) HS at 37 °C; the main chart represents total release (5-FU + TMZ), while the inner pane specifically indicates the trend of 5-FU and TMZ.

Fig. 23 TMZ and 5-FU co-release profiles from CS-PGA in A) SGF, B) PM, C) PS and D) HS at 37 °C; the main chart represents total release (5-FU + TMZ), while the inner pane specifically indicates the trend of 5-FU and TMZ.

Fig. 24 MS spectra of A) TMZ (control) and TMZ after release in B) physiological and C) preparation media at different time.

Fig. 25 MS spectra of A) 5-FU (control) and 5-FU after release in B) physiological and C) preparation media at different time.

Fig. 26 MS spectra of TMZ and 5-FU co-released from A) physiological and B) preparation media.

Fig. 27 Schematic representation of amide bond formation between CS amino groups and COOH group in PLA

Fig. 28 ATR-FTIR spectra of A) CS and various PLA and B) the obtained products

Fig. 29 A) Average dimension and B) z-potential of all prepared formulations, loaded and unloaded compared with unmodified chitosan (CS).

Fig. 30 Relationship between polymer/DS ratio (w/w) and average dimension (nm), ζ-potential and the μ_e of nanoparticles in preparation media pH 5.5

Fig. 31 Effect of pH on A) DOX and B) TMZ encapsulation efficiency in all formulation

Fig. 32 Relationship between average dimension of nanoparticles and temperature

Fig. 33 Cumulative co-release rate in PBS pH 7.4 at 37 °C of DOX and TMZ from A) CS, B) CS-g-PLA; C) CS-g-PLACA2% and D) CS-g-PLACA5%.

Fig. 34 First 6h Cumulative co-release rate in PBS pH 7.4 at 37 °C of DOX and TMZ from A) CS, B) CS-g-PLA; C) CS-g-PLACA2% and D) CS-g-PLACA5%.

Fig. 35 ATR-FTIR spectra of A) the obtained polymer and B) nanoparticles formulation loaded and unloaded with BSA

Fig. 36 ^{1}H NMR spectra of CS and CS-g-PLA.

Fig. 37 Relationship between CS and CS-g-PLA solution conductivity (mS/cm) and volume (mL) of NaOH 0.160 M.

Fig. 38 Effect of pH on the swelling properties of CS and CS-g-PLA

Fig. 39 Effect of different media composition on the swelling properties of CS and CS-g-PLA

Fig. 40 influence of polymer concentration on encapsulation efficiency (EE) and loading capacity (LC) of BSA in preparation media pH 5.5

Fig. 41 Release trend of BSA from CS and CS-g-PLA in different media; A) pH 2 and B) pH 7.4. BSA released in the first 6h after media contact in reported in panel C) pH 2 and D) pH 7.4

LIST OF ABBREVIATIONS

5-FU   5-Fluorouracil

CSA   Cyclosporine A`

CSNPs   CoreShell Nanoparticles

DDS   Drug delivery systems

DL   Drug Loading

DTX   Docetaxel

EE   Encapsulation Efficiency

HPMA   N-(2-Hydroxypropil Methacryamide)

NPs   Nanoparticles

PA   Polyacrylic

PAA   Polyacrylic acid

PCL   Polycaprolactone

PEG   Polyethylene Glycol

PGA   Polyglycolic acid

PLA   Polylactic acid

PTX   Paclitaxel

POE   Polyorthoesters

TMZ   Temozolomide

VCR   Vincristine

VEGF   Vascular Endothelial Growth Factor

VER   Verapamil

WOR   Phophatidyl inositol 3-kinase inhibitor

YP   Particles Yield

CURRICULUM VITAE

Name : Antonio Di Martino

Date of birth : 22nd August 1984

Address: Via Italia 125, 66052, Gissi, Italy

Nationality : Italian

Contact: dimartino@ft.utb.cz

Education:

2013-present

Tomas Bata University in Zlín, Faculty of Technology. Doctoral degree studies in Chemistry and material technology

2008-2011

University of Rome La Sapienza, Faculty of Mathematical, Physical and Natural Sciences. Master's degree studies in Industrial Organic Chemistry and Biochemistry

2008

Helsinki University, Faculty of Computer Sciences. Basic in Bioinformatics. Summer school

2004-2007

University of Rome La Sapienza, Faculty of Mathematical, Physical and Natural Sciences. Bachelor's degree studies in Industrial Chemistry

Training abroad:

03.2016-05.2016

National Research Tomsk Polytechnic University, Department of Technology of Organic Substances and Polymer Materials

01.2015 – 4.2015

National Research Tomsk Polytechnic University, Department of High Physics Technology. Tomsk, Russian Federation

09.2014 – 11.2014

Vilnius University, Faculty of Chemistry, Department of Polymer Science. Vilnius, Lithuania

Projects:

CZ.1.05/2.1.00/03.0111 Centre of polymer systems (2013-2015), provider: European Fund of the Research and Development for Innovations programme, namely the Priority Axis 2 - Regional R&D centres, Ministry of Education, Youth and Sports of the Czech Republic (MEYS). Researcher.

GJ15-08287Y Immobilization of specific bioactive natural substances in functionalized biodegradable polymer matrices (2015-2017), provider: Czech Science Foundation. Member of research team

QJ1310254 Research into the use of whey as dairy industry waste product, the production of antimicrobial compounds for the modification of hydrophilic polymer systems with the use in cosmetic and medical applications (2013-2017), provider: Ministry of Agriculture of the Czech Republic (MZe). Member of research team.

LE12002 The support centre for international cooperation in research and development in technical fields (2012-2015), provider: Ministry of Education, Youth and Sports of the Czech Republic (MEYS). Member of research team.

IGA/CPS/2015/003 Development of Advanced Biodegradable and Antimicrobial Polymer Systems (2015), provider: Internal Grant Agency of Tomas Bata University in Zlín. Member of research team.

LIST OF PUBLICATIONS

Journal articles:

1.   Bordi Federico, Chronopoulou Laura, Palocci Cleofe, Bomboi Francesca, Di Martino Antonio, Cifani Noemi, Pompili Barbara, Ascenzioni Fiorentina, Sennato Simona . Chitosan–DNA complexes: effect of molecular parameters on the efficiency of delivery. *Colloids and Surfaces A: Physicochemical and Engineering Aspects*, 2014, 460: 184-190.

2.   Di Martino Antonio, Sedlarik Vladimir. Amphiphilic chitosan-grafted-functionalized polylactic acid based nanoparticles as a delivery system for doxorubicin and temozolomide co-therapy. *International journal of pharmaceutics*, 2014, 474.1: 134-145

3.   Cifani Noemi, Chronopoulou Laura, Pompili Barbara, Di Martino Antonio, Bordi Federico, Sennato Simona, Di Domenico Enea Gino, Palocci Cleofe, Ascenzioni Fiorentina. Improved stability and efficacy of chitosan/pDNA complexes for gene delivery. *Biotechnology letters*, 2015, 37.3: 557-565.

4.   Urbanek Pavel, Di Martino Antonio, Gladyš Sviatoslav , Kuritka Ivo, Rík Mina, Pavlova Ewa, Bondarev Dmitrij. Polythiophene-based conjugated polyelectrolyte: Optical properties and association behavior in solution. *Synthetic Metals*, 2015, 202: 16-24.

5.   Di Martino, Antonio, Kucharczyk Pavel , Zednik Jiri, Sedlarik Vladimir . Chitosan grafted low molecular weight polylactic acid for protein encapsulation and burst effect reduction. *International journal of pharmaceutics*, 2015.

6.   Antonio Di Martino, Alena Pavelkova, Sandra Maciulyte, Saulute Budriene, Vladimir Sedlarik.Polysaccharide- based nanocomplexes for co-encapsulation and controlled release of 5-Fluorouracil and Temozolomide. *European Journal of Pharmaceutical Sciences* Available online 3 May 2016. In Press, Accepted Manuscript

Conference proceedings:

1.   Di Martino Antonio, Kucharczyk Pavel, Sedlarik Vladimir, Effect of polylactide molecular weight on doxorubicin and temozolomide release from chitosan-grafted polylactide nanoparticles, *Nanocon 2013*, Brno, *Czech Republic.*

2.   Di Martino Antonio, Kucharczyk Pavel, Sedlarik Vladimir, Study of pH and thermo-responsive properties of nanoparticles based on an amphiphilic co-polymer, *Plastko 2014*, Zlin, *Czech Republic*.

3.   Di Martino Antonio, Kucharczyk Pavel, Sedlarik Vladimir, Chitosan grafted carboxy functionalized polylactide nanoparticles for multidrugs controlled and sustained release. *"Siberian Youth Conference "Current Topics in Organic Chemistry"* 20-26 March 2015 Sheregesh, *Russian Federation*.

4.   Di Martino Antonio, Kucharczyk Pavel, Sedlarik Vladimir. Nanoparticles based on star-shaped carboxy-terminated polylactide and chitosan for controlled release applications. *Nanocon 2015*, Brno, *Czech Republic*.

5.   Di Martino Antonio, Kucharczyk Pavel, Sedlarik Vladimir. Novel pH sensitive chitosan -grafted- star shaped polylactide nanoparticles for sustained and controlled release application. *4th EPNOE International Polysaccharide Conference 2015*, Warsaw, *Poland*.

6.   Di Martino Antonio, Vladimir Sedlarik. Smart Polysaccharides nanoparticles for controlled release of protein. *2nd International Young Scientist School 'Nanostructured naterials'*.10-12 May 2016. Tomsk, *Russian Federation*.

7.   Di Martino Antonio, Kuchaczyk Pavel, Kucekova Zdenka, Humpolicek Petr, Sedlarik Vladimir. Improve temozolomide stability by loading in Chitosan-carboxy enriched polylactide NPs. In vitro evaluation. *7th International Conference 'Nanoparticles, Nanostructured coatings and microcontainers: technology, properties, applications'*. 12-15 May 2016, Tomsk, *Russian Federation*.

8.   Di Martino Antonio, Vladimir Sedlarik. Novel PLA-Chitosan nanocomplexes for controlled and sustained release of DNA-alkylating drugs. *XVII international scientific conference "chemistry and chemical engineering in XXI century"*. 17-20 May 2016. Tomsk, *Russian Federation*.

9.   Kurtukov.V.Viktor, Guselnikova A. Olga, Olshtrem A. Anastasia, Di Martino Antonio. Synthesis of Gd-based MRI contrast agent. *XVII international scientific conference "chemistry and chemical engineering in XXI century"*. 17-20 May 2016. Tomsk, *Russian Federation*.